U. S. DEPARTMENT OF COMMERCE
Charles Sawyer, Secretary
NATIONAL BUREAU OF STANDARDS
E. U. Condon, Director

AUGUST 1948
VOLUME • 41
NUMBER 2

JOURNAL OF RESEARCH

of the

NATIONAL BUREAU OF STANDARDS

Contents

RP		Page
1906	Strain test for evaluation of rubber compounds. Frank L. Roth and Robert D. Stiehler. (Price 10 cents)	87
1907	Strain tester for rubber. William L. Holt, Ellis O. Knox, and Frank L. Roth. (Price 10 cents)	95
1908	Barium aluminate hydrates. Elmer T. Carlson and Lansing S. Wells. (Price 10 cents)	103
1909	Aliphatic halide-carbonyl condensations by means of sodium. Edgar A. Cadwallader, Abraham Fookson, Thomas W. Mears, and Frank L. Howard. (Price 10 cents)	111
1910	Barium 2-ketolactobionate and the corresponding barium bromide double salt. William W. Walton and Horace S. Isbell. (Price 10 cents)	119
1911	Infrared prism spectrometry from 24 to 40 microns. Earle K. Plyler. (Price 10 cents)	125
1912	Mass spectra of octanes. Evelyn G. Bloom, Fred L. Mohler, J. H. Lengel, and C. Edward Wise. (Price 10 cents)	129
1913	Effects of substitute fuels on automotive engines. Clarence S. Bruce, Jesse T. Duck, and A. R. Pierce. (Price 10 cents)	135
1914	Applications of magnetochemistry to polymers and polymerization. Pierce W. Selwood. (Price 10 cents)	151

For sale by the Superintendent of Documents, U. S. Government Printing Office, Washington 25, D. C. - Price 50 cents
$4.50 per year on subscription

UNITED STATES GOVERNMENT PRINTING OFFICE, WASHINGTON : 1948

U. S. Department of Commerce
National Bureau of Standards

Research Paper RP1906
Volume 41, August 1948

Part of the Journal of Research of the National Bureau of Standards

Strain Test for Evaluation of Rubber Compounds[1]

By Frank L. Roth and Robert D. Stiehler

Measurements of elongation of rubber vulcanizates at a fixed stress have been made with a precision much greater than can be obtained in the usual measurements of stress at a specified elongation. Such measurements form the basis of a strain test developed to characterize rubber vulcanizates in control and research testing. Statistical analyses show that the errors introduced in the actual strain measurements are negligible compared to those introduced by variations during compounding and curing, whereas the errors introduced by the usual measurements of stress at a specified elongation are of the same order of magnitude. The high precision of strain testing has been used to detect variations within a single sheet of vulcanized rubber and variations among sheets cured from the same compounded batch. It has also been possible to determine with a single sheet its change in stiffness or modulus with age. The uniform treatment of specimens in the strain test makes them particularly useful for precise measurements of set. Further, it has been found that the decrease in elongation with time of cure apparently follows the laws of a second-order chemical reaction, and consequently it is possible to represent the data by an equation involving three vulcanization parameters.

I. Introduction

The inherent variability of measurements for determining the stress-strain properties of vulcanized rubber is notorious. It has been customary to ascribe the cause of the variability entirely to the rubber. This allegation may be largely true in the case of stress and elongation at failure, but measurements by means of the strain test definitely show that the measurements are responsible for a large portion of the observed variations of points on the stress-strain curve below failure.

Since the advent of the Government Synthetic Rubber Program in 1943, there has been an intensified effort to improve the precision of stress-strain testing. Measurements of the stress-temperature relationships for pure gum vulcanizates of GR–S and natural rubber by Roth and Wood [1, 2][2] suggested that the precision and accuracy of stress-strain measurements might be greatly improved by measuring the elongations of rubber specimens suspending predetermined loads. Strain tests made in late 1944 on vulcanizates of X–125 GR–S and in 1945 on vulcanizates of natural rubber at the Instituto Agronomico do Norte in Belem, Brazil [3] confirmed this suggestion. In the development of this test, strain measurements for the evaluation of vulcanized rubber have been found to yield information that has not been revealed by the usual stress-strain measurements.

II. Procedure

In the strain test, a predetermined load is applied to a specimen and the elongation is measured after the load has been applied for a specified time. The load is selected to produce a specified force per unit of cross-sectional area of the unstretched specimen.

The early tests were performed with extremely simple equipment that required manual application of the load to a standard dumbbell-shaped specimen having a reduced section 2 in. long. Most of the data reported here, however, were obtained by means of a tester developed by Holt, Knox, and Roth [4]. This tester is designed to minimize the number of manual operations and thereby to reduce the number of subjective errors.

[1] Presented before the Division of Rubber Chemistry at the 113th Meeting of the American Chemical Society, Chicago, Ill.

[2] Figures in brackets indicate the literature references at the end of this paper.

These authors also describe the preparation of the test specimens and the measurement of their thickness, in addition to the measurement of strain at the specified stress. Strip specimens approximately ¼ in. wide and 6 in. long are used, since specimens with enlarged ends are not required for this test. These specimens can be cut from the standard 6 by 6 by 0.075-in. test sheet and permit the distance between bench marks to be increased to improve precision. The bench marks are spaced 10 cm. apart, so that elongations can be read directly by means of a millimeter scale.

In early experiments, a stress of 1,000 psi (pounds per square inch) was used for vulcanized specimens of GR–S and GR–I prepared according to the Specifications for Government Synthetic Rubbers [5]. In the course of development of the method, the stress has been reduced in several steps to 400 psi which is employed at present for vulcanized tread-type compounds. The stress of 400 psi was selected because it is in the region where the ratio of elongation to stress attains a maximum value. A stress of 100 psi has been selected for gum vulcanizates of natural and other rubbers in order to avoid effects of crystallization. The stress of 100 psi can also be used for studying gum vulcanizates of GR–S.

For control testing and many research purposes, stresses of 100 to 400 psi are sufficient. Accordingly, the tester developed by Holt, Knox, and Roth [4], is provided with weights for applying a stress of 100, 200, or 400 psi. Stresses lower than 100 psi can be used, provided the elongation is above 50 percent. Minor modifications in the apparatus or procedure are necessary in order to measure precisely lower elongations. Stresses higher than 400 psi are obtained by suitable adjustment of the weights and are limited only by the strength of the specimen or the limiting extension of the specimen by the tester.

When the load is applied, the specimen elongates rapidly at first and then more slowly as time elapses. The precision of measurement increases as the rate of creep decreases, thus observations can be made with greater precision as the time after application of the load increases. It is necessary, however, in a control test to keep the time for making a test at a minimum compatible with the requisite precision.

Measurements have been made at various intervals between 10 sec and 10 min after application of the load. These measurements indicate that the elongation of the specimen increases approximately linearly with the logarithm of time. For example, in figure 1, the increase in elongation after the 10-sec reading is plotted against the logarithm of time. The test specimens were prepared from GR–S according to the Specifications for Government Synthetic Rubbers [5]. Vulcanizates cured 25 and 90 min at 292° F were employed. Specimens cured 25 min were tested with loads of both 100 and 400 psi to determine the effect of load. The specimens cured 90 min were tested only with a load of 400 psi.

As can be seen in the figure 1, the rate of creep is approximately the same for the two loads, whereas the rate of creep for specimens cured 90 min is approximately one-third of that for those cured 25 min. None of the natural or other synthetic rubber vulcanizates investigated, including some without fillers, had a greater rate of creep than the GR–S carbon-black compound

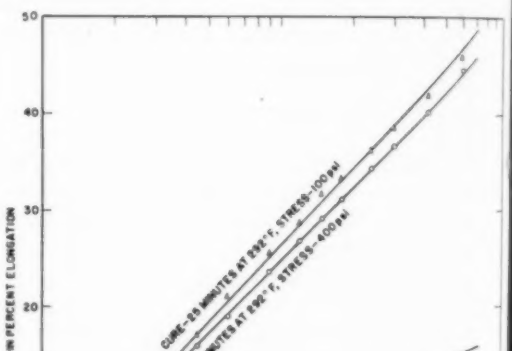
CHANGE IN PERCENT ELONGATION
TIME IN SECONDS
CURE–25 MINUTES AT 292°F, STRESS–100 psi
CURE–25 MINUTES AT 292°F, STRESS–400 psi
CURE–90 MINUTES AT 292°F, STRESS–400 psi

FIGURE 1. *Creep of GR-S specimens under tensile stress.*

The creep is shown as the difference between the elongation at any specified time and that at 10 seconds after application of the stress. The time scale is logarithmic.

cured 25 min at 292° F. In those cases where crystallization occurred, the rate of creep was a maximum at intermediate loads. This phenomenon is in accordance with the observations for unvulcanized natural rubber by Treloar [6] and for

vulcanized natural rubber by Field [7] and by Wildschut [8].

From these studies, a time interval of 60 sec was selected for making subsequent measurements, since observations made between 56 and 64 sec are less in error due to creep than to errors in determining cross-sectional area of the specimen. With the automatic timing of the tester designed by Holt, Knox, and Roth [4], it is possible to retain the same precision with shorter time intervals by reducing the period permitted for observation by a proportionate amount; that is, measurements made between 28 and 32 sec are as precise as those made between 56 and 64 sec. The absolute value of the elongation, however, will be lower at 30 sec than at 60 sec, as indicated in figure 1.

III. Precision of Test

The high precision of the strain test is achieved largely by measurement of the elongation under nearly static conditions, instead of taking observations as the specimen is being extended. This precision can be seen in table 1, which gives the standard deviations among specimens from the same sheet of vulcanized rubber. The values represent data obtained during the evaluation of reference lots of Government Synthetic Rubbers. With the exception of the values for X–125 GR–S, which were obtained with 2-in. dumbbell specimens and manually applied loads, the standard deviations are essentially identical for all rubbers tested during the past 3 years and are comparatively small. Because these values are in units of elongation, they cannot be compared directly with those for tensile stress. A comparison can be made, however, by converting one into the units of the other. In table 2 the standard deviations for strain are converted into equivalent stress values and compared with those for tensile stress as follows:

1. Six sheets from the same compounded batch of X–243 GR–S were cured for each of the times indicated; 3 sheets of each cure were used for measurements of tensile stress and three for those of strain.

2. The tensile stress at 300-percent elongation was measured on 6 specimens from each of the 3 sheets; the elongation was measured on 18 specimens from each sheet, 6 at a stress approximatelv equivalent to the average tensile stress at 300-percent elongation, 6 at a stress 50 psi lower, and 6 at a stress 50 psi higher. The mean values for each of these properties are shown in the first 4 lines of table 2.

3. The standard deviations among specimens were calculated for tensile stress and for strain measurements and are given in lines 5 and 6 of table 2. The change in elongation produced by a change in stress of 1 psi were calculated from the strain measurements in lines 2 to 4 and are shown in line 7. The values of the standard deviations in line 6 were divided by the corresponding values in line 7 to obtain the equivalent standard deviations in units of stress shown in line 8.

4. The ratios of the values in line 5 to those in line 8, given in the last line, indicate that the standard deviations for tensile stress measurements at 300-percent elongation are approximately 2½ times as large as the equivalent values for strain measurements.

Another comparison of the precision of measurements made by these two methods of test is

TABLE 1. *Precision of strain measurements*

Type of rubber	Date of tests	Number of sheets tested	Stress	Standard deviations of strains for specimens within a sheet		
				25 min [b]	30 min [b]	90 min [b]
			psi	*Percent*	*Percent*	*Percent*
GR–S X–125 [a]	Dec. 1944	2	1,000	7.5	5.9	4.3
X–179	Feb. 1945	22	1,000	2.8	2.5	1.4
X–224	July 1945	9	1,000	4.9	2.4	1.7
X–224	July 1945	9	1,000	3.8	2.2	1.9
X–224	July 1945	9	1,000	2.6	2.0	1.9
X–243	Dec. 1945	20	1,000	3.3	1.7	1.8
X–224	Apr. 1946	12	750	1.5	3.1	1.8
X–289	Apr. 1946	12	750	2.0	3.2	1.2
X–289	Jan. 1947	11	600	3.0	1.1	0.9
X–346	Jan. 1947	21	600	3.0	1.5	.8
X–346	July 1947	20	600	2.6	2.2	1.4
X–387	July 1947	40	600	3.1	2.0	1.4
X–387	Dec. 1947	16	600	3.2	1.5	1.8
X–418	Dec. 1947	36	600	3.5	2.1	1.3
X–412	Dec. 1947	30	600	3.8	1.5	2.8
X–418	Feb. 1948	54	400	2.5	1.2	<0.7
				20 min [d]	40 min [d]	80 min [d]
GR–I Y–100	Apr. 1945	20	1,000	3.3	2.9	2.3
Y–102	Jan. 1947	8	600	1.7	1.5	1.3
Y–103	Jan. 1947	16	600	1.6	1.1	1.2
				10 min [b]	10 min [d]	20 min [d]
GR–M (10 lots)	July 1946	20	600	3.1	2.5	2.2

[a] Used 2-in. dumbbell-shaped specimens and applied load manually.
[b] Time of cure at 292° F.
[c] Cured 100 min at 292° F.
[d] Time of cure at 307° F.

TABLE 2. *Comparison of precision of strain test with precision of usual tensile stress test*

Line	Test	Statistic	Compounds of X-243 GR-S vulcanized					
			25 min at 292° F		50 min at 292° F		90 min at 292° F	
			Stress	Strain	Stress	Strain	Stress	Strain
			psi	*Percent*	*psi*	*Percent*	*psi*	*Percent*
1	Stress	Mean	407	300	1,089	300	1,543	300
2	Strain	do	350	298.9	1,050	324.7	1,500	330.1
3	do	do	400	328.9	1,100	335.2	1,550	338.2
4	do	do	450	355.3	1,150	344.8	1,600	348.8
5	Stress	Std. dev.[a]	18.8		30.2		45.2	
6	Strain	do [a]		4.35		3.25		2.74
7	do	$\triangle E/\triangle S$[b]		0.564		0.201		0.187
8	do	Std. dev.[c]	7.72		16.2		14.7	
9		Ratio [d]	2.44		1.86		3.07	

[a] Standard deviation of specimens within a sheet.

[b] The change in elongation for a change in stress of 1 psi (line 4 minus line 2)/100.

[c] Standard deviation of strain measurements expressed in equivalent stress units, which is calculated by dividing the strain standard deviation by $\Delta E/\Delta S$, line 6/line 7.

[d] Ratio of standard deviation for tensile stress to that for strain both expressed in psi, line 5/line 8.

possible by subjecting the data obtained on reference lots of synthetic rubbers to an analysis of variance. Such an analysis for X–289 and X–346 GR–S is given in table 3. Column A lists for each property the variances (squares of standard deviations) among batch means, and column B lists the variances among specimens from the same batch. The values in column A may be resolved into two components, one due to variations from batch to batch and the other to variations among specimens from the same batch. Since five specimens from each batch were tested, the contributions from variations among specimens to the variances in column A are one-fifth of the variances in column B and are listed in column C. Column D expresses this contribution as a percentage of the observed variance among the batch means. In the case of elongation at 600 psi, testing variations account for approximately 34 percent of the observed batch-to-batch variations, which is about one-tenth the corresponding percentage for stress at 300-percent elongation. Similar results have been obtained in the evaluation of Y–102 and Y–103 GR–I. Other laboratories [9,10], have noted comparable improvements in precision of testing by means of the strain test.

TABLE 3. *Variances of stress and strain measurements* [a]

Type of GR–S	Cured at 292° F for —	Variances			
		A	B	C	D
		Batch means [b]	Specimens [c]	Col. B/5	Col. C/A
STRESS AT 300 PERCENT ELONGATION					
	min	*psi* [2]	*psi* [2]	*psi* [2]	*Percent*
X–346	25	509	1,320	264	52
	50	824	1,297	259	31
	90	708	1,801	360	51
X–289	25	133	276	55	41
	50	658	931	186	28
	90	1,847	1,120	224	12
STRAIN AT 600 PSI					
		Percent [2]	*Percent* [2]	*Percent* [2]	*Percent*
X–346	25	78.9	9.00	1.80	2.3
	50	24.6	2.16	0.43	1.8
	90	1.8	0.65	.13	7.2
X–289	25	56.0	8.86	1.77	3.2
	50	5.3	1.12	0.22	4.2
	90	8.9	0.73	.15	1.7

[a] Analysis of variances is treated in such books as *Statistical methods in research and production*, by O. L. Davies, published by Oliver and Boyd, London (1947) for Imperial Chemical Industries, Ltd., or *Statistical methods*, by George W. Snedecor, Iowa State College Press (1946).

[b] Variances apply to 27 batches of X–346 GR–S and 11 batches of X–289 GR–S.

[c] Variances apply to 5 specimens from a sheet from each batch, i. e., a total of 105 specimens of X–346 and 55 specimens of X–289 GR–S.

IV. Applications of Strain Test

The high precision of the strain test has made it possible to obtain a reliable evaluation of vulcanized rubber samples by means of relatively few measurements. For example, it has been possible to determine with little effort the variations intro-

duced during compounding and curing, the heterogeneity of a single sheet of rubber, and the change in stress-strain properties during storage of vulcanized rubber.

In table 3 the large variance among batch means compared to the variance among specimens for the strain data indicates that there was considerable variability in the compounding and curing operations. Similar data are shown in table 4, where values for individual specimens from five batches prepared on different days are given. The agreement among the specimens from a single sheet from each batch is excellent, but the batch averages vary considerably. In order to determine whether this variation is related to the compounding or curing procedure, 6 sheets from the same batch were vulcanized simultaneously. The average value for each of the 6 sheets is given in table 5. The variation among sheets cured from the same batch is considerably more than expected from specimen variations and is an appreciable fraction of the variation among batches noted in table 4. From an analysis of variance made on data, not reported here, for approximately 100 pairs of sheets of X–412 and X–418 GR–S vulcanizates, it was inferred that the true variance among batches is approximately two times the true variance among sheets within a batch.

TABLE 4. *Typical data for strain and set of individual specimens*

Date, 1946	Strain at 600 psi			Set [b]		
	25 min [a]	50 min [a]	90 min [a]	25 min [a]	50 min [a]	90 min [a]
	Percent	*Percent*	*Percent*	*Percent*	*Percent*	*Percent*
Oct. 22	450	245	190	10.5	4.5	3.0
	450	245	190	10.5	4.5	3.0
	452	242	192	10.5	4.6	3.2
	456	245	191	10.6	4.3	3.0
	457	245	191	10.6	4.5	3.2
	Avg. 453	244	191	10.5	4.5	3.1
Oct. 23	492	256	190	10.5	4.8	3.2
	485	256	190	10.8	4.8	3.4
	484	256	192	10.7	4.8	3.3
	488	255	190	10.7	5.0	3.3
	485	257	190	10.7	5.0	3.3
	Avg. 487	256	190	10.7	4.9	3.3
Oct. 24	486	248	193	13.4	5.0	3.0
	484	250	194	13.4	5.0	3.0
	481	250	194	13.4	4.9	3.5
	485	250	192	13.6	4.9	3.5
	485	249	193	13.6	5.0	3.5
	Avg. 484	249	193	13.5	5.0	3.3
Oct. 29	446	244	190	12.0	4.4	3.8
	446	241	190	12.3	4.4	3.8
	445	243	190	12.3	4.2	3.6
	448	242	190	12.4	4.3	3.7
	446	240	190	12.3	4.3	3.6
	Avg. 446	242	190	12.3	4.3	3.7
Oct. 30	486	252	193	13.5	5.0	3.4
	486	252	191	13.5	5.0	3.5
	486	250	190	13.2	5.0	3.5
	485	249	189	13.5	5.0	3.4
	487	247	188	13.4	4.9	3.5
	Avg. 486	230	190	13.4	5.0	3.5

[a] Time of cure at 292° F. X–289 GR–S vulcanizates prepared according to the Specifications for Government Synthetic Rubbers, effective Jan. 1, 1946.
[b] Set measurements made 1 hr after strain measurements on same specimens.

TABLE 5. *Strain and set data for sheets within a batch of X–289 GR–S vulcanizates*

Sheet	Strain at 600 psi			Set [b]		
	25 min [a]	50 min [a]	90 min [a]	25 min [a]	50 min [a]	90 min [a]
	Percent	*Percent*	*Percent*	*Percent*	*Percent*	*Percent*
1	471	254.6	194.3	12.15	4.50	3.23
2	484	255.7	193.7	[c] 14.85	4.74	3.16
3	468	251.2	192.9	[c] 12.66	4.54	3.15
4	498	258.0	191.5	[c] 14.07	4.91	3.36
5	465	253.0	192.9	[c] 12.70	4.68	3.36
6	468	253.6	191.9	12.48	.....	[c] 3.23
Avg	476	254.5	192.9	13.15	4.67	3.25

[a] Time of cure at 292° F.
[b] Set measurements were made 1 hr after strain measurements on same specimens.
[c] Mean for 6 specimens, other values are means for 20 specimens.

In addition to its use for detecting compounding and curing variables, the strain test is sufficiently sensitive to detect variations within a single sheet of vulcanized rubber. The narrow specimen used in this test makes it possible to cut 20 specimens from a sheet 6 in. square. The variations among 20 such specimens are seen in figure 2. This figure shows the individual strain values for the sheets vulcanized 25 and 90 min, respectively, and summarized in table 5. The elongation of each specimen is plotted in the order of its position in the sheet. The trends in values noted across most sheets are believed to be due to grain effects caused by flow during the early part of vulcanization. This conclusion

is supported by the studies of Gurney and Gough [11].

Since 20 specimens can be cut from a single sheet, it is possible to study the change in stress-strain properties of vulcanized rubber during storage. Figure 3 shows the average change in five sheets of each of three GR–S vulcanizates during the first 6 days of storage at 82° F. These data show the marked stiffening of undercured rubber during the first 24 hr after vulcanization

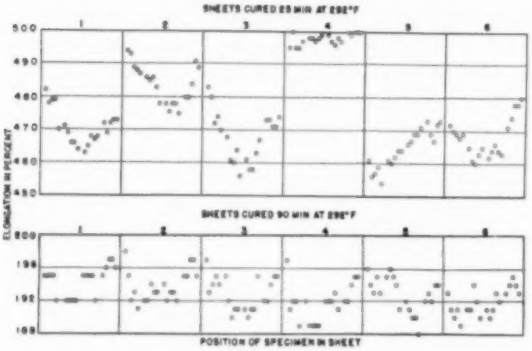

FIGURE 2. *Heterogeneity within and among sheets from same compounded batch.*

The mean value for each sheet and the conditions of test are given in table 5

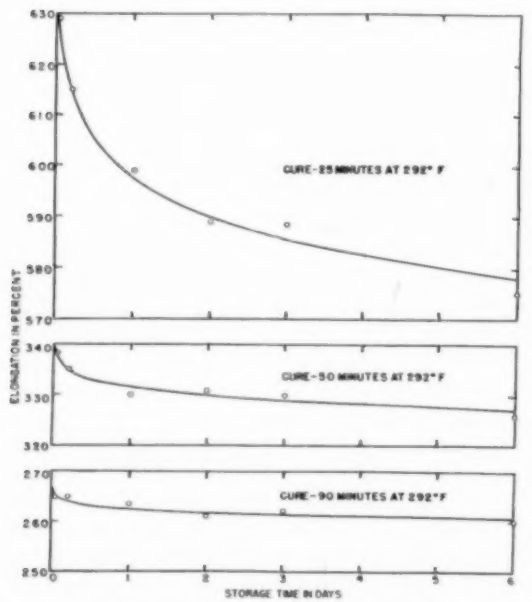

FIGURE 3. *Effect of storage at 82°F on elongation at 600 lb/in.² for vulcanizates of X-243 GR-S.*

and support the minimum aging period of 24 hr between vulcanization and testing required by ASTM Method D15–41 and of 16 hr by the Specifications for Government Synthetic Rubbers. It should be emphasized that the strain test made it possible to obtain these results from only one batch for each cure.

V. Method for Measuring Set

Specimens subjected to the strain test can be conveniently used for precise measurement of extension set for a specified stress, since the specimens are subjected to a uniform stress for a uniform period of time. Such measurements of set after the specimens have been allowed to recover for 1 hr are presented in table 4. As seen in this table, the dispersion of values for specimens from the same sheet is remarkably small, so that it is easy to detect variations among sheets or batches. The results of set measurements shown in table 5 indicate that there is an appreciable variation in set among sheets from the same batch, although not as large as that among batches shown in table 4.

VI. Determination of Vulcanization Parameters

In the usual measurements of tensile stress ("modulus") of rubbers vulcanized for different periods of time, considerable ambiguity arises in differentiating between cure characteristics and the inherent stiffness of the rubber compound. An examination of strain data plotted as a function of time of cure, as in figure 4, indicates that the curve is a rectangular hyperbola of the form $(t-a)\ (E-b)=c$, where E is the elongation at time of cure, t. On differentiation, this equation becomes: $-dE/dt=(E-b)^2/C$. This equation suggests that elongation at a fixed stress decreases with time of cure according to the laws of a second-order reaction, in which the reaction rate constant (k) is $1/C$. The parameter b is independent of the time of cure and corresponds to the elongation (E_∞) for infinite cure time. The parameter a is the constant of integration and corresponds to the time (t_0) at which the elongation begins to decrease. This time may be considered as the point of incipient cure or scorch time. Thus, strain data may be useful for determining three parameters of vulcanization; (1) scorch time, t_0, (2)

reaction rate constant, k, and (3) a structure factor, E_∞, which may be associated with the inherent stiffness of the rubber compound. This stiffness may be due to the structure of the polymer or the nature and concentration of the compounding ingredients. As seen in figure 4, E_∞, is a function of the applied stress; whereas t_0 is independent of it. The reaction rate constant, k, is also a function of the applied stress that must be considered in comparing compounds with different stress-strain characteristics.

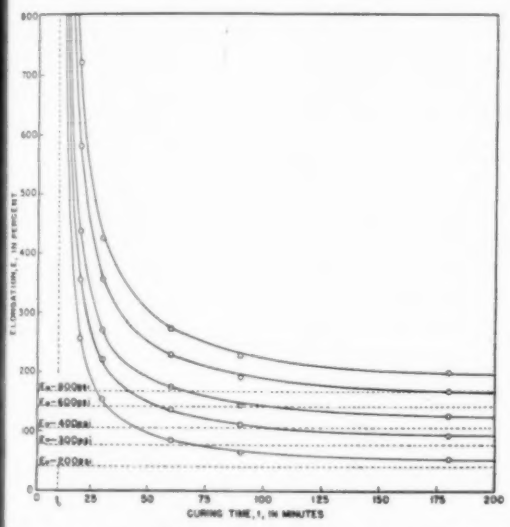

FIGURE 4. *Elongations for various stresses versus time of vulcanization of X–387 GR-S at 292° F.*

The solid lines are hyperbolas calculated from the equation, $(t-t_0)(E-E_\infty)=k$, with the following values for the parameters:

Stress	t_0	E_∞	k
lb/in.²	*min*	*%*	*(min × %)⁻¹*
200	11	41	0.000488
300	11	78	.000392
400	11	107	.000329
600	11	142	.000250
800	11	168	.000203

This relationship has been found to apply to vulcanized GR–S, GR–M, and natural rubber compounds. In the case of rubbers that crystallize on stretching, however, t_0 decreases and may become negative as crystallization increases. Accordingly, if t_0 is to be regarded as a scorch time, the stress should be sufficiently low to avoid crystallization. Reversion is another phenomenon that affects the vulcanization parameters. When reversion occurs, E reaches a minimum and then increases instead of approaching an asymptote as the cure time increases indefinitely. Further, the parameters are extremely sensitive to the observed variations between sheets noted in table 5. It is, therefore, essential to use the average value from several sheets in order to obtain reliable values for the parameters. Employing the average values obtained in the evaluation of X–289, X–346, and X–387 GR–S, the constants given in table 6 were calculated for the vulcanization parameters, t_0, k, and E_∞.

TABLE 6. *Vulcanization parameters derived from strain data*

Type of GR–S	Date tested	Scorch time, t_0	Reaction rate constant, k	Structure factor, E_∞ at 600 psi
		min	*(min×%)⁻¹*	*Percent*
X–289	Oct. 1946	13.0	0.000249	138
X–289	Jan. 1947	12.1	.000239	138
X–346	Jan. 1947	10.9	.000265	135
X–346	July 1947	11.0	.000247	130
X–387	July 1947	11.0	.000234	136

VII. References

[1] F. L. Roth and L. A. Wood, J. App. Phys. **15,** 749 (1944).

[2] L. A. Wood and F. L. Roth, J. App. Phys. **15,** 781 (1944).

[3] N. Bekkedahl, Private communication.

[4] W. L. Holt, E. C. Knox, and F. L. Roth, J. Research NBS **41,** 95 (1948) RP1907.

[5] Specifications for Government Synthetic Rubbers (Reconstruction Finance Corp., Office of Rubber Reserve, Washington 25, D. C., Jan. 1, 1947).

[6] L. R. G. Treloar, Trans. Faraday Soc. **36,** part 4, 538 (1940). Reprinted in Rubber Chem. Tech. **13,** 795 (1940).

[7] J. E. Field, J. App. Phys. **12,** 23 (1941). Reprinted in Rubber Chem. Tech. **14,** 555 (1941).

[8] A. J. Wildschut, Physica **10,** 571 (1943). Reprinted in Rubber Chem. Tech. **17,** 854 (1944).

[9] A. R. Crandall, Private communication.

[10] H. M. Leeper, Private communication.

[11] W. A. Gurney and V. E. Gough, Trans. IRI **22,** 132 (1946). Reprinted in Rubber Chem. Tech. **20,** 863 (1947).

WASHINGTON, April 16, 1948.

U. S. Department of Commerce
National Bureau of Standards

Research Paper RP1907
Volume 41, August 1948

Part of the Journal of Research of the National Bureau of Standards

Strain Tester for Rubber[1]

By William L. Holt, Ellis O. Knox, and Frank L. Roth

A tester for measuring the strain of rubber vulcanizates when subjected to a predetermined stress is described. The operation of the tester and a description of the apparatus for cutting and measuring the test specimens are presented. With this equipment, routine determinations of a point on the stress-strain curve can be made with greater accuracy and precision than has hitherto been possible with the usual stress-strain equipment. This strain test also requires less labor than the customary stress tests.

I. Introduction

The strain tester described herein was designed to measure the strain at a definite time after the application of a predetermined stress. In the usual testing procedure, stress is measured at a specified strain during the extension of the specimen at a relatively rapid rate. Interest in the development of the strain tester resulted from previous investigations [2], which showed that the replicate measurements of strain at a predetermined stress have a variance of approximately one-tenth the variance of the usual measurements of stress at a specified strain.

The apparatus was designed to permit routine measurements of strain at any selected stress below rupture to be made with the degree of precision found by Roth in the earlier investigation. In designing the strain tester, accuracy of measurement, as well as precision, was considered. The design features that are responsible for the improved precision and accuracy of measurements in the strain test are (1) Observation of bench marks when they are essentially at rest, (2) use of freely suspended weights to attain the desired stresses without friction effects, and (3) increase in distance between bench marks of from two to four times that possible with usual dumbbell-shaped specimens.

This test is not intended to measure stress-strain properties near or at rupture. For control testing, however, and for many research tests, a knowledge of the properties below the region of failure is sufficient. The improved precision of the strain test warrants a separate determination of the properties at failure in those cases where they are necessary.

II. Details of Construction

Three accessory instruments are required to prepare specimens for measurements in the strain tester. These are (1) a die to cut specimens from a sheet of rubber, (2) a device for placing bench marks on the specimen, and (3) a device for determining the average thickness of the specimen. The construction of each of these instruments and of the strain tester is described in turn.

1. Die for Cutting Specimens

The construction of the die used to cut specimens from a sheet of rubber is shown in figure 1. The cutting blades of the die consist of six strips of razor blade steel sharpened on one edge. Each strip is 6 in. long, ¾ in. wide, and 0.009 in. thick.[3] They are clamped between metal spacers 6 in. long, ⅝ in. wide, and 0.245 in. thick, so that the cutting edges project ⅛ in. The die is used in an arbor press or "clicking" machine.

With this device, five strips 0.254 in. in width are cut simultaneously. This width was chosen for its convenience in determining the load to be applied to the specimen to obtain the desired

[1] The tester was designed and constructed at the request of the Subcommittee on Test Methods of the Committee on Specifications for Synthetic Rubbers and was financed in part by funds transferred from the Office of Rubber Reserve, Reconstruction Finance Corp.

[2] Frank L. Roth and Robert D. Stiehler, J. Research NBS **41**, 87 (1948) RP1906.

[3] These blades were supplied through the courtesy of the Gillette Safety Razor Co., 125 Granite Street, Boston, Mass.

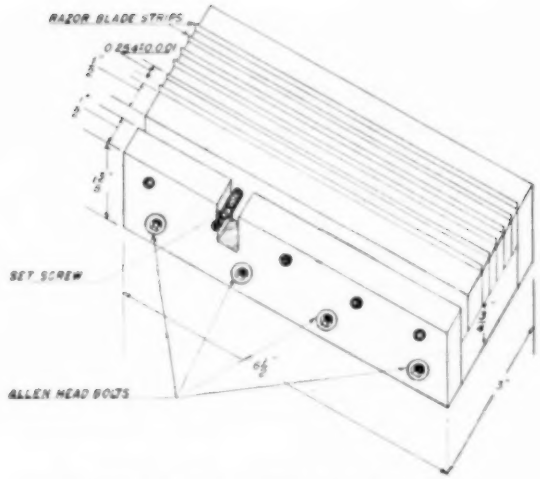

FIGURE 1. *Die for cutting five test specimens.*

stress based on the cross sectional area of the unstrained specimen. The width is one one-hundredth the numerical factor by which the thickness in millimeters must be divided in order to convert it to inches. Consequently the load, expressed in pounds, is equal to the numerical value of the thickness of the specimen measured in millimeters, multiplied by the numerical value of the desired stress expressed in "hundredweights" per square inch. For example, to obtain a stress of 400 lb/in.^{2}, the load to be applied to a specimen 2.03 mm in thickness and 0.254 in. in width would be $2.03 \times 400/100 = 8.12$ lb.

2. Bench Marker

Bench marks are placed 10 cm apart upon each specimen. This distance makes it convenient to measure elongation (strain) directly by means of a scale graduated in millimeters. The device used is essentially a metal bar with razor blades fastened on each end, as shown in figure 2. In order to prevent cutting of the specimen by the blade the edges are ground, as shown in the detailed section. With this marker, distinct lines not over 0.010 in. wide are easily made.

3. Thickness Gage

The thickness of specimens is measured with the gage shown in figure 3. This gage has a dial indicator graduated in hundredths of a millimeter. One revolution of the pointer corresponds to 1.0 mm, and the total range of the indicator is 2.5 mm. The indicator is mounted above an especially constructed base shown in figure 4. An important feature of this base is the pressure-bar arrangement. This metal bar is 10 cm long and is pressed upon the surface of the specimen with a force of 4 lb by means of a spring. The bar is attached to a ball joint, which possesses sufficient freedom of movement to average the thickness of wedge-shaped specimens. The dial indicator is adjusted to read zero for specimens 1.50 mm in thickness, as specimens of this thickness require a load corresponding to the basic weight of the weight assembly described in section II, 4. Additional thickness beyond 1.50 mm is read in hundredths of a millimeter.

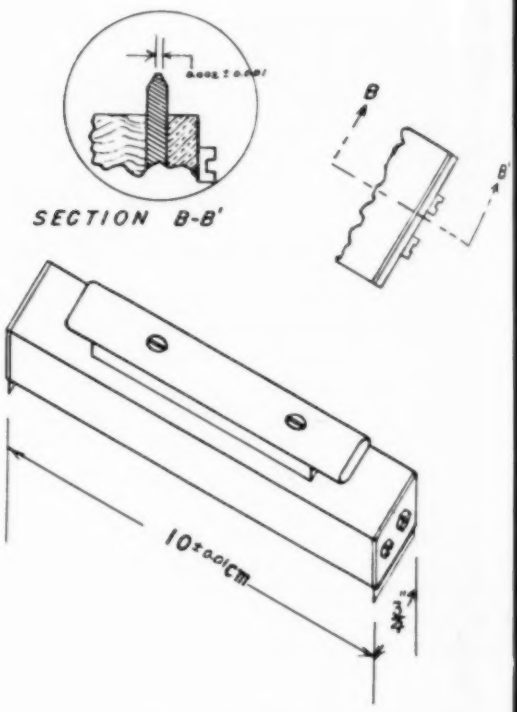

FIGURE 2. *Bench marker.*

4. Strain Tester

The strain tester is designed to apply automatically the selected weights to a specimen to produce the desired stress, to provide means for measuring the elongation accurately and easily, to assure that measurement of elongation is made

FIGURE 3. *Gage for obtaining average thickness of the specimen.*

at the proper time after application of the load, and to return automatically the specimen and tester to their starting positions after the measurement has been made. The design of the tester embodies mechanical and electrical features that are discussed separately.

(a) Mechanical Assembly

The strain tester is shown in figures 5 and 6. Essentially, the tester consists of two parts. The upper part comprises a vertical track, the driving mechanism for extending and suspending the specimen and the mechanism for measuring the elongation. The lower part consists of the weight assembly and mechanism for placing the proper load on the specimen.

The vertical track is constructed from five strips of cold-rolled steel 48 in. long. The basic steel strip is 2 in. in width and $\frac{3}{4}$ in. in thickness. To this strip, two strips, $\frac{5}{8}$ in. by $\frac{1}{8}$ in., and two strips,

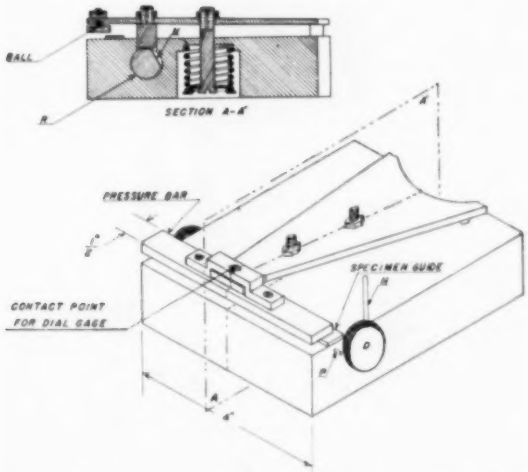

FIGURE 4. *Construction of the averaging mechanism of the thickness gage.*

The apparatus is shown with the pressure bar raised. The specimen is placed on the base under the bar and against the guide. When the knurled disk *D* is turned so that the handle *H* rests against the pin *P*, the notch *N* in the rod *R* is at the top, allowing the spring to pull the pressure bar down against the top side of the specimen.

FIGURE 5. *General view of rubber strain tester.*

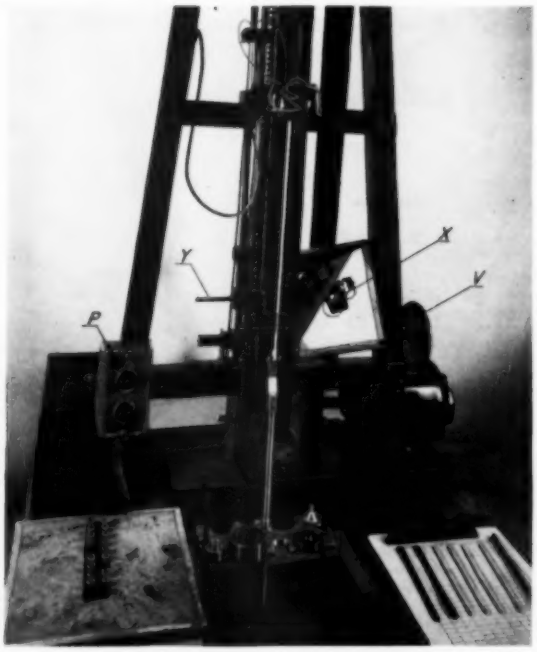

FIGURE 6. *Rubber strain tester from the perspective of the operator.*

P, Pilot in series with motor of time-cycle controller; *V*, hand wheel for alining upper positioner with upper bench mark; *X*, prism and specimen as seen in plane mirror; *Y*, handle for rotating positioners to the specimen and alining the lower positioner with the lower bench mark.

¾ in. by ⅛ in., are fastened to form a T-slot ¾ in. in width at the base and ½ in. at the throat. This slot serves as a guide for the grip, which stretches and supports the upper end of the specimen. The specimen grip also connects the two ends of a roller chain (Boston No. 35), which passes over sprockets at each end of the vertical track, and thence to a ⅛- or ¼-hp-ratio motor. The motor raises and lowers the specimen grip in the T-slot at a speed of 200 in./min. Two limit switches located fore and aft of the sprocket at the upper end of the track prevent the specimen grip from reaching the sprockets and damaging the tester.

A steel tape graduated in millimeters is used to measure the elongation. As the bench marks are placed on the specimen 10 cm apart, each millimeter of extension corresponds to an elongation of 1 percent. Two transparent plastic positioners with hair lines are used to locate the position of the bench marks on the millimeter tape. The end of the tape is fixed to the upper positioner, and the zero point on the tape is adjusted exactly 10 cm below the hair line on this positioner. Thus, when the positioners are placed on the bench marks, the elongation is read from the tape at the lower positioner directly in percentage. In order to permit the operator when seated at the tester to locate the hair line of the upper positioner on the upper bench mark arrangement, *X* in figure 6, is made to observe the hair line and the bench mark by means of a fixed plane mirror and a reflecting prism attached to the upper positioner. Lights attached to the prism illuminate the upper bench mark during the time an observation is to be made. The upper positioner, prism, and lights are moved up or down by means of a ladder chain and sprocket assembly. The assembly is driven by means of a hand wheel, *V* in figure 6, within easy reach of the seated operator. The lower positioner slides freely on a vertical square bar, which serves as a guide for both positioners and rotates them away from the specimen. A handle, *Y* in figure 6, on the lower positioner enables the operator to slide it and to rotate both positioners to the specimen in order to make observations without parallax.

The lower part of the apparatus, consisting of the weight-assembly and weight-loading mechanism, is centered around a plumb line from the upper grip. The weight assembly passes freely through a rectangular hole 4 in. by 8 in. cut in the table top that supports the upper and lower parts of the apparatus. The assembly consists of an aluminum rod (approximately 32 in. long), on which is fastened two weight holders, one at the lower end for the fixed weight and the other about 24 in. above for the additive weights. At the upper end of the rod is fastened the grip for the lower end of the specimen. The holder for the additive weights is constructed as shown in figure 7. Guide rods pass through the holes in the ends of the weight holder, and the additive weights are placed in the semicircular notches on the sides.

The combination of the weight assembly and weight loading mechanism is shown in figure 8. The eight additive weights are supported on arms that are normally inclined at an angle of about 8° from the vertical. When additive weights are needed, the arms supporting the selected weights are moved to a vertical position. The additive weights are then lifted from the ends of the arms by the upward movement of the weight holder at

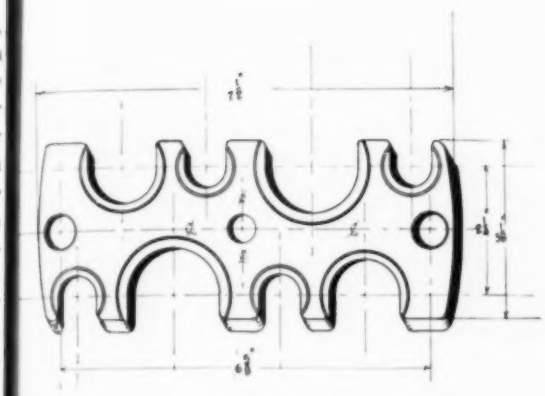

FIGURE 7. *Holder for additive weights.*

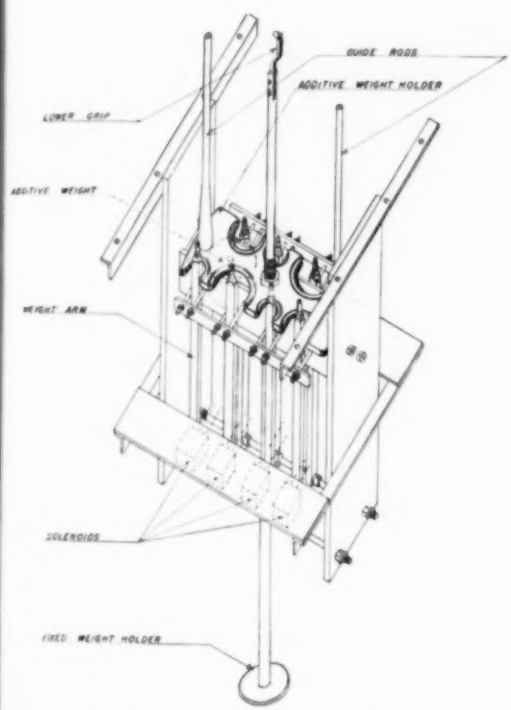

FIGURE 8. *Weight assembly and loading mechanism.*

The weight arms are shown in their vertical position. In operation there are never more than four arms in this position at one time. One of the additive weights is shown by dashed lines in position on the weight arm.

the time the specimen is elongated. The weights are returned to the arms during the retraction of the specimen.

The arms are moved to the vertical position by means of solenoids and returned to their normal position by the action of a coil spring after the circuit to the solenoid is broken. The mechanism for actuating the solenoids and the mechanism for indicating when the weight assembly is suspended freely are discussed in the section on the electrical circuit.

(b) Electrical Circuit

The mechanical operation of the tester is controlled by the electrical circuit shown in figure 9. The part of the circuit that controls the weight loading mechanism utilizes eight solenoids, *S*, (Guardian No. 12 AC) for moving the eight weight arms into their vertical positions and 18 normally open switches for selecting the proper solenoids to apply the desired load. The keys operating the switches are locked by means of an additional solenoid, *K*, while the weight assembly is suspended. During the time the switches are free to be changed for selection of the desired load, this part of the circuit is not excited.

Four of the solenoids are controlled by one decade of switches and the other four by a second decade. Four switches of each decade are single-pole, single-throw and control individual solenoids. The other five switches of each decade are either double-pole, single-throw, or split-contact single-throw (Micro-Switches BZ-3YLT were used) and control appropriate combinations of two solenoids. Thus with four weights, the selection of any additive load in a decade is obtained by closing one of nine switches. One decade can adjust the load to correspond to specimen thicknesses from 0.1 to 0.9 mm in steps of tenth-millimeters and the other decade from 0.01 to 0.09 mm in hundredth-millimeter steps. Thus the two decades can adjust the load for specimen thicknesses ranging from zero to 0.99 mm in hundredth-millimeter steps. To close these switches it is convenient to use two decades of keys and the keyboard mechanism from a Friden calculator. This assembly is arranged so that the closing of one switch in a decade opens the others. The keyboard mechanism also provides a convenient device for locking the keys while the tester is in operation.

The electrical circuit, which controls the weight loading mechanism, is excited when the main relay (4PST, 110 v AC, 6 amp) is closed. This relay is closed by pressing the start button at the start-stop station. Once closed the relay remains

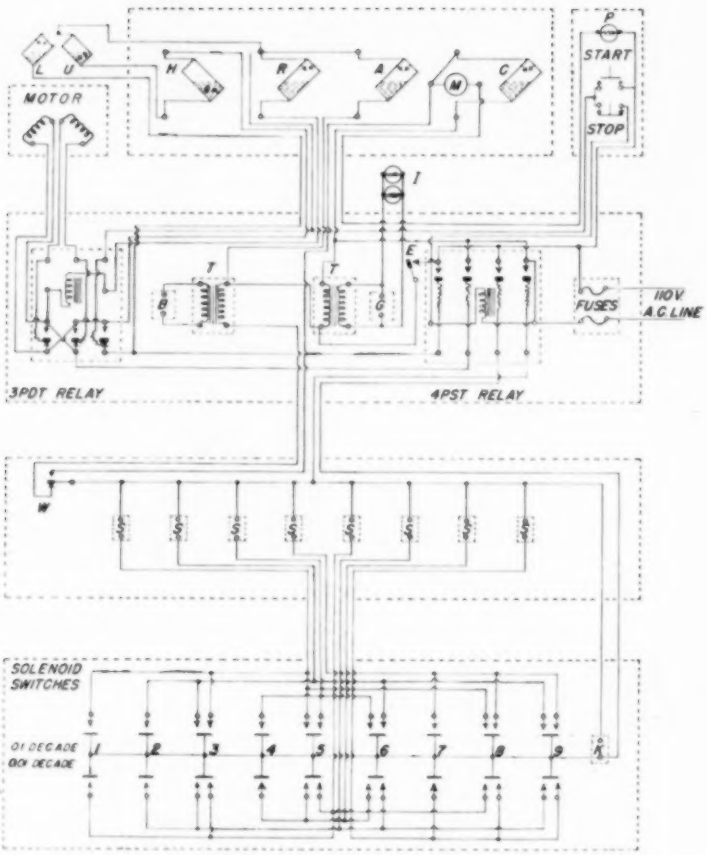

FIGURE 9. *Electrical circuit for the rubber strain tester.*

The positions of the switches and relays shown in the circuit are for the tester at rest. *A*, Switch for actuating single stroke bell or gong, *G*, and lamps, *I*; *B*, bell or buzzer; *C*, switch for stopping motor, *M*; *E*, switch for manual operation of lamps, *I*, when the tester is not in operation; *G*, single stroke bell or gong; *H*, switch for limiting the lift of the weight assembly after switch, *W*, is released; *I*, lamps for illuminating upper bench mark during the observation period; *K*, solenoid for locking the keyboard; *L*, switch for opening four PST relay when upper grip returns to starting position; *M*, time-cycle controller motor; *P*, pilot light for motor, *M*; *R*, switch operating 3 PDT relay to return upper specimen grip to rest position at end of test; *S*, solenoids for moving weight arms to their vertical position; *T*, bell transformers; *U*, switch for limiting upward travel of the upper grip; *W*, SPDT switch for starting motor, *M*, and when weight assembly is not freely suspended at time of measurement for ringing bell, *B*.

closed until the circuit to its exciting coil is broken either by the action of the limit switch, *L*, which opens when the upper grip returns to its starting position or by the pressing of the stop button by the operator. Besides exciting the circuit controlling the weight-loading mechanism, this relay starts the motor that lifts the upper grip and stretches the specimen.

When the weight assembly is freely suspended, a single-pole, double-throw precision snap switch, *W*, mounted on the weight loading mechanism starts the motor, *M*, on a time-cycle controller. The function of the other position of this double-throw switch is to actuate a signal that is described with the signaling devices.

The sequence of operations after the weight assembly is freely suspended is controlled by a time-cycle controller (Electric Switch Corp. model 602). This controller consists of four mercury switches that are opened and closed by the action of cams rotated by a synchronous clock motor, *M*. The functions of the mercury switches are as follows:

The height switch, *H*, limits the height to which the weight assembly may be raised (approximately 8 in.).

The signal switch, A, operates an alarm, which indicates the time the measurement of elongation is to be made.

The reversing switch, R, actuates a 3-pole double-throw relay, which reverses the motor at the end of a test, permitting the specimen to retract and the weight assembly to come to rest.

The cycle switch, C, stops the time-cycle controller at the end of the cycle. The four switches open and close at the following points in the revolution of the cams:

Switch	Opens	Closes
	Degrees	*Degrees*
Height	9	355
Signal	284	248
Reversing	355	293
Cycle	360	5

A rotation of 360° requires 80 sec. In order to indicate when the controller is in operation, a pilot lamp, P (6 v, 0.15 amp) is connected in series with the motor.

The signal switch of the controller closes the primary circuit of an 8-v transformer, T. Connected to the secondary of the transformer is a single-stroke bell or gong, G, which serves to indicate when the elongation of the specimen is to be observed. The lamps, I, which illuminate the upper bench mark, are connected to the same circuit. If the weight assembly is not freely suspended at the time the observation is to be made, the double-throw switch, W, attached to the weight-loading mechanism, connects a second transformer into the signal-switch circuit. Connected to the secondary of this transformer is a vibrating bell or buzzer, B. This signal warns the operator that the observation is in error.

One of the limit switches, U, on the vertical track is used to protect the tester in case a specimen has an elongation greater than the limit of the tester or breaks before the motor of the time-cycle controller starts. The other limit switch, L, breaks the circuit to the coil of the main relay at the end of each test when the upper grip returns to its starting position. This action breaks all of the circuits except the one to the motor of the time-cycle controller.

A switch, E, is provided for manual operation of the lamps, I, when illumination is desired for purposes other than the normal operation of the tester. For example, illumination is required when the zero position of the steel tape is being initially adjusted relative to the hair line on the upper positioners. This adjustment is conveniently accomplished by use of a separate millimeter scale held in the position of the specimen.

III. Method of Operation

Three steps are involved in the strain test procedure: namely, (1) the preparation of the test specimen from a rubber vulcanizate, (2) the measurement of the cross-sectional area of the specimen to determine the load to be applied, and (3) the measurement of the elongation of the specimen at a definite time after the load is applied.

1. Preparation of Specimen

From the usual test sheet of rubber vulcanizate, 6 in. square and about 0.075 in. in thickness, five specimens are cut by means of the die described in section II, 1. Using the marker described in section II, 2, bench marks 10 cm apart are placed upon each specimen. The marking compound should be of a contrasting color to that of the specimen; e. g., if the specimen is dark in color, red or white marks are convenient.

2. Determination of Load

If the die is properly constructed and in good condition, the width of each specimen will be 0.254 in. (6.45 mm) to within 0.001 in. Then only a measurement of the average thickness of each specimen by means of the gage described in section II, 3 is required to determine the cross-sectional area.

For measurements at a stress of 100 lb/in.^{2}, changes in thickness will require changes in load, in pounds, which are numerically equal to the thickness change in millimeters. Consequently, by setting the zero position of the dial gage to the numerical value of the fixed weight, one needs merely to make the additive weights equal to the dial reading obtained with the different specimens. To obtain the same convenient arrangement at 200 lb/in.^{2}, the fixed load and each additive weight must be doubled. This is accomplished by the substitution of a different weight assembly. Analogously, weight assemblies corresponding to any other desired stress can be used, if desired.

734450—48——2

The tester in our laboratory is equipped with three sets of weights for applying stresses of 100, 200, and 400 lb/in.^{2}. Alternatively, the fixed weight can be manually adjusted for each stress, and a table used to obtain the key board settings corresponding to different dial-gage readings.

3. Measurement of Strain

The specimen is placed in the grips of the tester by the operator with the bench marks facing him. After depressing the proper keys controlling the additive weights, he presses the start button. This action engages the appropriate additive weights and stretches the specimen. The pilot light indicates when the weights become freely suspended, and the time cycle begins. Fifty-five seconds later when the signal sounds, the operator holds the positioners against the specimen with his left hand and superimposes the hair line of the upper positioner on the upper bench mark by turning the hand wheel with his right hand. After this positioner is adjusted, he superimposes the hair line of the lower positioner on the lower bench mark by sliding the positioner with his left hand. Approximately 8 sec are allowed for these two operations. The operator observes the elongation in percentage directly from the position of the hair line of the lower positioner on the millimeter tape. There is ample time to observe and record the elongation while the upper grip and weight assembly return automatically to their starting position. A new specimen can be inserted and the keys changed while the controller completes its cycle. Thus each specimen requires about 1½ min of machine operation. The operator, however, has about 1 min of this time free during which he could either operate a second machine or prepare specimens for measurement.

IV. Comments on Performance

The strain tester constructed in this laboratory has operated very satisfactorily for more than a year. In the usual stress-strain measurements, the errors in testing have been found to be of the same order of magnitude as those arising in the preparation of the vulcanizate. On the other hand, it has been found that the errors of testing with the strain tester are negligible in comparison to those arising in the preparation of the vulcanizate. This improvement in precision and accuracy of testing has been useful in both control and research testing. Data showing the improvement of precision have been omitted from this paper, as they are a part of a separate paper (see footnote 2).

An advantage of this test, in addition to the improved testing, is the reduction in man-hour requirements. This reduction is due in large part to obtaining the data in tabular form at the time of test. At the same time, the ease and convenience of the test has improved the morale of the testing personnel. The operation of the tester from a sitting position, the ease of changing weights, and the elimination of following two moving bench marks simultaneously have been the prime factors in this respect.

Washington, October 24, 1947.

U. S. Department of Commerce
National Bureau of Standards

Research Paper RP1908
Volume 41, August 1948

Part of the Journal of Research of the National Bureau of Standards

Barium Aluminate Hydrates

By Elmer T. Carlson and Lansing S. Wells

Methods of preparation, optical properties, and X-ray diffraction data are reported for six barium aluminate hydrates. Three of these were obtained successively by precipitation from supersaturated barium aluminate solutions at 30° C. The first, designated by the empirical formula $1.1BaO.Al_2O_3.6H_2O$, is metastable with respect to the second, $BaO.Al_2O_3.7H_2O$, which in turn is metastable with respect to $BaO.Al_2O_3.4H_2O$. Two lower hydrates, $BaO.Al_2O_3.2H_2O$ and $BaO.Al_2O_3.H_2O$, were prepared hydrothermally. $2BaO.Al_2O_3.5H_2O$ was obtained from boiling barium aluminate solutions.

I. Introduction

For several years, the calcium aluminates and their hydration products have been studied by a number of investigators in various countries. The widespread interest in these compounds resulted chiefly from their importance in relation to hydraulic cements. In spite of the large amount of work that has been done, it cannot be said that the relationships of the various hydrated calcium aluminates are fully established. Among the difficulties connected with the problem are the low solubilities of the hydrates, extreme fineness of precipitates, slowness of approach to equilibrium, and persistence of metastable phases.

In view of these difficulties it was considered possible that a study of the aluminates of barium might disclose a series of analogous compounds from which might be drawn some inferences as to the nature of the calcium aluminates. It was known that the solubilities of the barium compounds were much higher, and it seemed not unlikely that the other difficulties might also be minimized. During the course of this investigation it soon became apparent that the hydrated aluminates of barium were in no way analogous to those of calcium; nevertheless, the study was continued because of the importance of the barium compounds themselves. The barium aluminates have found application in water purification, and it has been proposed that barium compounds might replace those of calcium in cements for special purposes.

The hydrated barium aluminates have been studied by several investigators, notably E. Beckmann [1] [1] and G. Malquori [2]. The latter gives a solubility diagram for the system BaO-Al_2O_3-H_2O at 20° C, and indicates that the compounds $BaO.Al_2O_3.6H_2O$ and $2BaO.Al_2O_3.5H_2O$ occur as primary phases at this temperature. Beckmann reports a compound $3BaO.Al_2O_3.XH_2O$, in addition to the other two, and the $BaO:Al_2O_3$ ratio of the 1:1:6 compound is said to be variable. Neither optical nor X-ray data were found in the literature for any of the barium aluminate hydrates.

II. Methods

The general method used in the present investigation was similar to that employed in the study of the calcium aluminates [3]. Supersaturated solutions of alumina in barium hydroxide were prepared and allowed to stand, with occasional shaking, at 30° C. The precipitates were observed under the microscope from time to time, and changes in concentration of the solutions were determined by analysis. Various methods were used for preparation of the supersaturated solutions. The most satisfactory was the treatment of anhydrous barium aluminate with sufficient water to cause practically complete hydrolysis and precipitation of hydrated alumina, followed by boiling with barium hydroxide solution to dissolve the alumina. The solution was then filtered promptly while still hot. The anhydrous aluminate used for the purpose was either $BaO.Al_2O_3$

[1] Figures in brackets indicate the literature references at the end of this paper.

or $3BaO.Al_2O_3$ or a mixture of the two, as desired, prepared by heating a mixture of barium carbonate and gibbsite ($Al_2O_3.3H_2O$), in the desired proportions, at about 1,300° C. The products usually contained a little insoluble material, probably corundum, but this did not affect their usefulness.

Other methods of preparation of the solutions included treatment of gibbsite with boiling barium hydroxide solution, similar treatment of freshly precipitated alumina, and the interaction of barium hydroxide and aluminum sulfate in solution. Reagent grade chemicals were used except in the case of the gibbsite, which was a commercial product containing 0.30 percent of soda. Solutions were handled as rapidly as possible and flasks were tightly stoppered, but no other precautions were taken to avoid the action of carbon dioxide. Carbonation proceeded rapidly whenever the strongly basic solutions were exposed to the air, but the amount formed appeared insufficient to seriously affect the analysis of the solid phases.

The general procedure outlined above was designed to yield data from which a diagram of equilibrium at 30° C could be drawn. It has been found, however, that equilibrium in this system is not attained even after several months, and further work will be required before the equilibrium diagram can be established. The following generalizations may be made, however: (1) From solutions low in BaO, hydrated alumina is precipitated as the primary phase; (2) From solutions sufficiently high in BaO, hydrated barium hydroxide, $Ba(OH)_2.8H_2O$, is precipitated as the primary phase. The limiting concentration for this phase, with no alumina present, is about 50 g BaO per liter and increases somewhat with increasing alumina concentration; (3) From solutions intermediate in BaO, three hydrated barium aluminates are precipitated successively, if the alumina concentration is about 15 g/liter or higher. From solutions lower in alumina, the second member of the series is formed directly. These three hydrates all have $BaO:Al_2O_3$ ratios close to 1:1. The fact that they are sometimes formed in contact with solid $Ba(OH)_2.8H_2O$ suggests that no more basic barium aluminate hydrate exists as a stable phase at 30° C.

In addition to the hydrates precipitated at 30° C, one compound was obtained from boiling solutions, as described below, and two were prepared by hydrothermal synthesis. In the latter procedure, the material to be treated was placed in a 3-ml platinum thimble, which was capped loosely and then placed in a bomb-type autoclave containing sufficient water to saturate the enclosed air at the temperatures used. The thimble was supported above the water level by means of a coiled wire in order to minimize the loss of dissolved substances. The autoclave was heated in a specially designed furnace [4] or, at the lower temperatures, in an ordinary laboratory oven.

In the chemical analysis of the products synthesized, the percentage of water was calculated from the ignition loss at 900° C, with no correction for carbon dioxide. Microscopic examination indicated that the amount of carbonation was negligible. Alumina and barium oxide were determined by the usual gravimetric methods.

The refractive indices reported are for sodium vapor light. X-ray powder patterns were made on an X-ray spectrometer with a Geiger-counter and automatic recorder, using copper Kα radiation.

III. Results

The various hydrates synthesized are described below:

$1.1BaO.Al_2O_3.6H_2O$—The compound that is precipitated first from highly supersaturated barium aluminate solutions, as described above, may be designated by this empirical formula. Analyses of six preparations indicated $BaO:Al_2O_3$ ratios of 1.14, 1.12, 1.12, 1.14, 1.12, and 1.11, respectively. The ratios of H_2O to Al_2O_3 in the same preparations were 6.1, 6.2, 6.0, 6.1, 6.0, and 5.9. The slight variation in $BaO:Al_2O_3$ ratio bore no observable relation to the concentration of the solution, and may be ascribed to experimental error. The departure from a 1:1 ratio is in agreement with the findings of E. Martin [5], who claims to have isolated a compound, $11BaO.10Al_2O_3.xH_2O$. Beckman [1] and Malquori [2] also reported ratios greater than unity. The actual stoichiometric ratio remains in doubt. Thermal analysis indicates that most of the water is liberated below 160° C.

This compound was precipitated from solutions of proper concentration, but formed rather slowly. From one solution in which the concentration of Al_2O_3 exceeded 17 g/liter, precipitation commenced almost at once, but in more dilute solutions pre-

cipitation was first observed after several days. Constant agitation appeared to have little if any effect at first, but probably accelerated precipitation after it had once started. The compound exists in the form of needle-shaped crystals (fig. 1)

FIGURE 1. $1.1BaO.Al_2O_3.6H_2O$

Magnification, ×120.

and imparts to the reaction mixtures the "silky" appearance characteristic of crystals of this shape. Optically it is slightly birefringent, biaxial positive; $\alpha=1.535$, $\gamma=1.540$; the elongation is positive. X-ray diffraction data are given in table 1.

Precipitation of this compound continues slowly for approximately a week, after which there appears a new crystal phase, described in the following paragraph. The needle crystals simultaneously disappear, and the excess BaO goes into solution. The transformation requires several days for completion, the time being somewhat variable.

$BaO.Al_2O_3.7H_2O$—This compound is produced by transformation of the 1.1:1:6 hydrate described above, and is also precipitated as the primary phase

TABLE 1. *Interplanar spacings and relative intensities of X-ray diffraction bands for the barium aluminate hydrates*

$1.1BaO.Al_2O_3.6H_2O$		$BaO.Al_2O_3.6H_2O$		$BaO.Al_2O_3.4H_2O$	
d	Intensity	*d*	Intensity	*d*	Intensity
A		*A*		*A*	
10.7	S	7.6	VS	5.46	W
8.5	VW	4.28	M	4.91	VS
6.0	VW	3.74	S	4.47	VW
5.39	S	3.61	W	3.61	VW
4.97	VW	3.44	VW	3.22	VS
3.99	M	3.28	M	2.88	W
3.61	VS	2.81	VW	2.68	M
3.39	M	2.71	W	2.47	VS
3.11	M	2.50	S	2.40	VW
2.82	M	2.41	W	2.28	VW
2.72	W	2.28	VW	2.15	S
2.61	M	2.22	VW	2.10	VW
2.48	M	2.05	M	1.99	W
2.25	S	1.89	VW	1.92	W
2.16	W	1.71	W	1.82	W
1.87	W	1.44	VW	1.69	W
1.81	M	.....	.....	1.64	VW
1.70	M	.....	.....	1.62	W
1.55	VW	.....	.....	.....	.....
1.40	W	.....	.....	.....	.....

$BaO.Al_2O_3.2H_2O$		$BaO.Al_2O_3.H_2O$			$2BaO.Al_2O_3.5H_2O$	
d	Intensity	*hkl*	*d*	Intensity	*d*	Intensity
A			*A*		*A*	
5.81	W	110	4.85	S	6.31	VS
4.56	VW	111	3.94	W	3.98	M
3.86	W	200	3.42	VS	3.76	M
3.50	M	210	3.06	W	3.25	M
3.37	VW	211	2.79	VS	3.03	VS
3.20	S	220	2.42	M	2.89	W
2.81	W	300	2.28	S	2.71	M
2.56	VW	310	2.16	M	2.60	S
2.33	VW	222	1.97	W	2.51	M
2.26	VW	320	1.90	VW	2.37	VS
2.09	VW	400	1.71	W	2.24	W
1.98	W	410	1.66	VW	2.09	VS
1.91	VW	331	1.57	M	2.03	W
1.75	VW	332	1.45	W	1.81	VW
		500	1.36	M	1.76	M
		511	1.31	W	1.66	S
		Unit cell: $a=6.81A$			1.61	VW
					1.49	VW
					1.43	M

from solutions of somewhat lower alumina content. Three analyses of one preparation gave an average molar ratio of $0.97\ BaO:1Al_2O_3:6.75H_2O$. In another preparation, the ratio of BaO to Al_2O_3 was the same, but in two separate samples filtered off at different times, the ratio of H_2O to Al_2O_3 was 6.80 in one case and 6.65 in the other. These samples had been washed with alcohol and ether, and it is believed that part of the water of

crystallization is so loosely bound that it is removed by such treatment. Thermal analysis indicates that most of the water is driven off below 120° C. Microscopic examination revealed the presence of a small amount of impurity believed to be hydrated alumina. This would explain the slight excess of Al_2O_3 over BaO. The compound appears in the form of exceedingly thin flakes, approximately rectangular in outline (fig. 2). The crystals obtained were too small to permit a determination of optical character and sign. The indices of refraction are $\alpha=1.538$, $\gamma=1.556$. The elongation is positive. X-ray data are given in table 1.

FIGURE 2. $BaO.Al_2O_3.7H_2O$.

Magnification, ×120.

On standing for several months, the reaction mixtures continued to precipitate this compound slowly until the concentration of Al_2O_3 was of the order of 8 g/liter.

$BaO.Al_2O_3.4H_2O$—This compound was first observed in one of the reaction mixtures described above. It had stood at 30° C for 4 months, and apparently a state of equilibrium had been reached between the solution and the precipitate of $BaO.Al_2O_3.7H_2O$. The new phase occurred as prismatic crystals, averaging 2 mm in length (fig 3). Because of their size, they were readily separated from the hexahydrate for examination and analysis. The $BaO:Al_2O_3:H_2O$ ratio was calculated to be 0.97:1:3.90, from which it was assumed that the formula was $BaO.Al_2O_3.4H_2O$. Later the same phase, in considerably different crystalline habit (fig. 4) appeared in several other reaction mixtures. X-ray diffraction and optical data showed it to be identical with the prismatic form. Analysis of two preparations gave the following ratios: $0.98BaO:1Al_2O_3:3.94H_2O$ and $0.99BaO:1Al_2O_3:3.94H_2O$. Refractive indices of the tetrahydrate are $\alpha=1.625, \beta=1.628, \gamma=1.650$. It is biaxial positive. The crystals of prismatic habit are usually twinned. X-ray data are given in table 1.

FIGURE 3. $BaO.Al_2O_3.4H_2O$, *prismatic form.*

Reflected light, magnification, ×5.

The three compounds described above were the only barium aluminate hydrates formed at 30° C in any of the reaction mixtures studied. It is obvious that the first two are metastable with respect to the third, at least over a certain range

FIGURE 4. $BaO.Al_2O_3.4H_2O$, *rhombohedral form.*
Magnification, ×250.

of concentration not yet defined. It appears certain, also, that the heptahydrate is less stable at higher temperatures. This is supported by the following experiment. A sample of $BaO.Al_2O_3.7H_2O$ in contact with barium aluminate solution was withdrawn from a reaction mixture that had stood for 4 months at room temperature without apparent change. The sample was held at 60° C for 7 days, at the end of which time it was found to have been changed completely to $BaO.Al_2O_3.4H_2O$.

$BaO.Al_2O_3.2H_2O$—By hydrothermal treatment of the heptahydrate preparation described in the preceding paragraph, a new crystalline compound was obtained. The molar ratio indicated by analysis was $0.99BaO:1Al_2O_3:2.00H_2O$; it may thus be considered a dihydrate of $BaO.Al_2O_3$. The same compound, with minor variations in crystal habit, was obtained from samples held at various temperatures ranging from 124° to 215° C, for periods of 2 to 4 days. (See table 2.) At lower temperatures the tetrahydrate was formed (see above), while at higher temperatures the monohydrate described below was produced.

TABLE 2. *Hydrothermal treatment of* $BaO.Al_2O_3.7H_2O$ *in contact with barium aluminate solution*

Temperature	Duration of treatment	Product
°C	*Days*	
60	7	$BaO.Al_2O_3.4H_2O$
102	5	Do.
124	4	$BaO.Al_2O_3.2H_2O$
156	4	Do.
175	3	Do.
195	5	Do.
215	2	Do.
222	2	$BaO.Al_2O_3.2H_2O$ and $BaO.Al_2O_3.H_2O$
228	2	$BaO.Al_2O_3.H_2O$
248	3	Do.
295	6	Do.

The dihydrate occurs as flat plates, usually grown together in foliated aggregates. A fragment of one of these aggregates is shown in figure 5, photographed under crossed nicols. The crystals are biaxial positive, with very low birefringence, and parallel extinction. The indices of refraction are: $\alpha = 1.610$; $\gamma = 1.613$.

FIGURE 5. $BaO.Al_2O_3.2H_2O$.
Crossed nicols, magnification, x100.

$BaO.Al_2O_3.H_2O$—A crystalline compound (fig .6) approximating this formula was first obtained by hydrothermal treatment of anhydrous $BaO.Al_2O_3$ for 7 days at 275° C. The same compound was later prepared in the same manner at temperatures ranging from 260° to 350° C, also by hydrothermal treatment of gibbsite in contact with $Ba(OH)_2$ solution. In all cases there was a considerable amount of contamination by other substances, often unidentified. A better product was obtained by hydrothermal treatment of $BaO.Al_2O_3.5H_2O$ in contact with barium aluminate solution, at temperatures ranging from 222° to 295° C (table 2). Similar treatment of $2BaO.Al_2O_3.5H_2O$ (described below) at 280° C yielded the same compound. In this case the excess BaO remained in solution in the supernatant liquid. Analyses of three preparations gave the following molar ratios: $BaO:Al_2O_3:H_2O = 1.14:1:1.08$; 1.16:1:1.01; 1.12:1:0.99. The relatively good agreement suggests that the departure from a 1:1 ratio may not be due to impurities, as was first believed. It may indicate, instead, that the simple formula given is incorrect, or that solid solution may occur. In the absence of further evidence, however, the formula $BaO.Al_2O_3.H_2O$ will be used for convenience.

This compound belongs to the cubic system and has an index of 1.644. X-ray data are given in table 1.

$2BaO.Al_2O_3.5H_2O$—This compound is precipitated at boiling temperature from barium aluminate solutions over a wide range of concentration. It may be prepared readily by boiling a mixture of gibbsite and barium hydroxide solution, the concentration of the latter being of the order of 50 g BaO per liter. The hydrate forms a caked mass around the particles of gibbsite. If the solution is then filtered and the filtrate concentrated by boiling, a reasonably pure preparation of $2BaO.Al_2O_3.5H_2O$ will be obtained. The product is coarse grained and relatively resistant to attack by water and dilute HCl (fig. 7). Analyses of two such preparations gave the molar ratios

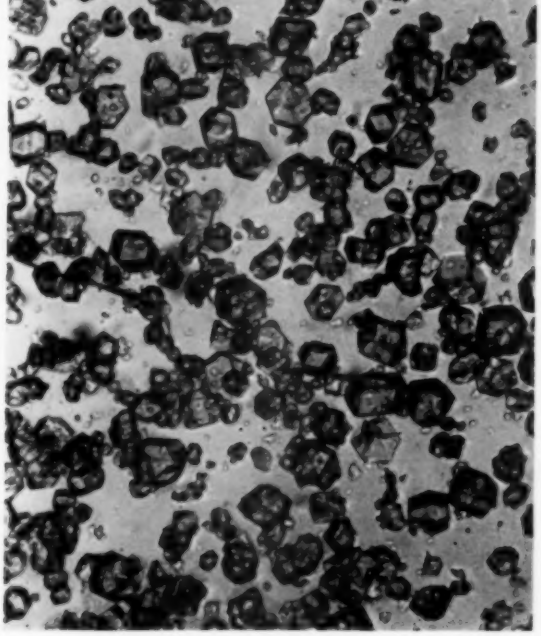

FIGURE 6. $BaO.Al_2O_3.H_2O$.

Magnification, ×120.

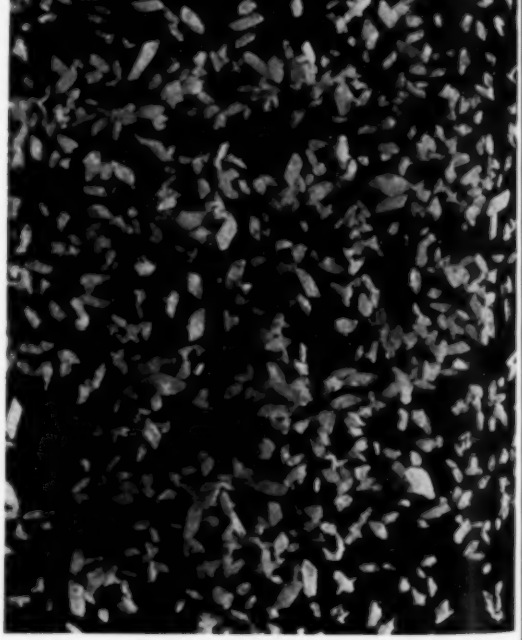

FIGURE 7. $2BaO.Al_2O_3.5H_2O$.

Reflected light, magnification, ×11.

1.96:1:4.85 and 1.93:1:4.75. The departure from a 2:1:5 ratio probably is due to the presence of a small amount of hydrated alumina. Most of the water can be driven off below 250° C.

The crystals are biaxial positive; indices are: $\alpha=1.642$, $\beta=1.655$, $\gamma=1.676$. The density is 3.42. X-ray data are given in table 1.

Malquori's solubility diagram [2] indicates that $2BaO.Al_2O_3.5H_2O$ is the stable solid phase in contact with barium aluminate solution over a certain range of concentration at 20° C. In the present investigation it has been obtained only from boiling solutions; at 30° C only the 1:1 (or 1.1:1) barium aluminate hydrates have been precipitated, even from solutions saturated with respect to $Ba(OH)_2.8H_2O$. As a preliminary determination of the stability of the 2:1:5 compound at room temperature, equal quantities of the solid were placed in contact with barium aluminate solutions of five different concentrations up to saturation with respect to $Ba(OH)_2.8H_2O$, and kept for several months. The solutions were analyzed from time to time. In every case, the solid dissolved slowly and incongruently with a slow increase in the ratio of BaO to Al_2O_3 in solution. These results require further confirmation but they strongly suggest that $2BaO.Al_2O_3.5H_2O$ is not stable in contact with barium aluminate solutions at room temperature. The slowness with which it reacts with water may easily lead to an erroneous assumption of equilibrium.

The X-ray powder diagrams and the photomicrographs were made by Mrs. E. Golovato and the thermal analyses by E. S. Newman, both of this Bureau.

IV. References

[1] E. Beckmann, J. prakt. Chem. [2] **26,** 385–421, 474–503 (1882); **27,** 126–152 (1883).
[2] G. Malquori, Gazz. Chim. ital. **56,** 51 (1926).
[3] L. S. Wells, W. F. Clarke, and H. F. McMurdie, J. Research NBS **30,** 367 (1943) RP1539.
[4] E. P. Flint, H. F. McMurdie, and L. S. Wells, J. Research NBS **21,** 617 (1938) RP1147.
[5] E. Martin, Chimie & industrie **23,** 564 (1930).

Washington, April 14, 1948.

U. S. Department of Commerce
National Bureau of Standards

Research Paper RP1909
Volume 41, August 1948

Part of the Journal of Research of the National Bureau of Standards

Aliphatic Halide-Carbonyl Condensations by Means of Sodium

By Edgar A. Cadwallader, Abraham Fookson, Thomas W. Mears, and Frank L. Howard

As a part of an investigation of the synthesis of highly branched aliphatic hydrocarbons that is being conducted at the National Bureau of Standards for the National Advisory Committee for Aeronautics, the Navy Bureau of Aeronautics, and the Army Air Forces, several compounds have been prepared by interaction of alkyl halides and various carbonyl compounds in the presence of sodium. This reaction makes possible the synthesis of certain highly branched compounds not easily obtainable by other means.

I. Introduction

The use of the Grignard reaction for synthesis of highly branched compounds is limited by undesirable side reactions, which become progressively more pronounced as the degree of branching of the reactants is increased. These side reactions involve the reduction and enolization of the adduct rather than the desired addition of the alkyl group.

The recent work of Bartlett and Schneider [1] [1] and previous work by Morton and Stevens [13] indicate that the reaction between an alkyl halide and an ester or ketone under the influence of sodium may be used to prepare certain compounds more easily than by the Grignard reaction, or may be used in some cases in which the Grignard reaction fails completely as a synthetic tool. In this paper, are described the results of a few reactions that were designed to give information concerning the scope of the reaction and the effect of various solvents and temperatures of reaction. The work of Bartlett and Schneider has been extended to include a few additional reactants.

II. Experimental

The apparatus used in making small-scale runs was the conventional three-neck flask of appropriate size, fitted with a stirrer, reflux condenser, and thermometer. A separatory funnel was placed at the top of the condenser. Heating and cooling of the reaction mixture was effected by application of hot or cold oil baths. In some cases, particularly with low-boiling solvents, both small necks of the flask were fitted with reflux condensers with the elimination of the thermometer.

Sodium sand was prepared batch-wise by heating a weighed amount of sodium in a purified light mineral oil until melted, and then shaking the liquid sodium vigorously in a closed Erlenmeyer flask until the desired state of subdivision was obtained. After the particles of sodium had cooled sufficiently, they were washed by decantation with three or four portions of the solvent to be used, transferred to the reaction vessel, and immediately covered with solvent.

A few of the first reactions tried in this series were conducted in *n*-pentane (boiling range 34° to 38° C), but later ones were conducted in isooctane [2] (boiling point, 99° C). It was found that the vigorous reactions were more easily controlled when the higher-boiling solvent was used. Also the use of isooctane as a solvent facilitated the use of higher temperatures for the reactions.

Bartlett and Schneider carried out their reactions by adding all of the alkyl halide to the sodium at once and then adding the carbonyl compound over a period of time. In attempting to use this

[1] Figures in brackets indicate the literature references at the end of this paper.

[2] This is the commonly used name for 2,2,4-trimethylpentane, which is a primary standard for octane number measurements. The commercially obtained material is exceptionally pure and serves admirably as an inert solvent for reactions of this type. The common name is used throughout this paper.

technique in our applications of the reaction, we often found that the reaction was so vigorous that the sodium was completely consumed before all of the carbonyl compound could be added. Apparently in these cases there is a self-sustaining reaction between the sodium and the alkyl halide that needs only a starting impetus given by the carbonyl compound. In order to minimize this effect only a small portion of the alkyl halide was added at the start of the reaction, and the remainder was mixed with the carbonyl compound for gradual addition during the reaction.

After the reaction had been carried to completion, the mixture was decomposed either by pouring it into ice water or by direct addition of water to the mixture in the flask. If any sodium was visible in the flask, the treatment with water was preceded by the addition of small amounts of ethyl alcohol. After complete hydrolysis, the two layers were separated and the organic layer washed with several portions of water. The organic substance was finally dried over a suitable drying agent. In those cases where the products of reaction were well known, only those physical constants that were deemed necessary to identify the product were determined.

Some of these reactions have been used for large-scale synthesis; the equipment used in these cases has been described previously [8].

Methyl isobutyrate, *t*-butyl chloride, methyl *n*-butyrate, isobutyl chloride, *n*-propyl chloride, and *n*-butylchloride were all made by standard procedures. Ethyl trimethylacetate and hexamethylacetone (2,2,4,4-tetramethyl-3-pentanone) were prepared by methods previously described [8]. Pentamethylacetone (2,2,4-trimethyl-3-pentanone) was prepared by a large-scale run of the reaction between ethyl trimethylacetate and isopropyl chloride by the method described herein. Pinacolone (3,3-dimethyl-2-butanone) [8] was prepared by the oxidation of 3,4,4-trimethyl-2-pentene [8] with sulfuric acid-dichromate solution in a manner analogous to that used previously for the preparation of 4,4-dimethyl-2-pentanone [8]. The other materials were obtained commercially.

Only constant-boiling materials that were collected from distillation in a 180 by 2.5-cm Whitmore and Lux [16] column were used in the synthesis. Several of these columns were used; some were packed with glass helices, the others were packed with stainless steel helices, but all were equipped with the type of distilling head recently described [7].

Solvents used for the reactions were removed by distillation through these columns; the residues were distilled (generally at reduced pressures) in a Podbielniak Hyper-cal column or in a Claisen flask fitted with a short fractionating column.

Yields were calculated on the basis of the amount of carbonyl compound that was added to the reaction. Table 1 summarizes data obtained on the several products, together with results reported in the literature.

1. Diisopropyl Ketone and *n*-Propyl Chloride

Sodium sand (69 g, 3 g atoms) was added to 1 liter of isooctane in the reaction vessel. The contents was heated to 80° C, and a solution of 114 g of diisopropyl ketone (1 mole) and 157 g of *n*-propyl chloride (2 moles) was gradually added. After the reaction began, the temperature rose to 95° C, which caused considerable refluxing. The characteristic [3] greenish-black color appeared, and addition of the ketone-halide solution was continued at such a rate as to insure vigorous refluxing. Addition time was approximately 2 hours. After standing overnight the reaction mixture was hydrolyzed, and the organic layer was washed and dried. Isooctane and unreacted *n*-propyl chloride were removed by distillation, and the residue was distilled at reduced pressure (Claisen flask). There was obtained 40 g of recovered diisopropyl ketone, and 51 g of 2-methyl-3-isopropyl-3-hexanol (32% yield). This carbinol has been prepared by George [5] in 36-percent yield by the reaction of *n*-propyl-magnesium halide and diisopropyl ketone. The residue (50 g) was a viscious material (boiling point >200° C, n_D^{20} 1.4590), and presumed to be a bimolecular product from condensation of diisopropyl ketone.

2. Diisopropyl Ketone and Isobutyl Chloride

A solution of 155 g of isobutyl chloride (1.68 moles) and 96 g of diisopropyl ketone (0.84 mole) was diluted with 200 ml of isooctane and added

[3] This reaction is visualized as starting with the formation of a sodium ketyl as the first step. This ketyl is colored an intense dark blue, blue-green, purple, or black, depending, it seems, on one or a combination of several factors. It has been noted that in several reactions tried, where reaction failed to occur, no characteristic color was observed. It is significant that this color appears first on the surface of the sodium. At this stage, if only a very small amount of ketone is present in relation to the amount of halide, the color often disappears as the ketone reacts.

TABLE 1. *Reaction products*

Reaction	Product	Yield percentage of theory [1]	Boiling point	Refractive index, n_D^{20}	Density, D^{20}	Reference
			°C/*mm* Hg			
Diisopropyl ketone and *n*-propyl chloride.	2-methyl-3-isopropyl-3-hexanol	32	90 to 95/22 [2] 178 to 182/760	1.4439	0.8504	
			[1] *132/125* *182/760*	*1.4444*	*.8554*	[5]
Diisopropyl ketone and isobutyl chloride.	2,5-dimethyl-3-isopropyl-3-hexanol	14	105 to 110/38 180 to 185/760	1.4430	0.8486	
			140/125 *190/760*	*1.4423*	*.8470*	[5]
Pentamethylacetone and methyl bromide.	2,2,3,4-tetramethyl-3-pentanol	43	111 to 112/128 175/760	1.4397	0.8550	
			94/50 *179/760*	*1.4405*	*.8565*	[8]
Pentamethylacetone and methyl iodide.	2,2,3,4-tetramethyl-3-pentanol	29	86 to 90/55 *94/50*	1.4410 *1.4405*	0.8555 *.8565*	[8]
Pentamethylacetone and ethyl bromide.	2,2,4-trimethyl-3-ethyl-3-pentanol	44	93 to 97/35 185 to 189/760 *188 to 191/760*	1.4479 *1.4481*	0.862 *.8628*	[14]
Pentamethylacetone and isopropyl chloride.	2,2,4-trimethyl-3-isopropyl-3-pentanol.	42	105 to 107/35 *103 to 104/27*	1.4550 *1.4559*		[1]
Hexamethylacetone and *n*-propyl chloride.	2,2-dimethyl-3-*t*-butyl-3-hexanol [4]	38	117/22	1.4563	0.8595	
Pinacolone and *n*-butyl chloride	2,2,3,6,6-pentamethyl-3-heptene-5-one.		103 to 107/30 [3] 83/10.5	1.4487 [5] *1.4498*	.8439 [5] .8432	
Hexamethylacetone and *t*-butyl chloride.	No product					
Methyl *n*-butyrate and *t*-butyl chloride (small run).	2,2-dimethyl-3-hexanone [6]	9	48 to 52/20 148 to 152/760 *148 to 148/760*	1.4115 *1.4085*		[6]
Methyl-*n*-butyrate and *t*-butyl chloride (large run).	2,2-dimethyl-3-hexanone	6.6	76.2 to 77.7/86 to 89 *146 to 148/760*	1.4098 *1.4095*		[6,12,10]
	2,2-dimethyl-3-hexanol	4.8	156/760 90 to 91/87 to 89 70 to 78/28 to 30	1.4262		
			155 to 157/760 *153 to 156/755*	1.4280 (at 17° C).		[6,12,10]
Methyl isobutyrate and *t*-butyl chloride.	Hexamethylethane		99 to 102	Solid		
	Pentamethylacetone	50	62/89 *136/760*	1.4067 *1.4059*		[8]
	2,2,4-trimethyl-3-pentanol	7.3	155/760 83/82 152/760 [7]	1.4280 [7] 1.4280		
	2,2,4,4-tetramethyl-3-isopropyl-3-pentanol.	19	113/37 *180 to 182/50*	1.4655 *1.4623*		[2]
Diethylcarbonate and *t*-butyl chloride.	Ethyl trimethylacetate	9	118 *118*	1.3912 *1.3906*		[8]
	Hexamethylacetone	9	151 *153*	1.4198 *1.4192*		
	Pivaloin		Melting point, 78° C	Solid		

See footnotes at end of table.

TABLE 1. *Reaction products*—Continued

Reaction	Product	Yield percentage of theory [1]	Boiling point	Refractive index, n_D^{20}	Density, D^{20}	Reference
			° C/mm Hg			
Ethyl trimethylacetate and isopropyl chloride.	Pentamethylacetone	4	136 *136*	1.4059 *1.4059*		[8]
	2,2,4-trimethyl-3-pentanol	4	151 *152*	1.4287 *1.428*		[6]
	2,2,4-trimethyl-3-isopropyl-3-pentanol.	54	110/33 *103 to 104/27*	1.4576 *1.4559*		[1]
Paraldehyde and *t*-butyl chloride	No product					
Paraformaldehyde and *t*-butyl chloride.	do					
Acetamide and *t*-butyl chloride	do					
Acetic anhydride and *t*-butyl chloride.	do					

[1] Yields based upon the carbonyl or ester compound.
[2] The temperature conversion to 760 mm Hg was done by a method described by Lippencott [11].
[3] The data in italics are from the literature.
[4] A freezing point of −10.1° C for this compound was made by E. H. Rich.
[5] The values for a known sample of 2,2,3,6,6-pentamethyl-3-heptene-5-one, as measured in this laboratory.
[6] Obviously, a mixture of ketone and carbinol.
Constants from the carbinol previously prepared in this laboratory.

over a period of 3 hours to a suspension of 69 g of sodium sand (3 g atoms) dispersed in 1 liter of isooctane at 80° C. The reaction mixture turned purplish blue as soon as the addition was begun, and the temperature rose quickly to 98° C. Stirring was continued for 1 hour after the addition was completed. The reaction mixture was hydrolyzed after standing overnight, and the organic layer washed several times with water and dried. The solvent and unreacted isobutyl chloride were distilled off, and the residue was distilled under reduced pressure (Claisen flask) to give 20 g (14% yield) of 2,5-dimethyl-3-isopropyl-3-hexanol.

3. Pentamethylacetone and Methyl Bromide

A suspension of 69 g of sodium sand (3 g atoms) in a solution of 128 g of pentamethylacetone (1 mole) and 1 liter of isooctane was heated to 80° C. An excess of methyl bromide was added from a methyl bromide dispenser [4] through a tube extending below the surface of the liquid. The reaction began in the usual manner, with the temperature rising quickly to 98° C, and the appearance of the blue color. Stirring was continued for 1 hour after all of the methyl bromide had been added, and the contents of the flask was allowed to stand overnight. The reaction mixture was worked up in the usual manner, and the isooctane and unreacted methyl bromide were removed by distillation. The residue, which was distilled at reduced pressure (Podbielniak still), yielded 62 g of 2,2,3,4-tetramethyl-3-pentanol, (0.43 mole, 43% yield).

4. Pentamethylacetone and Methyl Iodide

Pentamethylacetone (128 g, 1 mole) and 284 g methyl iodide (2 moles) were diluted with 200 ml of isooctane and added over a period of 2 hours to a suspension of 69 g of sodium sand (3 g atoms) in 300 ml of isooctane at 80° C. A rapid rise in temperature occurred, followed by the appearance of the characteristic blue color. After standing overnight the reaction mixture was hydrolyzed, and the organic layer washed several times with water and dried. The solvent and unreacted methyl iodide were removed by distillation, and the residue, which was distilled under reduced pressure, (Claisen flask) gave 41.5 g (29% yield) of 2,2,3,4-tetramethyl-3-pentanol.

5. Pentamethylacetone and Ethyl Bromide

A solution of 163 g of ethyl bromide (1.5 moles) and 64 g of pentamethylacetone (0.5 mole) was

[4] Arrow Products Co., Carlstadt, N. J.

added to 72 g of sodium sand (3.1 g atoms) suspended in 900 ml of isooctane. The reaction began in the usual manner with the appearance of the blue color and a rise in the temperature from 80° to 98° C. After standing overnight the reaction mixture was hydrolyzed, and the organic portion was washed and dried. Isooctane was removed by distillation, and the residue was distilled at a reduced pressure (Claisen flask) to give 35 g (44% yield) of 2,2,4-trimethyl-3-ethyl-3-pentanol. Nasarow [14] prepared the same carbinol in 7-percent yield by using pentamethylacetone and ethylmagnesium bromide.

A large run of this reaction has been carried out as a part of a synthesis. More precise data on the physical properties of the carbinol, its dehydration, and identification of 4,4-dimethyl-3-isopropyl-2-pentene as the dehydration product will be reported when further work, which is now in progress, has been completed.

6. Pentamethylacetone and Isopropyl Chloride

A solution of 64 g of pentamethylacetone (0.5 mole) and 98 g of isopropyl chloride (1.25 mole) was diluted with 250 ml of isooctane and added to a reaction flask containing 72 g (3.1 g atoms) of sodium sand in 300 ml of isooctane at 80° C. The usual procedure was carried out, and the organic layer was worked up in the usual manner. After removing the solvent, the residue was distilled at reduced pressure (Claisen flask) to give 36 g (42% yield) of 2,2,4-trimethyl-3-isopropyl-3-pentanol. This carbinol was prepared by Bartlett and Schneider [1] in 6-percent yield from the reaction of diisopropyl ketone with *t*-butyl chloride by means of sodium.

7. Hexamethylacetone and *n*-Propyl Chloride

A solution of 142 g of hexamethylacetone (1 mole) and 157 g of *n*-propyl chloride (2 moles) was diluted with 200 ml of isooctane. This solution was added to 69 g of sodium sand (3 g atoms) in 600 ml of isooctane at 80° C over a period of 2 hours. A sudden rise in temperaure occurred and was followed by the appearance of the usual blue-black color in the reaction mixture. After standing overnight the contents of the flask was hydrolyzed, washed, and dried. Isooctane and unreacted *n*-propyl chloride were removed, and the residue was distilled at reduced pressure in a Claisen flask. There was obtained a 38-percent yield of 2,2-dimethyl-3-*t*-butyl-3-hexanol. Two analyses [5] on this carbinol gave (1) C, 77.6 percent H, 14.3 percent and (2) C, 77.6 percent; H, 14.7 percent. The calculated values are: C, 77.42 percent; H, 13.98 percent. The molecular refractions were determined: MR (observed), 58.97, MR (calculated),[6] 58.86.

It is presumed that the carbon and hydrogen analyses are high due to the presence of some olefinic material formed by the dehydration of the carbinol during distillation.

8. Hexamethylacetone and *t*-Butyl Chloride

A solution of 71 g of hexamethylacetone (0.5 mole) and 138 g of *t*-butyl-chloride (1.5 moles) was added to 69 g of sodium sand (3 g atoms). The reaction began at 78° to 80° C, but it did not proceed well. Considerable gas, probably isobutylene, was given off during the reaction. The ketone-halide solution was added to the reaction mixture over a period of 2 hours. The contents of the flask was worked up in the usual manner, and the solvent was removed at atmospheric pressure. The residue (85 ml) was distilled from a Claisen flask at reduced pressure to give: 25 ml of residual isooctane, 36 g of recovered hexamethylacetone, boiling point 65° to 72° C at 32 mm Hg, $n_D^{20}=1.4133$ to 1.4195, and 3 ml of heavy viscous material of unknown composition. An attempt to crystalize tri-*t*-butyl carbinol [1] from a pentane solution of the residue by using first an ice-salt mixture and secondly a dry ice and acetone mixture, failed to yield any solid material.

9. Pinacolone and *n*-Butyl Chloride

A solution of 100 g of pinocolone (1 mole) and 185 g of *n*-butyl chloride (2 moles) in 700 ml of isooctane was added to 69 g of sodium sand (3 g atoms) in 300 ml of isooctane at 80° C over a period of 2 hours. The reaction that ensued was similar to those already described. After standing overnight, the reaction mixture was worked up in the previously described manner. The isooctane and unreacted *n*-butyl chloride were removed at atmospheric pressure, and the residue was distilled at reduced pressure in a Claisen flask. There was obtained 43 ml of material having these properties: boiling point, 103° to

[5] We are indebted to the Analytical Chemistry and Standard Samples Sections, NBS, for the carbon and hydrogen determination.

[6] Lorentz-Lorenz equation.

107° C at 30 mm Hg, $n_D^{20}=1.4487$ $D^{20}=0.8439$. The reported constants for the expected product, 2,2,3-trimethyl-3-heptanol, are boiling point, 84° to 87° C at 13 mm Hg, n_D^{20} 1.4409, D^{20} 0.8487 [3]. Since the constants of the fraction obtained do not agree with the reported values, it was presumed that pinacolone had dimerized in the presence of sodium to yield, after dehydration, 2,2,3,6,6-pentamethyl-3-heptene-5-one, boiling point, 83° C at 10.5 mm Hg, $n_D^{21}=1.4498$, $D^{21}=0.8432$. A carbon and hydrogen determination gave C, 79.1 percent; H, 12.6 percent. The calculated values for the dimer are: C, 79.12 percent; H, 12.08 percent, and for 2,2,3-trimethyl-3-heptanol, C, 76 percent; H, 13.92 percent. The formation of the dimer was expected rather than the addition reaction, because pinacolone, being a methyl ketone, easily aldolizes in the presence of sodium.

A 2,4-dinitrophenylhydrazone was prepared from some of this material, which melted 146.5° to 147° C. The same derivative was prepared from an authentic sample of 2,2,3,6,6-pentamethyl-3-heptene-5-one and melted at 147° to 147.5° C. A mixture of the two derivatives melted at 146.0° to 146.5° C. Hence the main produce from this reaction was the dehydrated bimolecular product from pinacolone.

10. Methyl *n*-Butyrate and *t*-Butyl Chloride

A solution of 102 g of methyl *n*-butyrate (1 mole) and 368 g of *t*-butyl chloride (4 moles) was added over a period of 3 hours to 46 g (2 g atoms) of sodium sand in 200 ml of isooctane at 80° C. After standing overnight the mixture was hydrolyzed, and the organic layer was washed several times with water and dried over anhydrous sodium carbonate. The isooctane was removed, and the residue was distilled at reduced pressure in a Claisen flask. There was obtained thereby 11 g (9% yield) of 2,2-dimethyl-3-hexanone.

Since more information was desired on this reaction than was afforded by the small-scale run, a large run was made. A solution of 17.6 kg of *t*-butyl chloride (190 moles) and 7.54 kg of ethyl *n*-butyrate (65 moles) was added over a period of 7 hours to 6.9 kg of sodium sand (300 g atoms) in 10 gal of isooctane at a temperature of 55° to 60° C under a nitrogen atmosphere. The reaction mixture turned greenish-black during the course of the addition and evolved large quantities of gas, probably isobutylene. The reaction mixture was stirred overnight at a temperature of 56° C.

Five gallons of 95-percent ethanol was then added over a half-hour period, and the mixture was kept at reflux temperature all day in order to remove as much as possible of the excess sodium. This was followed by 10 gal of water, which was added cautiously to the cooled reaction mixture under a nitrogen atmosphere during 6 hours. After the last traces of sodium had disappeared, the mixture was washed three times with a large amount of water. About 8 to 10 gal of organic material was obtained, which was dried over calcium chloride prior to distillation.

The isooctane was removed at atmospheric pressure, and the residue, 2,500 ml, was submitted to vacuum distillation (Podbielniak). There were obtained 552 g of 2,2-dimethyl-3-hexanone (4.3 moles, 6.6%) and 408 g of 2,2-dimethyl-3-hexanol (3.1 moles, 4.8%) [10]. There were no fractions that could be identified as the desired product, 2,2-dimethyl-3-*t*-butyl-3-hexanol.

The poor recovery of starting materials is indicative of the fact that little coupling occurred; the boiling points of the coupling products are all well above that of isooctane, and they would certainly have appeared in the residue left upon stripping the isooctane. Hence their absence can only be accounted for as a consequence of side reactions. The *t*-butyl chloride was lost partly as isobutylene during the course of the reaction, and the remainder distilled with the isooctane during the stripping operation. The ester must have been lost as a consequence of alkaline hydrolysis when the reaction mixture was worked up, the hydrolysis products being discarded with the raffinates.

11. Methyl Isobutyrate and *t*-Butyl Chloride

In a 50-gal stainless steel reactor, 6.9 kg of sodium sand (300 g atoms) was prepared in 10 gal of isooctane. To this was added 17.6 kg of *t*-butyl chloride (191 moles), and the mixture was heated to 45° C, after which 6.4 kg of methyl isobutyrate (62.8 moles) was added over a period of 6 hours. The reaction mixture was stirred overnight and hydrolyzed. The organic layer was separated, washed, and dried. Isooctane and unreacted *t*-butyl chloride were distilled at atmospheric pressure. The following compounds were isolated from the residue by distillation on a

Podbielniak column: 59 g of hexamethylethane, 1,036 g of pentamethylacetone (50% yield), 599 g of 2,4,4-trimethyl-3-pentanol, and 2,229 g of 2,2,4,4-tetramethyl-3-isopropyl-3-pentanol (19% yield). The latter carbinol was prepared in 15-percent yield by Bartlett and Schneider [1] by the reaction of pentamethylacetone, *t*-butyl chloride, and sodium.

12. Diethylcarbonate and *t*-Butyl Chloride

Ethyl trimethylacetate (9% yield) and hexamethylacetone (9% yield) were obtained from the reaction of 277 g of *t*-butyl chloride (3 moles) and 236 g of diethylcarbonate (2 moles) in the presence of 92 g of sodium sand (4 g atoms) using petroleum ether as the solvent. There was considerable difficulty in starting the reaction, but once started the reaction became very vigorous. The sodium turned black, then bronze, and the reaction mixture thickened considerably so that additional solvent was required to permit stirring. After hydrolyzing the reaction mixture, the organic layer was worked up in the usual manner. After removing the petroleum ether, the residue was distilled in a Podbielniak column to give 0.185 mole of ethyl trimethylacetate, and 0.176 mole of hexamethylacetone.

A second run was made by using the same quantity of materials, but isooctane was used as the solvent. From the residue 25 g of solid (melting point, 78° C), which was identified as pivaloin (melting point, 80° C), and a very high boiling material were obtained. There were no fractions isolated having the properties of either ethyl-trimethylacetate or hexamethylacetone.

13. Ethyl Trimethylacetate and Isopropyl Chloride

In a 50-gal stainless steel reactor, 15.4 lb of sodium sand (300 g atoms) was prepared in 10 gal of isooctane. To this there was added, over a period of 6 hours, a solution of 180 moles of isopropyl chloride and 60 moles of ethyl trimethylacetate. The reaction mixture exhibited the characteristic appearance of a blue color accompanied by a rise in the temperature to 54° C. The reaction was kept at 50° to 70° C by means of warm water in the kettle jacket. After standing overnight, excess sodium was destroyed by 5 gal of 190-proof ethyl alcohol, followed by ample quantities of water for hydrolysis. The organic layer was separated, washed several times with water, and dried over anhydrous calcium chloride. Isooctane was distilled off, and the residue was distilled at reduced pressure in a Podbielniak column. The following products were isolated and identified from their physical constants: 2.5 moles (4% yield) pentamethylacetone, 2.73 moles (4% yield) 2,2,4-trimethyl-3-pentanol, and 32.6 moles (54% yield) 2,2,4-trimethyl-3-isopropyl-3-pentanol. Distillation data are shown in figure 1.

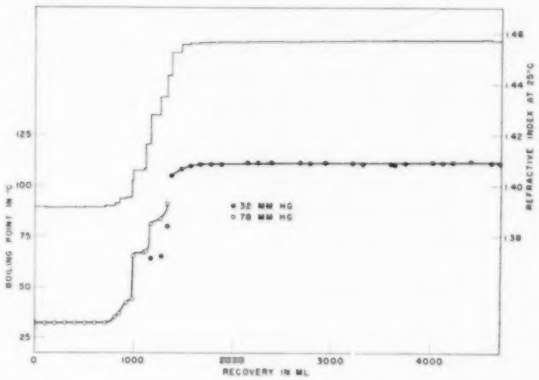

FIGURE 1. *Results of distillation of the products from interaction of ethyl trimethylacetate and isopropyl chloride.*

The small plateau in the boiling point curve, beginning at about 1,000 ml. distilled, represents pentamethylacetone; the next small plateau represents 2,2,4-trimethyl-3-pentanol. The long plateau represents 2,2,4-trimethyl-3-isopropyl-3-pentanol. These curves are similar to those obtained in the other experiments.

14. Paraldehyde, Paraformaldehyde, and *t*-Butyl Chloride

An attempt was made to extend the Bartlett-Schneider reaction to include the reaction of an aldehyde with an alkyl halide. Because monomeric aldehydes aldolize under alkaline conditions, it was decided to try paraldehyde and paraformaldehyde.

A mixture of 132 g of paraldehyde (0.5 mole) and 138 g of *t*-butyl chloride (1.5 mole) was added in small portions to 39 g of sodium sand in 400 ml of isooctane. The temperature of the reaction mixture was maintained at 80° C until all of the mixture had been added. There was no evidence of reaction at this temperature; consequently the mixture was heated to 90° C for 1 hour. After standing overnight, no reaction had taken place. The experiment was discontinued.

791450—48——3

A similar attempt was made with paraformaldehyde and *t*-butyl chloride as reactants, but no reaction was observed.

15. Acetamide and *t*-Butyl Chloride

Small portions of 59 g of acetamide (1 mole) and 277 g of *t*-butyl chloride (3 moles) were added to a reaction vessel containing 69 g of sodium sand (3 g atoms) in 1 liter of isooctane. The reaction was very sluggish with evolution of a gas (probably isobutylene), and the temperature did not rise above the initial temperature of 80° C. After hydrolysis with ethyl alcohol and water, a strong odor of ammonia developed indicating hydrolysis of the acetamide to acetic acid. Fractionation gave a cut (boiling point 78° C $n_D^{20}=1.3862$) identified as ethyl acetate [9]. This is not surprising, since acetic acid and ethyl alcohol could esterify under conditions of the experiment. No other reaction product was obtained.

16. Acetic Anhydride and *t*-Butyl Chloride

In a large Erlenmeyer flask, 94 ml of acetic anhydride was added to 23 g of sodium sand in 100 ml of isooctane. The mixture was heated to 75° C, and 217 ml of *t*-butyl chloride was added in small amounts. From time to time the flask was heated on a hot plate. There were no visible signs of reaction, nor did any reaction occur when the contents of the flask was heated to the boiling point of isooctane (boiling point, 99° C). The addition of *t*-butyl chloride was discontinued, and the reaction mixture was allowed to stand overnight. No change had taken place during the night, and the experiment was therefore discontinued.

III. Summary

In the study of these condensation reactions, seventeen runs were made, of which nine were of the aliphatic ketone-aliphatic halide type, four were of the aliphatic ester-aliphatic halide type, and four were a miscellaneous type. In those reactions that produced desirable compounds, the yields were as good or better than where the Grignard reagent was employed.

This reaction is apparently, applicable to compounds whose carbonyl group is sufficiently removed from influences that cause enolization, aldolization, or hydrolysis. Table 1 is a résumé of results obtained in this work.

IV. References

[1] P. D. Bartlett and A. Schneider, J. Am. Chem. Soc. **67,** 141 (1945).
[2] G. Calingaert, H. Soross, V. Hnizda, and H. Shapiro, J. Am. Chem. Soc. **66,** 1389 (1944).
[3] J. B. Connant and A. H. Blatt, J. Am. Chem. Soc. **51,** 1227 (1929).
[4] A. Faworsky, J. Prakt. Chim. **88,** 651 (1913).
[5] Richard Stanley George, PhD Thesis, Pennsylvania State College (1943).
[6] A. Haller and E. Bauer, Compt. rend. **150,** 586 (1910).
[7] F. L. Howard, Anal. Chem. **19,** 144 (1947).
[8] F. L. Howard, T. W. Mears, A. Fookson, P. Pomerantz, and D. B. Brooks, J. Research NBS **38,** 365 (1947) RP1779.
[9] E. H. Huntress and S. P. Mulliken, Identification of pure organic compounds, p. 378 (John Wiley & Sons, Inc., New York, N. Y., 1941).
[10] M. J. Lerodie, Ann. Chim. Phys. [9] **16,** 369 (1921).
[11] S. B. Lippencott and Margaret M. Lymen, Ind. & Eng. Chem. **38,** 320 (1946).
[12] R. Locquin and L. Leers, Compt. rend. **178,** 2097 (1924); Bul. soc. chim. [4] **39,** 434 (1926).
[13] A. Morton and J. R. Stevens, J. Am. Chem. Soc. **53,** 2244 (1931).
[14] I. N. Nasarow, Ber. deut. chem. Ges. **69B,** 21 (1936).
[15] F. C. Whitmore, J. M. Church, and R. U. McGrew, J. Am. Chem. Soc. **56,** 176 (1934).
[16] F. C. Whitmore and A. R. Lux, J. Am. Chem. Soc. **54,** 3451 (1932).

Washington, January 26, 1943.

U. S. Department of Commerce
National Bureau of Standards

Research Paper RP1910
Volume 41, August 1948

Part of the Journal of Research of the National Bureau of Standards

Barium 2-Ketolactobionate and the Corresponding Barium Bromide Double Salt [1] [2]

By William W. Walton and Horace S. Isbell

As a preliminary step in the development of methods for the preparation of 2-ketoaldobionic acids for use in the synthesis of glycosidic derivatives of ascorbic acid, the preparation of 2-ketolactobionic acid has been studied. By oxidation of lactose osone with bromine in the presence of barium carbonate, barium 2-ketolactobionate was obtained and separated in the crystalline state. In addition to the normal barium salt, a double salt containing barium bromide was found. This salt is unique in that it is the first and only crystalline barium bromide salt of a sugar acid reported in the literature. It crystallizes freely and is useful for the separation and identification of 2-ketolactobionic acid.

I. Introduction

In consideration of the relationship between the carbohydrates and vitamin C and the prevalence of glycosides in natural products, it seemed desirable to undertake the preparation and study of some glycosidic derivatives of ascorbic acid. The most natural course for the synthesis of the glycosidic derivatives of ascorbic acid is through the intermediate production of 2-ketoaldobionic acids. The esters of certain 2-keto acids undergo lactonization and enolization with the formation of ascorbic acids [1, 2, 3].[3] Thus one might expect that methyl 2-ketomelibionate on treatment with sodium methylate in methanol would give the following reaction:

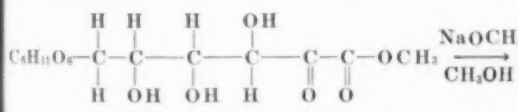

Methyl 2-ketomelibionate

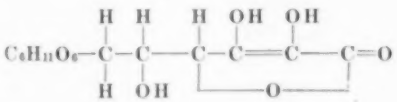

6-galactosylisoascorbic acid

The facility with which esters of 2-ketoaldonic acids yield ascorbic acid derivatives has led to the development of methods for their production. The most generally used method consists of oxidation of ketoses with potassium permanganate. With this method, it is necessary to protect the hydroxyl groups other than those attached to carbons one and two, as for instance by preparing acetone derivatives. It has been found, however, that L-sorbose [4] and D-fructose [5] can be oxidized directly with nitric acid to 2-keto-L-gluconic acid and 2-keto-D-gluconic acid, respectively. In some cases the aldonic acids or their esters can be oxidized, and the keto acid or its ester can be obtained directly. This has been accomplished by several methods, notably by anodic oxidation of a salt of the aldonic acid [6] and by oxidation of the aldonic acid, its lactone, or ester with a chlorate in the presence of vanadium pentoxide [7]. The latter method requires the presence of an acid and is not suitable for the preparation of keto acids containing easily hydrolyzable glycosidic groups.

A method that does not require the presence of an acid consists of the production of the sugar osone followed by oxidation with bromine in sub-

[1] Abstracted from a thesis submitted by William W. Walton in June 1947 to the faculty of the Graduate School of the University of Maryland, represented by Nathan L. Drake, in partial fulfillment of the requirements for the degree of Doctor of Philosophy.

[2] Presented before the Division of Sugar Chemistry and Technology of the American Chemical Society at New York, Sept. 1947.

[3] Figures in brackets indicate the literature references at the end of this paper.

stantially neutral solution. The procedure is suitable for use with osones derived from both monosaccharides and disaccharides, and it has been applied to a number of osones including maltosone [8]. The product from maltosone was reported to be amorphous and was undoubtedly an impure salt of 2-ketomaltobionic acid. As mentioned before, the enolization and lactonization of certain 2-ketoaldobionic acids would be expected to yield ascorbic acid derivatives of the desired type. 2-Ketomaltobionic acid and 2-ketolactobionic acid, however, contain substituents on the fourth carbon atom that prevent ring closure to that carbon atom. For this reason they cannot yield ascorbic acid derivatives. Nevertheless, on account of the ready availability of lactose it was selected for preliminary study of oxidation methods.

II. Barium 2-Ketolactobionate and Its Barium Bromide Double Salt

As an intermediate in the preparation of 2-ketolactobionic acid, it was necessary to prepare lactose osone. Ordinarily osones are obtained by reaction of phenylhydrazine with the sugar followed by treatment of the resulting phenylosazone with benzaldehyde [9] to remove the phenylhydrazine. In some cases osones have been obtained by direct oxidation of the sugar with copper acetate [10]; but this method is not applicable to disaccharides, because the reaction is slow and considerable hydrolysis takes place. Hence, the first method was adopted. The lactose osone was oxidized with bromine in the presence of barium carbonate, the resulting barium bromide was removed by treatment with silver sulphate, and barium 2-ketolactobionate was crystallized from the solution. Barium 2-ketolactobionate is the first crystalline metallic salt of a 2-ketoaldobionic acid to be prepared. It is quite soluble and does not crystallize easily. It was found, however, that barium 2-ketolactobionate forms a double salt with barium bromide, which crystallizes readily. The salt appears to be somewhat analogous to calcium lactobionate-calcium bromide [11]. Nevertheless, it is unique in that it is the first and only crystalline salt of a sugar acid to contain barium bromide. Photomicrographs of the normal salt and the double salt are shown in figure 1.

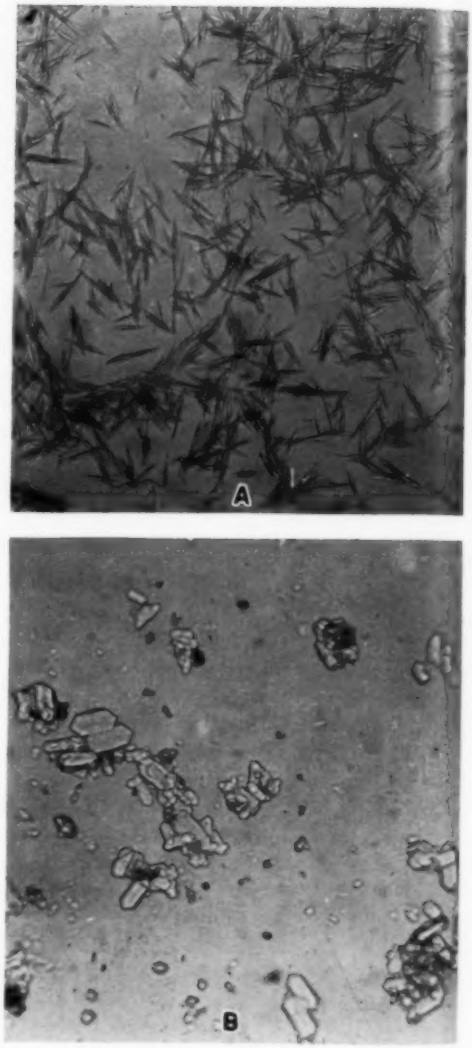

FIGURE 1. *A, Barium 2-ketolactobionate dihydrate,* $[\alpha]_D^{20} = -37.9°$, *B, Barium 2-ketolactobionate-barium bromide tetrahydrate,* $[\alpha]_D^{20} = -28.2°$. (×250).

The double salt is particularly suitable for the separation of 2-ketolactobionic acid from the mixture obtained by the oxidation of lactose osone with bromine because it crystallizes freely from the impure mixture, and the barium bromide necessary for the formation of the salt is a byproduct of the reaction. The salt is characteristic of the 2-ketolactobionic acid structure and should be useful for identification purposes.

III. Structure of Barium 2-Ketolactobionate and its Barium Bromide Double Salt

To establish that the normal barium 2-ketolactobionate and the barium bromide double salt are derivatives of the same 2-ketoaldobionic acid, the normal salt was prepared from the double salt by removal of the barium bromide with silver sulfate followed by crystallization. Furthermore, by the addition of a mole of barium bromide, the double salt was regenerated from the normal salt.

Since the synthesis began with lactose, (4-β-D-galactosyl-D-glucose), in order to establish the structure of the new compound it was necessary (1) to prove that the biose linkage was still present and (2) to identify the products of hydrolysis as D-galactose and 2-keto-D-gluconic acid. Enzymatic hydrolysis of the substance with a sample of lactase [4] established the existence of the biose linkage. Galactose was separated from the products of hydrolysis and identified by its melting point and optical rotation. Its presence in the hydrolytic mixture was also shown by the action of a galactose-fermenting yeast. The 2-ketogluconic acid was identified by separation of the characteristic phenylhydrazine salt of the phenylhydrazone.

This experimental work shows that the new compound is the barium salt of 4-β-D-galactosyl-2-keto-D-gluconic acid (2-ketolactobionic acid). The freshly dissolved salt gave a specific rotation of $-36.4°$, 4 minutes after dissolution, which changed to $-37.9°$ in 45 minutes. The lack of a more extensive mutarotation is peculiar in light of the similarity of the substance to fructose and lactulose. 2-Ketolactobionic acid, like lactulose, has the fructose structure; it differs from lactulose (4-β-D-galactosyl-D-fructose) in having a carboxyl group in place of the terminal hydroxymethyl group. Fructose crystallizes in the pyranose form but establishes an equilibrium containing a substantial proportion of the furanose modification. Lactulose crystallizes in the furanose form, but its equilibrium state is very similar to that of fructose [12]. Since crystalline sugars having the fructose structure are thus known to exist in both furanose and pyranose forms, it is not possible to draw a conclusion concerning the ring structure of the crystalline barium salt by analogy to similar compounds.

It has been shown previously that an equilibrium state involving both pyranose and furanose modifications is particularly sensitive to changes in temperature, and that this equilibrium can be studied by measurements of optical rotation at various temperatures. A comparison of the equilibrium rotations of barium 2-ketolactobionate, lactulose, and levulose at two temperatures is given in table 1. In each case the optical rotation is appreciably altered by a change in temperature, and in the same direction. The like behavior of the compounds is evidence that they establish similar equilibrium states. Hence, barium 2-ketolactobionate, like fructose and lactulose, establishes an equilibrium state containing substantial amounts of both pyranose and furanose modifications. The lack of a more extensive mutarotation for the salt must be explained by changes too rapid to be detected, or by the presence of more than one modification of the sugar entity in the barium salt at hand.

TABLE 1. *Comparison of optical rotation*

Substance	Equilibrium rotation	
	0° C	20° C
Barium 2-ketolactobionate	[a]−42.3	−37.9
Lactulose	−24.8	−23.0
Levulose	−46.6	−42.7

[a] Temperature 0.6° C.

IV. Experimental Details

1. Preparation of Lactose Phenylosazone

One hundred and eighty grams of lactose was dissolved in 1 liter of water, and 164 ml of phenylhydrazine and 328 ml of a 50-percent aqueous solution of acetic acid were added. The mixture was heated in a water bath for 2 hours at 80°C, cooled, and stored in a refrigerator overnight. The osazone was removed by filtration, washed with dilute acetic acid, water, and finally with ether. The product was recrystallized from 20-percent aqueous alcohol. The yield was 38 percent.

[4] The lactase was kindly supplied by the research laboratories of Rohm & Haas, Philadelphia, Pa.

2. Preparation of Lactose Osone

Seventy grams of lactose phenylosazone was dissolved in 6 liters of hot water, 56 g of benzaldehyde was added, and the mixture was stirred vigorously while being heated on the steam bath in an atmosphere of nitrogen for 4 hours. The solution was cooled and filtered and the filtrate extracted several times with ether to remove excess benzaldehyde. The aqueous solution was then treated with a decolorizing carbon, filtered and concentrated under reduced pressure to a volume of 800 ml. The yield on several preparations was about 65 percent.

3. Preparation of Barium 2-Ketolactobionate-Barium Bromide

The aqueous solution of lactose osone obtained above, 800 ml in volume, was saturated with carbon dioxide and cooled in an ice bath. Thirty-five grams of barium carbonate and 12 ml of bromine were added, and the mixture was stirred. After 5 minutes the flask was removed from the ice bath and the contents was stirred for ½ hour at room temperature. Most of the excess bromine was removed with a rapid stream of carbon dioxide and the last trace by reaction with linseed oil. After separation from the oil, the mixture was filtered, treated with 10 g of a decolorizing carbon and refiltered. The colorless filtrate was concentrated under reduced pressure to a volume of approximately 50 ml and transferred to a beaker with about 20 to 25 ml of washings. In one preparation crystals separated at this point; in subsequent preparations the sirup was seeded and allowed to stand in a vacuum desiccator over sulfuric acid for a period of a day or two. The crystals were separated, washed with cold water, and air-dried. The yield in different preparations varied widely; the highest yield was 28.3 g and the lowest was 4 g.

The material was recrystallized as follows: Twenty-five grams of the barium 2-ketolactobionate-barium bromide was dissolved in 475 ml of water at room temperature, and the solution was filtered with the aid of a little decolorizing carbon. The filtrate was concentrated under reduced pressure to a volume of about 75 ml and allowed to stand overnight at room temperature. The crystals that formed were collected on a funnel, washed with cold water and air-dried. Nineteen grams of pure barium 2-ketolactobionate-barium bromide was obtained. Analysis: Calculated for $Ba(C_{12}H_{19}O_{12})_2.BaBr_2.4H_2O$: C, 23.7; H, 3.8; Ba, 22.6; Br, 13.1. Found: C, 23.9; H, 3.8; Ba, 22.6; Br, 13.2. At equilibrium, the specific rotation $[\alpha]_D^{20} = -28.2°$ (water c=2).

4. Preparation of Barium 2-Ketolactobionate

Barium 2-ketolactobionate was prepared by oxidation of lactose osone in a manner analogous to the preparation of the double salt. However, after treatment of the oxidized solution with carbon, the barium bromide was removed from the filtrate by treatment with silver sulfate and filtration. The solution was concentrated to about 50 ml under reduced pressure, and 50 ml of methanol was added. The solution was seeded with crystals of barium 2-ketolactobionate and allowed to crystallize for 2 days.

The material was recrystallized as follows: Seven grams of barium 2-ketolactobionate was dissolved in 20 ml of water, and the solution was filtered with the aid of a little decolorizing carbon. About 25 ml of methanol was slowly added to the filtrate and the solution was seeded and allowed to crystallize overnight. About 6 grams of recrystallized material was obtained. Analysis of the air-dried salt: Calculated for $Ba(C_{12}H_{19}O_{12})_2.2H_2O$: C, 32.6; H, 4.8; Ba, 15.5. Found: C, 32.7; H, 4.8; Ba, 15.7. At equilibrium, the specific rotation $[\alpha]_D^{20} = -37.9°$ (water c=2); $[\alpha]_D^{0.6} = -42.3°$.

5. Structure of Barium 2-Ketolactobionate

(a) Enzymatic Hydrolysis

A 1.105-g sample of barium 2-ketolactobionate was treated with an equivalent amount of 0.5 *N* sulfuric acid and the solution was stirred for 1 hour. Twenty-five hundredths gram of calcium carbonate was added, and the solution was stirred for 2 hours and filtered. The pH of the solution was adjusted to 6.7 with carbon dioxide. The optical rotation of the solution was −8.55° S (4-dm tube). Three-tenths gram of lactase was then added, the solution was covered with toluene to prevent mold formation and stored at 30° C for 4 days. The optical rotation indicated that hydrolysis was 70 percent completed. An additional 0.3 g of lactase was added, and the solution was stored at 30° C for an additional 7 days. The optical rotation at that time was −1.32° S (4 dm tube), indicating complete hydrolysis.

(b) Identification of Galactose

The hydrolyzed solution obtained in (a) was separated from the toluene and filtered. A small quantity of a galactose-fermenting yeast and 1 ml of a nutrient medium were added, and the solution was stored at 37° C for 24 hours. The optical rotation indicated the destruction of 18 percent of the theoretical amount of galactose in 1 day. This solution was reserved for part (c).

In a separate experiment, 2 g of barium 2-ketolactobionate was hydrolyzed by dissolving it in 25 ml of 7.5-percent sulfuric acid and heating the solution on the steam bath for 4 hours. About 2.5 g of calcium carbonate was added to the cool solution, and the mixture was allowed to stand overnight. It was then filtered and passed successively through a cation exchange resin and an anion exchange resin to remove calcium 2-ketogluconate. The filtrate was evaporated to a sirup, 10 ml of methanol was added, and the solution was seeded with galactose and allowed to crystallize overnight. The crystals were separated, dried over calcium chloride, and weighed. A yield of 51 percent of the theoretical amount of galactose was obtained. The material was recrystallized from a water-methanol solution and the melting point found to be 165° C. Mutarotation measurements were made, and the following values were found: initial rotation $[\alpha]_D^{20}=140.5°$; final rotation $[\alpha]_D^{20}=80.2°$; mutarotation constant 0.009. The corresponding values reported for galactose are: melting point, 165° to 167° C; initial rotation, $[\alpha]_D^{20}=150.7°$; final rotation $[\alpha]_D^{20}=80.2°$; mutarotation constant 0.008 to 0.009 depending on the carbon dioxide content of the water.

(c) Identification of 2-Ketogluconic Acid

The solution from (b) in which the galactose had been partially destroyed by fermentation was filtered and concentrated to a volume of 4 ml. Five drop of acetic acid and 5 drops of phenylhydrazine were added, and the solution was seeded with crystals of the phenylhydrazine salt of the phenylhydrazone of 2-ketogluconic acid. Crystals formed readily, and were separated by filtration, washed with ether, and dried. The melting point was 95° to 97° C with decomposition. The melting point of the phenylhydrazine salt prepared from authentic 2-ketogluconic acid was 96° to 98° C with decomposition. A mixed melting point of the two preparations was 95° to 97° C.

V. References

[1] T. Reichstein and A. Grüssner, Helv. chim. Acta, **17,** 311 (1934).
[2] K. Maurer and B. Schiedt, Ber. deut. chem. Ges. **66,** 1054 (1933).
[3] T. Reichstein, Helv. chim. Acta. **17,** 996, 1003 (1934).
[4] British Patent 443,901 (Sept. 1, 1934).
[5] H. Ohle, H. Erlbach, and H. Carls, Ber. deut. chem. Ges. **67,** 324, 555 (1934).
[6] R. Pasternack and P. Regna, U. S. Patent 2,222,155 (Nov. 19, 1940).
[7] R. Pasternack and P. Regna, U. S. Patent 2,207,991 (July 16, 1940).
[8] T. Kitasato, Biochem. Z. **207,** 217 (1929).
[9] E. Fischer, Liebigs Ann. Chem. **288,** 145 (1895); Ber. deut. chem. Ges. **35,** 3142 (1902).
[10] I. Stone, U. S. Patent 2,206,374 (July 2, 1940).
[11] H. S. Isbell, J. Research NBS **17,** 331 (1936) RP914.
[12] H. S. Isbell and W. W. Pigman, J. Research NBS **20,** 773 (1938) RP1104.

WASHINGTON, April 22, 1948.

U. S. Department of Commerce
National Bureau of Standards

Research Paper RP1911
Volume 41, August 1948

Part of the Journal of Research of the National Bureau of Standards

Infrared Prism Spectrometry from 24 to 40 Microns*

By Earle K. Plyler

A prism of KRS–5 (thallium-bromide-iodide) has been used to measure the transmission of various substances in the infrared region from 24 to 40 microns. The prism was installed in a Perkin-Elmer spectrometer, and a Golay detector was employed for measuring the energy. Transmission data were obtained for polystyrene, polyethylene, and different samples of KRS–5. Also measurements have been made on the cut-off of KBr, AgCl, and other crystals. The rotational spectrum of the water-vapor molecule has been measured to 39.2 microns, and the known frequencies of these absorption bands have been used for the calibration of the prism.

I. Introduction

Some of the optical properties of the thallium halides have been known for a considerable time. The residual rays of some of these substances were measured by Rubens and Wartenberg [1] in 1914. The maxima of the reflection bands were 91.9 μ for TlCl, 117 μ for TlBr, and 152 μ for TlI. These reflection maxima fall in the long wavelength region of the infrared. This fact indicated that the absorption of the material would not be intense for moderate thicknesses to about 40 or 50 μ. Thallium iodide does not form cubic crystals and usually exists as a powder. In order to use it for infrared studies, a mixed crystal with TlBr from the fused mixture is grown. During the war such mixed crystals were grown in Jena. The material was called KRS–5 and consisted of about 42 percent of TlBr and 58 percent of TlI. A mixed crystal of TlCl and TlBr was called KRS–6 and other materials that were used in the infrared region were also included in the KRS series. The KRS–5 is highly resistant to water and was found useful on field instruments. Preliminary measurements in Germany showed that the TlBr-I crystal has a high index of refraction in the visible and the infrared regions and that in thicknesses of 2 mm it is transparent beyond 40μ.

In 1945 plans were made at Fort Belvoir and at the National Bureau of Standards for the growing of synthetic crystals of the thallium halides. At first, considerable difficulty was experienced in producing single crystals of sufficient size for prisms. Also many of the early crystals became opaque beyond 30 μ. This difficulty was overcome when great care was takn in purifying the thallium bromide and thallium iodide.

II. Experimental Procedure

A single crystal of KRS–5 was grown by Francis Phelps of this Bureau, and from it a prism with a refracting angle of 26° was cut and polished in the Optical Shop. The prism was annealed before the final polishing. Some experiments on the polishing were carried out by Edgar Robinson, and he was able to get good surfaces that are flat to a few wavelengths of monochromatic yellow light over a considerable part of the prism face. The refracting angle of 26° was selected, in part, so that the prism could be used in a Perkin-Elmer spectrometer with a minimum of changes in the instrument. The KRS–5 has a high dispersion in the visible region, and the yellow mercury lines are well separated. It is possible to obtain an image of about 0.25 mm of a single visible spectral line by using an extremely narrow entrance slit.

The difficulty of obtaining very narrow images appears to be due to lack of homogeneity of the prism. If the composition of the crystal varies in such a manner that the proportions of TlBr and TlI differ for different regions within the crystal, corresponding variations in the index of refraction will result for the same regions. A

[1] H. Rubens and H. V. Wartenberg, Berl. Ber (1914).

*Presented in part at the meeting of the Optical Society of America, Mar. 5, 1948, J. Opt. Soc. Am. **38**, 664 (1948).

prism, obtained from another laboratory that was recently examined, produced four images of a single spectral line. The lack of sharpness of the image is not of great importance in the region from 25 to 40 μ. Because of the small amounts of energy radiated by the globar in this region, it is necessary to use slits up to 1 mm.

A Golay detector with a KRS–5 window was used as the detecting unit. The energy from the exit slit was focused on the blackened receiver by means of a lens made from KRS–5.

The energy is further reduced by the reflection losses of the prism. For example, at 28 μ the index of refraction is about 2.3, and a 26° prism loses about 50 percent of the energy by reflection when it is traversed twice. Under the same conditions, a 36° prism loses about 72 percent of the incident energy by reflection. Small scratches on the surface of the prims do not modify its properties for long wavelength energy to any great extent but may produce scattering of radiation in the short wavelengths.

III. Results

The infrared spectrometer, containing the KRS–5 prism as the dispersing unit, was calibrated for wavelength determinations by the use of the known absorption bands of many substances in the region from 2 to 40 μ. A graph was made by plotting the drum readings of the spectrometer as a function of the wavelength. On account of the low dispersion of the KRS–5 prism in the region from 2 to 15 μ, it is not advantageous to use a prism of this material for this region. Good resolution is obtained in the region from 24 to 40 μ, and a more detailed calibration curve has been obtained for this range of wavelengths. By the positions of the absorption bands of chloroform, bromoform, carbon disulfide, and carbon tetrachloride, the rotation lines of the water vapor absorption spectrum were identified. The wave numbers of these lines in the 24- to 40-μ region are well known from the work of Randall, Dennison, Ginsburg, and Weber.[2] Their work was carried out with a grating spectrometer, and the resolution is much higher than that obtained with the KRS–5 prism. However, many of the absorption lines are single and show up distinctly on the recorder traces. Where some of the lines of the water vapor molecule are not separated by the KRS–5 prism, an average value is used for the region of maximum absorption. The calibration curve is shown in figure 1. The graph was drawn through the experimentally determined wavelengths, and a smooth curve was obtained. The dispersion of the prism in this region is very good, six and one half turns of the spectrometer drum being necessary to change from 22 to 39 μ.

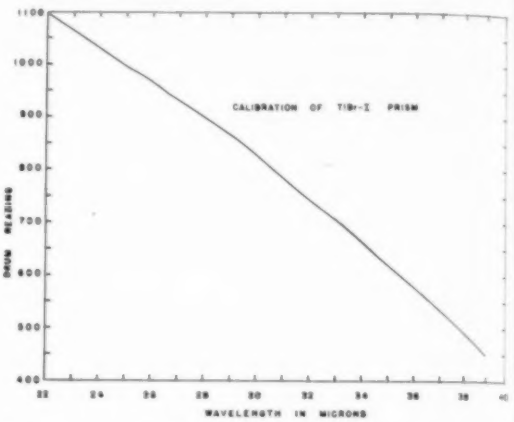

FIGURE 1. *Calibration curve for the* KRS–5 *prism used in a Perkin-Elmer infrared spectrometer.*

In the measurement of the water vapor spectrum, stray radiation became quite appreciable at 34 μ, and increased to about 65 percent of the total energy at 40 μ. In figure 2 is shown the water vapor spectrum as measured with an aluminum reflector in the source box. The two lines that are resolved in the region of 30.6 μ are separated by 4 cm^{-1}. The spectral slit width of the instrument using slits of 0.5 mm is much less than 4 cm^{-1}, and the practical limit is about 2 cm^{-1}.

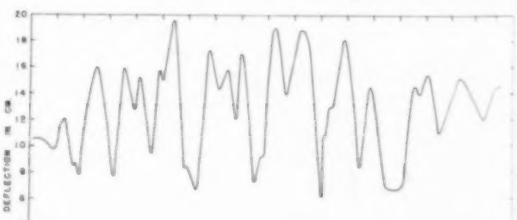

FIGURE 2. *Absorption spectrum of water vapor measured with an aluminum mirror in the source box of the spectrometer.*

[2] H. M. Randall, D. M. Dennison, N. Ginsburg, and L. R. Weber, Phys. Rev. *52*, 160 (1937).

In figures 3 and 4 are shown the water vapor spectrum for the same region using reflectors of CaF_2 and NaF. The stray radiation is reduced to about 5 percent at 37 μ, but there is also a reduction of the total energy. It is possible to extend the measurements with a KRS–5 prism to beyond 40 μ, but the energy is greatly reduced. Small amounts of energy are transmitted by the prism to 41 μ, but only an approximate measurement of the transmission of substances can be made at that wavelength.

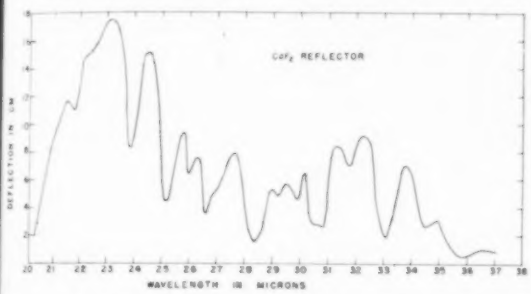

FIGURE 3. *Absorption spectrum of water vapor measured with a* CaF_2 *reflector.*

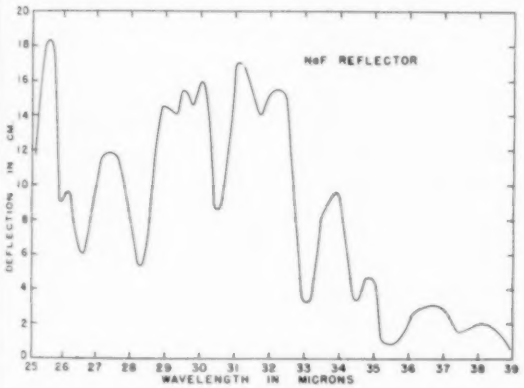

FIGURE 4. *Absorption spectrum of water vapor measured with a* NaF *reflector.*

The infrared spectrometer with the KRS–5 prism and filters has been used to measure the infrared transmission of different solids. Other materials were sought that would be transparent in the 24 to 40 μ region. In figure 5 is shown the percentage transmission of polystyrene, polyethylene, KRS–5, KBr, and AgCl. Polystyrene shows the highest transmission in this region of any substance measured. The high transparency is partly caused by the fact that the layer is only 25 μ thick. When a 1-mm window was used, only 25 percent of the incident radiation is transmitted at 33 μ. However, for coatings and windows, thin films of polystyrene are useful. A layer of polyethylene 240 μ in thickness also shows high transmission in this region. Thinner layers show somewhat higher transmission. The irregular form of the transmission curve is probably caused by absorption in the polyethylene. Films of $(C_2F_4)_x$-$(C_2H_2F_2)_x$, and $(C_2H_2Cl_2)_x$ were also measured, but they have low transmission in this region. The KBr sample is 6.4 mm thick and transmits about 10 percent at 31.5 μ. Thus, in thicknesses of 1 mm or less, KBr will be useful as a window to 30 μ. A sheet of AgCl, 2.1 mm thick, transmits 10 percent at 27.5 μ. However, the sample is slightly discolored and may not have as high transmission as a clear specimen.

Many samples of KRS–5 have been examined, and in figure 5 is shown the transmission of a clear specimen. The transmission at 24.5 μ is approximately 70 percent, about the same as at 20 μ. Most of the loss of energy is caused by reflection. As the wavelength is increased, the transmission decreases and is about 45 percent at 37 μ.

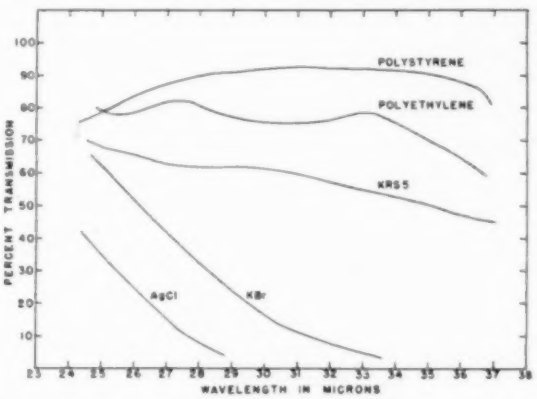

FIGURE 5. *Transmission of polystyrene 25 microns thick, polyethylene 240 microns,* KRS–5 *4 mm,* KBr *6.4 mm, and* AgCl *2.1 mm.*

In figure 6 is shown the transmission of other samples of KRS–5. The lower curve is for a sample that probably contained impurities. One sample, for which the measurements are not plotted on the graph, became opaque at 26 μ.

In figure 7 is shown the transmission of four chlorides. The $PbCl_2$ and TlCl samples were obtained from the Naval Research Laboratory and

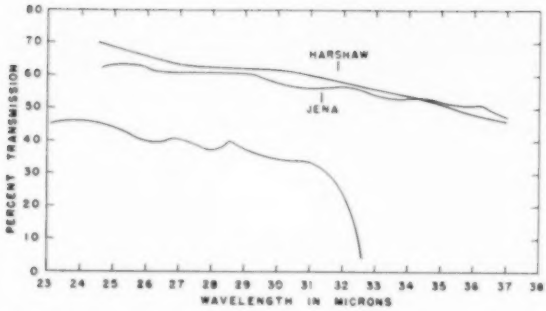

FIGURE 6. *Transmission of three different samples of* KRS–5, *thickness 8 mm.*

the AgCl and KCl samples from Harshaw Chemical Co. All of these materials are well suited for window materials, but the AgCl is the only one of these substances that is not attacked by water.

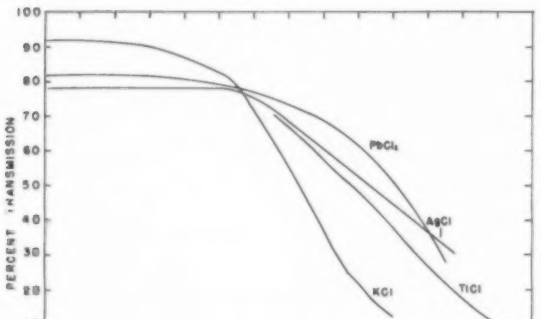

FIGURE 7. *Transmission of* $PbCl_2$ KCl, TlCl, *and* AgCl, *6 mm in thickness.*

In figure 8 is shown the transmission of KCl and TlCl–Br in the near infrared region. The KCl sample transmitted about 92 percent of the incident energy at 16 μ. The TlCl–Br reached a value of about 80 percent at 12 μ.

In figure 9, the transmission of four thallium halides is given. The two samples of TlCl–Br were obtained from different sources. The samples were not annealed and that accounts, in part, for their irregular transmission curves. Some of the small dips in the graph may represent impurities in the sample. Also impurities may cause the different transmitting properties of the two samples of TlCl–Br.

The technique of growing the thallium halide

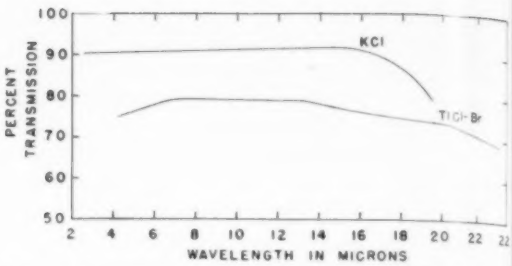

FIGURE 8. *Transmission of* KCl *and* TlCl–Br, KCl, *12 mm in thickness,* TlCl–Br, *6 mm in thickness.*

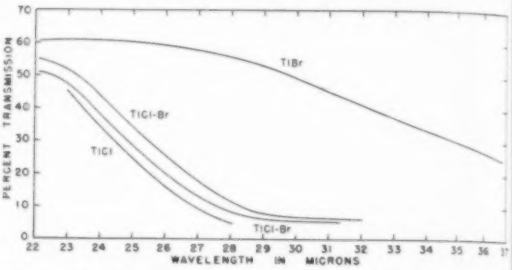

FIGURE 9. *Transmission of* TlBr, *of 2 different samples of* TlCl–Br *and of* TlCl.

All the samples were approximately 6 mm in thickness.

crystals has improved in the last year, and recent samples of KRS–5, in 6-mm thicknesses, have shown good transmission to 40 μ. However, it is difficult to obtain samples that have the same value for the index of refraction over a large cross section. Some transparent sections would not make good prisms because of the blurring of the image at the exit slit of the spectrometer. This problem is now being studied. The KRS–5 prism is a valuable addition to the other materials that are in use for infrared spectrometry.

The measurements made in this work were carried out with a prism cut from a single crystal, and it has been possible to obtain partial resolution of water-vapor lines separated by 2 cm^{-1}. However, in actual operation the spectral slit widths are about 4 cm^{-1} at 33 μ. In the region from 23 to 25 μ, better resolution is obtained with the KRS–5 than with the KBr prism. The lower resolution of the KBr prism in this region probably results from absorption by the KBr prism at 23 μ and longer wavelengths.

Further studies on the transmission of liquids and vapors in the 24- to 40-μ region are being carried out and will be reported in a future paper.

WASHINGTON, May 11, 1948.

U. S. Department of Commerce
National Bureau of Standards

Research Paper RP1912
Volume 41, August 1948

Part of the Journal of Research of the National Bureau of Standards

Mass Spectra of Octanes

By Evelyn G. Bloom, Fred L. Mohler, J. H. Lengel, and C. Edward Wise

Mass spectra of the 18 isomers of octane have been measured. The sensitivity at the maximum peaks in each spectrum relative to *n*-butane is computed as well as the total ionization relative to *n*-butane. Tables and plots of relative intensities in the mass spectra are given, and some correlations with structure are found. All isomers with a tertiary butyl radical have similar spectra. The other isomers tend to dissociate at carbon atoms with one or two side chains attached to them. This determines whether the loss of two or three carbon groups in dissociation is probable. Loss of four carbon groups is probable whenever the molecule ion can break in half in a single dissociation process.

I. Introduction

Mass spectra of the 18 isomers of octane have been obtained as part of a systematic survey of mass spectra of pure hydrocarbons.[1] It is of interest to compare the spectra of these isomers and look for possible correlations between the structure of the molecules and the mass spectra. These octanes are the highest molecular weight saturated hydrocarbons for which pure samples of all the isomers are available.

Unpublished mass spectra of the octanes have also been computed by the Consolidated Engineering Corporation for users of their mass spectrometer. A paper on mass spectrometer analyses of some liquid hydrocarbon mixtures[2] describes the practical problems of analysing mixtures containing octanes by means of these mass spectra.

II. Experimental

Mass spectra have been obtained on a 180° Consolidated mass spectrometer equipped with automatic control of the electron current and automatic temperature control of the ionization chamber. Standard procedures have been followed, and these are given in detail in the API Catalog (see footnote 1). Mass spectra were measured with 50- and 70-v ionization potential, and the values at 50 v are quoted here.

Relative intensities of mass peaks are expressed in terms of the maximum peaks taken as 100 percent and include intensities down to 0.01 percent. The sensitivity at the maximum peaks is measured in terms of the scale divisions of galvanometer deflection per micron pressure in the gas reservoir. The sensitivity at the mass 43 peak of *n*-butane is recorded for each octane spectrum, and the ratio of sensitivity of an octane to that of *n*-butane is a molecular property nearly independent of the arbitrary units used. Details of the mass spectral data are given in the API mass spectral catalog (see footnote 1).

The compounds used were with one exception National Bureau of Standards standard samples of specified purities between 99.5 and 99.94 mole percent. Tetramethylbutane (the only solid octane) was a sample of better than 98 mole percent purity obtained from the Ethyl Corporation by API Research Project 6.

III. Results

Sensitivity and total ionization.—Table 1 gives data on the sensitivity and total ionization of the octanes as compared with *n*-butane. Column 1 lists the 18 isomers in the order of increasing complexity of side chains. Column 2 gives the maximum mass peak in each spectrum, and in most cases it is mass 43. Four isomers have the maximum at 57, and these are the isomers that have a tertiary butyl radical $C(CH_3)_3$, and in the case of 2, 2,3,3-tetramethylbutane, both halves of the mole-

[1] Catalog of mass spectral data, American Petroleum Institute, Research Project 44, National Bureau of Standards, Washington 25, D. C.

[2] R. A. Brown, R. C. Taylor, F. W. Melpolder, and W. S. Young, Anal. Chem. 20, 5 (1948).

cule have this structure. Evidently molecule ions containing this grouping have a high probability of splitting in half.

Column 3 gives values of the ratio of sensitivity at the maximum octane peak to the sensitivity at the 43^+ peak of *n*-butane. This ratio ranges in value from 1.40 to 2.76 with no obvious relation between the value and the molecular structure.

The sum of all the mass peaks in a spectrum multiplied by the sensitivity gives the total ionization in arbitrary units, and this number divided by the total ionization of *n*-butane is a molecular property nearly independent of instrumental factors. This ratio given in column 4 of table 1, is 3.12 for *n*-octane and 1.86 for 2,2,3,3-tetramethylbutane with most other values intermediate. It is evident that total ionization depends on molecular structure though the correlation with structure is again not obvious.

Relative intensities.—Table 2 lists the relative peak heights of 17 mass peaks in the octane spectra

TABLE 1. *Octane mass spectral sensitivity*

Compound	Maximum peak	Sensitivity at maximum peak (relative to *n*-butane*)	Total ionization (relative to *n*-butane)
n-Octane	43	2.46	3.12
2-Methylheptane	43	1.87	2.52
3-Methylheptane	43	1.60	2.42
4-Methylheptane	43	2.13	2.29
2,2-Dimethylhexane	57	2.76	2.14
2,3-Dimethylhexane	43	1.63	1.94
2,4-Dimethylhexane	43	1.42	2.07
2,5-Dimethylhexane	43	1.56	2.08
3,3-Dimethylhexane	43	1.58	1.97
3,4-Dimethylhexane	56	1.40	1.84
3-Ethylhexane	43	2.45	2.43
2,2,3-Trimethylpentane	57	2.24	2.09
2,3,3-Trimethylpentane	43	1.80	2.15
2,3,4-Trimethylpentane	43	1.99	2.15
2,2,4-Trimethylpentane	57	2.53	2.03
2-Methyl, 3-ethylpentane	43	1.98	2.20
3-Methyl, 3-ethylpentane	43	2.14	2.25
2,2,3,3-Tetramethylbutane	57	2.44	1.86

* Corrected to 0.675 A magnet current from 0.535 A values.

TABLE 2. *Mass spectra of octanes*

Compound	Percentage of maximum peak at *m/e* values indicated																
	114	112	99	85	84	71	70	69	57	56	55	43	42	41	29	27	15
(1) *n*-Octane	6.9	0.02	0.1	30.0	6.0	23.5	12.2	1.3	34.2	18.1	10.2	100	15.8	38.9	34.5	26.2	2.2
(2) 2-Me heptane	4.9	.04	12.6	1.8	0.8	12.9	17.2	1.3	73.3	8.1	11.1	100	41.9	38.2	27.7	25.3	3.1
(3) 3-Me heptane	3.0	.02	0.8	49.0	27.3	3.1	2.5	2.7	67.5	38.3	11.2	100	7.9	45.9	40.7	27.8	2.8
(4) 2,4-Me_2 hexane	1.7	.....	1.1	46.1	9.0	14.9	9.8	4.2	72.8	29.6	9.9	100	11.0	43.4	32.4	24.2	3.6
(5) 2,5-Me_2 hexane	3.8	2.02	17.3	0.7	0.2	18.8	9.7	1.4	80.2	7.6	10.9	100	34.0	38.2	21.1	23.3	4.4
(6) 3,4-Me_2 hexane	2.2	.....	0.3	38.1	7.3	1.5	1.9	3.3	79.2	100	9.9	68.1	4.0	56.5	48.0	24.5	2.7
(7) 3-Et hexane	1.6	.....	.1	28.5	22.6	13.5	12.9	2.5	12.4	5.9	11.6	100	6.7	22.8	19.8	19.3	1.7
(8) 2-Me,3-Et pentane	1.3	.....	.1	18.1	4.3	24.7	50.0	3.3	14.8	2.9	17.9	100	14.2	27.0	18.7	19.2	2.2
(9) 3-Me,3-Et pentane	0.00	.....	1.9	64.3	16.8	0.5	0.6	5.8	27.0	2.6	8.0	100	2.4	25.0	21.2	17.5	1.7
(10) 2,2-Me_2 hexane	.03	.....	5.6	0.02	0.01	.7	.3	0.8	100	32.2	4.6	15.9	1.8	26.3	18.6	11.3	2.4
(11) 2,2,3-Me_3 pentane	.03	0.01	3.0	2.9	.2	.4	.5	1.2	100	57.5	5.8	22.8	2.2	33.4	23.0	11.4	2.9
(12) 2,2,4-Me_3 pentane	.02	.....	4.7	0.01	.05	.8	.2	0.5	100	32.7	4.0	23.1	2.0	27.4	15.4	10.7	3.6
(13) 2,2,3,3-Me_4 butane	.03	.....	6.2	.03	.3	.3	.1	1.3	100	27.3	4.5	17.7	1.5	28.2	16.2	7.0	4.7
(14) 3,3-Me_2 hexane	.01	.01	5.1	36.1	7.6	47.0	17.1	3.5	40.7	5.3	11.9	100	3.7	29.4	22.8	20.8	3.0
(15) 2,3,3-Me_3 pentane	.01	.....	3.5	25.0	3.5	45.3	35.5	3.5	35.8	1.5	15.7	100	5.4	28.6	16.0	18.2	3.2
(16) 4-Me heptane	3.1	.02	0.9	4.5	3.0	52.7	46.1	1.3	14.4	2.4	15.3	100	13.5	26.6	22.8	22.5	2.4
(17) 2,3-Me_2 hexane	1.7	.....	.4	1.5	0.4	46.4	58.3	1.6	16.7	1.6	19.8	100	18.9	28.6	19.0	21.6	2.9
(18) 2,3,4-Me_3 pentane	0.3	.....	.2	0.2	1	61.9	40.6	0.9	16.3	2.0	17.1	100	7.4	24.5	13.6	18.2	3.3

and figures 1, 2, and 3 show graphically 15 of the mass spectra and include all peaks greater than 2 percent of the maximum peak. In table 2 the compounds are listed in an arbitrary order to bring together groups with similar mass spectra, and the compounds are numbered consecutively. These numbers are used in the three figures for convenience of cross reference. The figures include structural formulas that omit the hydrogen atoms. In mass computations it is to be remembered that the valence of the carbon atom is four, and the appropriate number of hydrogen atoms must be added. Rearrangement peaks are indicated by *R*.

The spectra of the first nine isomers of table 2 and figures 1 and 2 show a great variety of intensity distributions and are very sensitive to molec-

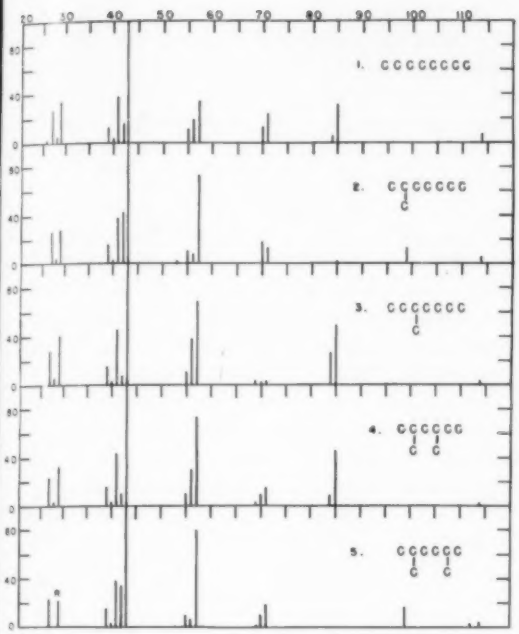

FIGURE 1. *Mass spectra of octanes numbers 1 to 5 of table 2.*

Abscissas are molecular weights, and ordinates are relative peak heights on a scale of 100 for the maximum peak. R indicates a mass peak involving rearrangement of atoms before dissociation.

ular structure. The other nine can be divided into three groups that are similar within each group.

Isomers number 10 to 13, inclusive, are the four compounds with a tertiary butyl radical which, as noted above, are characterized by having the maximum peak at 57. It is seen in table 2 that these spectra are very similar with no large peaks of mass greater than 57. Only one of these, number 10 of figure 2, has been plotted. If it is assumed that it is predominantly the $C(CH_3)_3$ half of the molecule that is ionized when the molecule ion dissociates, then the similarity of the four spectra is understood.

There is also a marked similarity between compounds 14 and 15 and between compounds 16, 17, and 18 shown in figure 3. This is a consequence of some empirical relations between spectra and structure noted in the following paragraphs.

Mass spectra and structure.—The parent peak, 114^+, has a maximum value for the normal compound, and this seems to be a general rule for saturated hydrocarbons. With a few exceptions the height of the peak decreases with increasing number of side chains. In table 2 it is seen that compounds number 9 to 15, inclusive, have much smaller values of 114^+ than any other octanes. These values are 0.03 or less, and other values are 0.3 or greater. This group comprises all the octanes containing carbon atoms with two side chains.

Only one compound, 2,5-dimethylhexane, has an appreciable 112^+ peak. This peak is accompanied by a relatively large metastable transition peak at 110^+, which comes from the delayed dissociation of 114^+ into 112^+ and two hydrogen atoms, after the parent ion has passed through the ion accelerating field.[3]

The 99^+ peak resulting from the loss of a CH_3 radical from 114^+ has a wide range of values from 17.3 to 0.1 percent with no obvious relation between peak height and structure.

There seems to be a qualitative relation between

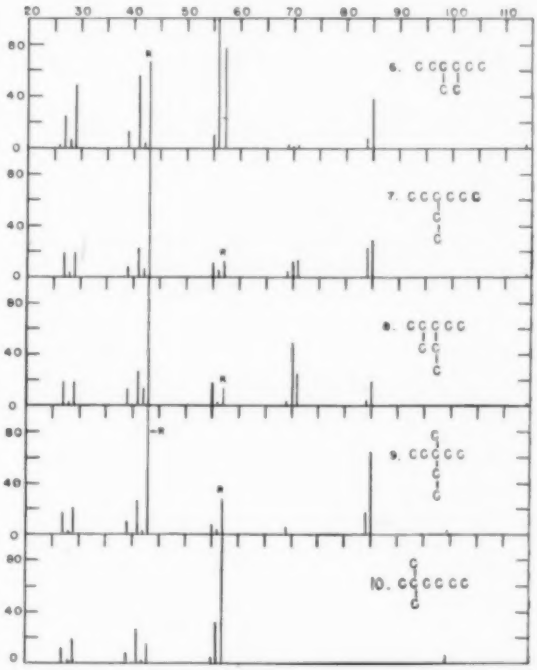

FIGURE 2. *Mass spectra of octanes numbers 6 to 10 of table 2.*

Abscissas are molecular weights, and ordinates are relative peak heights. R indicates mass peaks involving rearrangement of atoms before dissociation.

[3] Metastable transitions in mass spectra of 56 hydrocarbons, by Evelyn G. Bloom, Fred L. Mohler, J. H. Lengel, and C. E. Wise, J. Research NBS **40**, 437 (1948) RP1888.

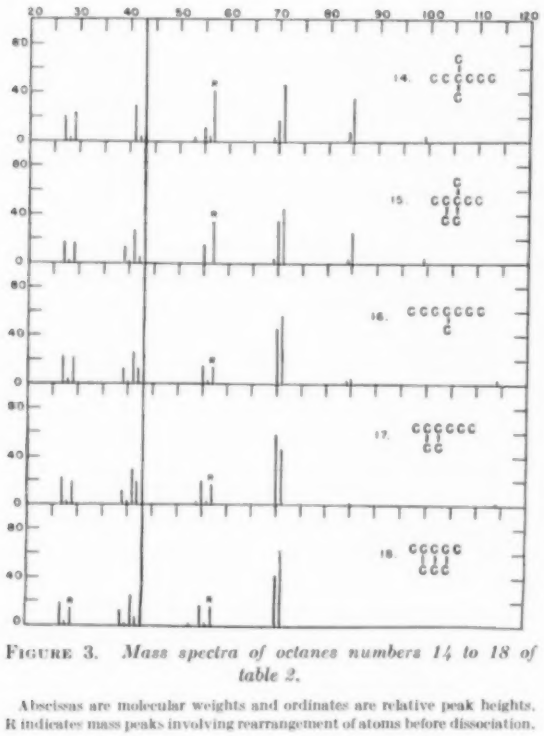

FIGURE 3. *Mass spectra of octanes numbers 14 to 18 of table 2.*

Abscissas are molecular weights and ordinates are relative peak heights. R indicates mass peaks involving rearrangement of atoms before dissociation.

structure and the relative probability of losing two or three carbon groups from the molecular ion. Molecules with side chains tend to dissociate on either side of the carbon atom to which one or two side chains are attached. The four isomers with a tertiary butyl radical can be excluded from consideration, as their spectra depend primarily on this radical and not on the rest of the structure. There remain 13 other isomers with one or more side chains to consider.

Molecules with an ethyl radical, CH_3CH_2, at either or both ends of the molecule attached to a carbon atom with one or two side chains tend to lose this radical and give a large 85^+ peak. The eight isomers that satisfy this condition have 85^+ peaks ranging from 64.3 to 18 percent. Three that have ethyl radicals at either end but not attached to branch points have 85^+ peaks of 4.5 to 1.5 percent, and two that do not have ethyl radicals at the end have values of 0.7 and 0.2 percent.

Molecules with a propyl radical, $CH_3CH_2CH_2$ or an isopropyl radical, $(CH_3)_2CH$ at the ends tend to lose these and give a large 71^+ peak. Ten isomers have propyl groups attached to branch points or have isopropyl groups at the ends and give values of 71^+ that range from 61.9 to 12.9 percent. One has a propyl group not attached to a branch point, and for this 71^+ is 3.1 percent. Two without terminal propyl groups have peaks of 1.5 and 0.5 percent.

Splitting in half to give 57^+ is probable in all cases except *n*-octane, in which the molecule can break in half in a single dissociation whether or not the break occurs at a carbon atom with side chains. As noted before this peak is 100 percent for the four isomers with a tertiary butyl radical. It ranges from 80.2 to 67.5 percent for the other five branched isomers that can break in half while it ranges from 40.7 to 12.4 percent where a rearrangement of hydrogen atoms or a double dissociation is required. In *n*-octane however, 57^+ is 34 percent, which falls in the lower range.

Loss of a 5-carbon group to give 43^+ is not obviously correlated with the structure except that it is relatively small, 15.9 to 23.1 percent, in all the isomers with a tertiary butyl radical. It is 68.1 percent in 3,4-dimethylhexane and 100 percent in all the others. In 3-methyl, 3-ethylpentane, and 3,4-dimethylhexane this highly probable ionization process requires a rearrangement of atoms to give mass 43.

The height of the 29^+ peak covers a smaller range of values and again is not obviously related to structure. In four cases a rearrangement of atoms is required to give $C_2H_5^+$, these peaks tend to be smaller, but there are exceptions.

The 15^+ peaks cover a small range from 4.7 to 1.7 percent. 2,2,3,3-tetramethylbutane with six CH_3 radicals has the largest CH_3^+ peaks, but in general there is not a close correlation between the peak height and the number of CH_3 radicals.

The similarity between 3,3-dimethylhexane and 2,3,3-trimethylpentane results from the above empirical rules. Both molecules can lose 2 carbon groups from one end or three from the other end by breaking at a carbon atom with side chains, and neither molecule can break in half (see fig. 3). This makes 85^+ and 71^+ relatively large and 57^+ small. Again in the last three isomers of table 2, the similarity comes from the fact that all three tend to lose three carbon groups but not two or four.

IV. Conclusions

Chemical analysis. The great variety of octane spectra makes it easy to identify a nearly pure

octane. To analyze a mixture of many octanes is necessarily difficult because of the large number of octanes. Also because of the variety of patterns, there is no basis for selecting an average pattern to analyze for octanes as a group when small amounts are mixed with other hydrocarbons.

To simplify analysis of a complicated mixture, one can use average patterns for the three groups of table 2: 10 to 13; 14 and 15; and 16 to 18. This reduces the number of unknowns in an octane mixture from 18 to 12. In the absence of cyclics and olefines, the 112^+ peak is characteristic of 2,5-dimethylhexane and can be used to identify this if over 2 percent of the compound is present. The problem of analyzing for octanes can thus be reduced to 11 unknowns and 11 simultaneous equations. Electric computing machines capable of handling 12 unknowns are used in routine analyses [4], so the problem could be solved by routine methods, but practical experience indicates that the precision would be low.

Brown, Taylor, Melpolder, and Young (see footnote 2) have made synthetic mixtures containing 16 of the octane isomers as well as C_8 cyclics and have made use of the grouping described above. They find that for good precision of analysis, these mixtures have to be divided into three or more fractions by a fractionating column and the fractions analysed and summed.

Correlation of structure and spectra.—The possibility of deducing the structure of complicated molecules from the mass spectrum is still far from realization. A serious difficulty is that the phenomenon of rearrangement of hydrogen atoms that sometimes occurs in the process of ionization is not understood. This results in ions of masses that would not be expected from simple dissociation of the molecule. The empirical relations pointed out in the preceding section seem to apply with some generality to saturated hydrocarbons. However, they appear to be mutually inconsistent. Apparently in octanes, the high probability of ionizing a tertiary butyl radical almost completely masks the other possible ionization processes. Complications of this latter type are of course to be expected in molecules containing many atoms and many alternative steps in the dissociation process.

WASHINGTON, May 3, 1948.

[4] C. E. Berry, D. E. Wilcox, S. M. Rock, and H. W. Washburn, J. Appl Phys. 17, 262 (1946).

794450—48——4

U. S. Department of Commerce
National Bureau of Standards

Research Paper RP1913
Volume 41, August 1948

Part of the Journal of Research of the National Bureau of Standards

Effects of Substitute Fuels on Automotive Engines

By Clarence S. Bruce, Jesse T. Duck, and A. R. Pierce

Tests were made to determine the operating characteristics of automotive engines with respect to cylinder wear, carbon deposits, life of accessories, and vapor lock. Fuels circulating through standard type pumps for a period equivalent to 200,000 miles had no visible effect on pump diaphragms. Cylinder wear with various fuels was determined by an optical instrument, the McKee wear gage. Wear is determined from changes in lengths of indentations made in cylinder walls with a precisely shaped diamond tool. The wear with alcohol was about half that with leaded gasoline. Carbon deposits also were much lower. There was no indication of dilution of crankcase oil by alcohol. The temperature limits for operation without vapor lock were established for various blends of alcohol with ether and with acetone.

I. Introduction

During the early months of the war, transportation of essential gasoline supplies to our allies became a serious problem. As enemy submarine warfare became more and more aggressive, petroleum reserves in these countries dwindled. Operation of automotive equipment with substitute fuels became common. However, equipment designed for use with gasoline frequently required modification before substitutes could be successfully used, and many operational difficulties were experienced.

In 1942 the National Bureau of Standards began a comprehensive study of the problems involved in the use of substitute motor fuels. This investigation was carried out at the request of the Board of Economic Warfare (later the Foreign Economic Administration) and included studies of the following special problems: (1) Effects of variations in compression ratios, (2) knock ratings, (3) power and fuel consumption with standard type automotive engines, (4) engine tests of gaseous fuels, (5) the effects of mixture distribution on engine performance, (6) starting characteristics at low temperatures and at altitudes, (7) fuel-pump life, cylinder wear, and corrosion, and (8) vapor lock with blends. The results of the first six studies [1 to 6] [1] listed above have been reported in the Journal of Research of the National Bureau of Standards. This report is the last of the series and includes all phases of the work not covered by the six earlier publications. The field to be investigated is very large, and some parts of it could not be completed in the time available. Further study of the causes of cylinder wear and methods of measuring it seem especially desirable. The test results support the widely accepted theory that much cylinder wear is due to corrosion occurring in low-temperature operation. A brief summary of each of the preceding papers follows:

RP1660 Single cylinder engine tests of substitute motor fuels.—Single-cylinder engine tests of nonhydrocarbon fuels and gasoline at fixed compression ratio and at the compression ratio for trace knock for each fuel show no material difference in performance other than those associated with differences in heats of combustion and of vaporization. All of the nonhydrocarbon fuels could be used at compression ratios higher than was permissible with gasoline, with corresponding increases in power and thermal efficiency.

RP1673 Knock ratings of gasoline substitutes.—Knock ratings of gaseous paraffins and olefins through C_4 and of carbon monoxide were determined by current motor and aviation test methods. Auxiliary apparatus and modifications of test engines necessary to rate gases are described.

Antiknock qualities of ethyl and normal butyl alcohol, and acetone, both alone and in blends were determined by current motor fuel rating procedures. Blending characteristics of these materials with straight-run gasoline and naphthas were investigated.

The tests indicated that blends containing up to 45-percent diethyl ether in alcohol should give relatively

[1] Figures in brackets indicate the literature references at the end of this paper.

knock-free performance under conditions of steady operation.

RP1681 The utilization of nonpetroleum fuels in automotive engines.—A number of substitute fuels and blends were tested to determine their relative efficiencies in operation of common types of engines. The tests showed that the maximum power developed with alcohol and with some of the other fuels was slightly greater than with gasoline. The specific fuel consumption with the various fuels was approximately in inverse proportion to the heat of combustion. Analysis showed that the mixture distribution was less uniform with the substitute fuels than with gasoline. Tests made with low-proof alcohols showed that an engine can be operated on a blend as low as 70-proof, but it is ordinarily impractical to use a blend much below 190-proof because of the excessive volumes required.

RP1698 Engine test with producer gas.—Bench tests with a four-cylinder stationary combustion engine were made using gasoline and producer gas from charcoal as fuels. The maximum power of an engine operating on producer gas is about 55 percent of that developed by the same engine when gasoline is used as a fuel. About 11.4 lbs. of charcoal is equivalent to 1 gallon of gasoline. Spark setting studies show that when operating on producer gas the spark should be advanced beyond the setting for maximum power with gasoline.

RP1712 An analysis of the effects of fuel distribution on engine performance.—From an empirical equation based on single cylinder engine test data, and relating engine power to fuel consumption, engine performance curves are derived analytically for typical examples of poor distribution. Investigation of the resulting information shows that the minimum specific fuel consumption is a satisfactory criterion of distribution quality.

RP1811 Cold-starting abilities of various substitute fuels.—Tests of various nonhydrocarbon fuels in a standard eight-cylinder engine showed the starting abilities of some single constituent fuels to be rather limited, but the addition of small percentages of more volatile fuels lowered the minimum starting temperature to a very marked degree.

A limited number of tests under altitude conditions also showed a further reduction in minimum starting temperature for each of the fuels used. This should compensate to some degree for the lower average temperatures usually encountered at higher altitudes, so that for any one area it would be possible to obtain satisfactory starting with a minimum number of blend changes.

In the six papers previously submitted it is indicated that several of the substitute fuels compare favorably with gasoline in general performance. However, most of the test data given relates to performance during comparatively short periods of operation—not long enough to show definitely the effects of physical and chemical properties of the fuels on the engines and their operation. In this report these properties are considered as they affect (1) life of fuel pumps, (2) relative rate of evaporation of fuels, (3) cylinder wear and corrosion, (4) combustion chamber deposits, (5) crankcase oil dilution, and (6) temperature limits for operation without vapor lock.

II. Life of Fuel Pumps

As it was believed possible that parts of the fuel pump might deteriorate through corrosive or solvent action of some of the substitute fuels used, a number of diaphragm type pumps of a given make were set up to deliver a quantity of fuel that would be comparable to normal life operation in an automobile. Six fuel pumps were mounted as shown in figure 1. The pumps were

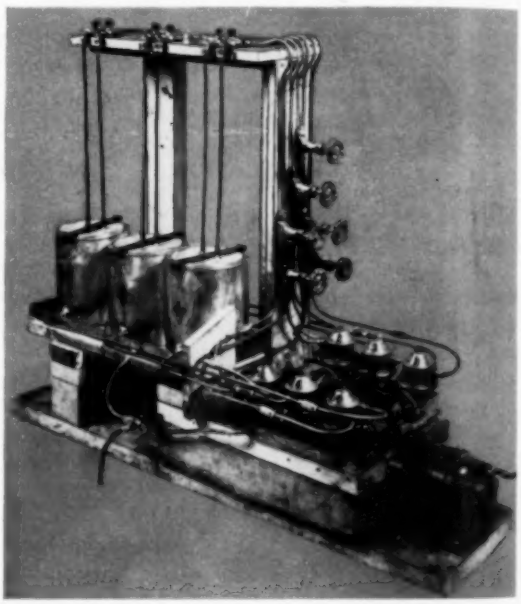

FIGURE 1. *Fuel-pump mounting for pump life and evaporation tests.*

operated by an oscillating arm driven by an electric motor. The stroke of each pump was adjusted so that the unrestricted flow was 600 ml per minute. The outlet of each pump was then throttled until the delivery was 300 ml per minute, approximately the requirement for operation at 70 mph on gasoline. The test setup comprised three 1-gallon tanks with two pumps connected to draw fuel from and return it to each tank through ¼-in. copper tubes discharging 1½ in. above a designated fuel level in the tanks. The open ends of the discharge lines were conducted through

1¼-in. lengths of ⅜-in. copper tubing. By this arrangement, a small amount of aeration, as well as a vent for breathing, was provided. Each tank was filled to the designated level at the beginning of the test. The pumps were equipped with standard valves and diaphragms, the latter being of the paint-base drying-oil type. The pumps operated without failure for 3,500 hr over a period of 5 mo. This is equivalent to more than 200,000 miles of operation, and is considered satisfactory performance as it is somewhat more than the life of the average automobile. Diaphragms impregnated with synthetic rubber were not tested, but it is believed that they would show at least equal resistance to these fuels and blends.

III. Relative Rate of Evaporation of Fuels

The fuel-pump endurance runs afforded an opportunity to find the relative evaporation losses of the test fuels as compared with gasoline. In each test, gasoline was run in one unit so that the effect of ambient conditions might be minimized by correcting to gasoline evaporation. Figure 2 shows the evaporation of gasoline during a 24-hr run. As each unit has a capacity of 3,100 ml of fuel, the loss is about one-fourth of the total volume in 24 hr. All of the relative evaporation loss values given in the following table are based on the loss during 6 hr of operation of the endurance run equipment. This corresponds to an assumed tank loss of 10 percent with gasoline, as shown in figure 2.

TABLE 1. *Relative evaporation loss of fuels*

Fuel	Relative loss rate
Gasoline	52
Acetone	28
n-Butanol	1
Alcohol (190 proof)	10
72% acetone, 28% 190-proof alcohol	43
12% ether, 88% 190-proof alcohol [a]	20

[a] Blend to start at 10°F.

It is seen that the evaporation loss with each of these fuels is materially less than with gasoline. The evaporation loss of the acetone-alcohol blend is somewhat higher than for either of the pure fuels. The ASTM distillation curves for the two blends are shown in figure 3.

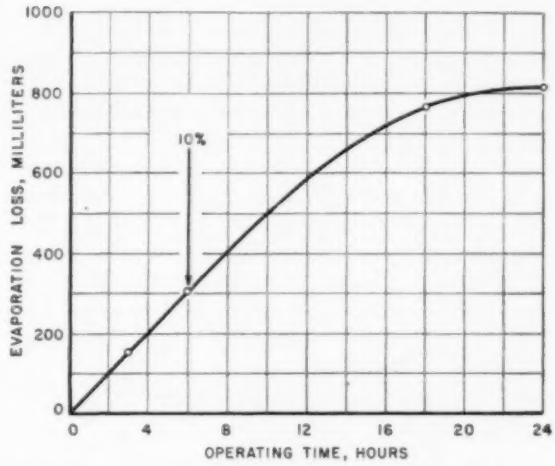

FIGURE 2. *Gasoline evaporation and pump operating time.*

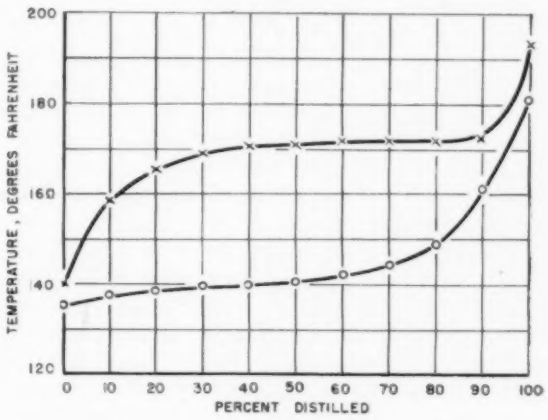

FIGURE 3. *ASTM distillation curves for fuel blends.*

Distillation was started at 10°F. ○, 72-percent acetone in 190-proof alcohol; ×, 12-percent ether in 190-proof alcohol.

IV. Cylinder Wear and Corrosion

1. Types of Cylinder Wear

Cylinder wear may be of three types: (1) Abrasion due to foreign particles in the oil film or intake air, (2) attrition caused by metal-to-metal contact of the pistons or rings and the cylinder bore, and (3) corrosive action on the pistons, rings, or cylinder wall.

Air cleaners and oil filters and changes in engine design have brought about a considerable reduction in cylinder wear during recent years. It is reasonable to assume that the greater part of the

reduction in wear must be due to better protection from abrasion and attrition. It is believed that a large proportion of cylinder wear at present is due to corrosion, but no satisfactory method has been developed to determine how much. Operation of engines with various substitute fuels and with gasoline may offer a good basis for evaluation of corrosion wear, as all conditions that may affect abrasion and erosion are equal. A substantial reduction in cylinder wear with a substitute fuel would indicate more corrosion with gasoline and vice versa. In this connection it has been found [7] that a large proportion of the wear with leaded gasoline is probably due to the presence of the lead compound.

2. Development of the Method

The method used for measuring wear in this investigation was developed a few years ago at the National Bureau of Standards by S. A. McKee at the suggestion of and with the collaboration of H. C. Dickinson. The method utilizes a form of indenting tool similar to that developed by Frederick Knoop, also of the National Bureau of Standards, [8] for determining the hardness of materials. The original wear test apparatus was designed for the measurement of wear in the cylinders of aircraft engines. A full description of the instrument and of the development of the method is given in a paper by McKee [9].

The method is covered by U. S. Patent 2,233,403, granted to Dickinson and McKee on March 4, 1941, and assigned by them to the United States Government. The instrument was modified for use with automobile engines and manufactured by the American Instrument Co., Silver Spring, Md., under license issued by the Secretary of Commerce.

With the McKee gage the wear is determined on the cylinder wall by observing changes in length of indentations made on the wall with a precisely shaped indenting tool. The length of the indentation is accurately measured by a special microscope, and its depth is computed from the length measured. The amount of wear at any given point is considered to be the difference in the computed depths of an indentation before and after a period of operation.

Wear observations made under good conditions with this apparatus are reproducible to 0.00002 in., and amounts smaller than this can be detected.

3. Description of Wear Test Instrument

The instrument is shown in detail in figure 4. There are three essential parts: (1) *A precisely shaped diamond indenting tool.*—The indenter can be adjusted to make marks from ½ to 2 mm in length. In practice a mark about 1 mm long has been found convenient. When the indentations are made in the cylinder wall, the indenter is held securely in place by: (2) *an indentation locater.*—The core of the locater can be rotated within its

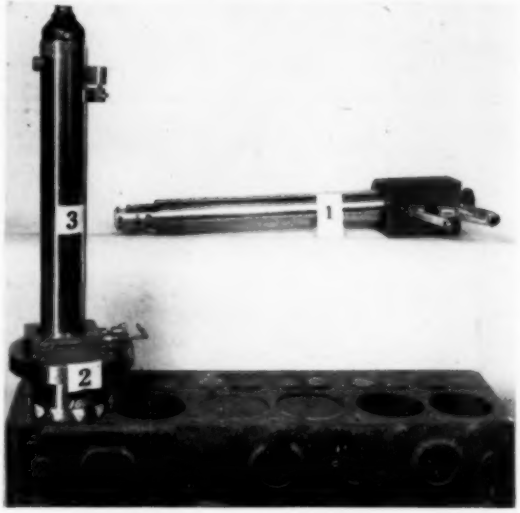

FIGURE 4. *McKee wear gage.*

1, Indenting tool; 2, indentation locator; 3, microscope.

base so that marks can be made at 30-degree intervals around the cylinder wall. (3) *A microscope.*—The microscope fits into the locater exactly in the same way as the indenter, so that when the locater is in the indenting position the indentation is in the field of view. A calibrated scale is superimposed on the image of the indentation so that the length of the indentation is represented by a given number of scale units. Each scale unit represents about 0.01 mm of length. It has been determined that the error of the scale does not exceed 0.2 percent.

4. Analysis of the Indentation

As the depth of the indentation is a function of its length, the depth at any given time may be computed from the length measured on the optical scale. The wear during any period of operation

is represented by the difference in the depths computed before and after the operating period.

The indenter is a pyramid whose base has the shape of a rhombus. The longitudinal axis of the base is several times longer than the transverse axis. The indentation as seen in the microscope is not visible in depth but is seen as an outline of its base. The four triangular faces of the pyramid have equal apex angles.

The width of the indentation has no significance in computations of depth. The depth is computed from the length of the image of the indentation as seen on the optical scale of the microscope. The computations are based on the imaginary triangle formed by joining the ends of the indentation with its apex. In figure 5 the line

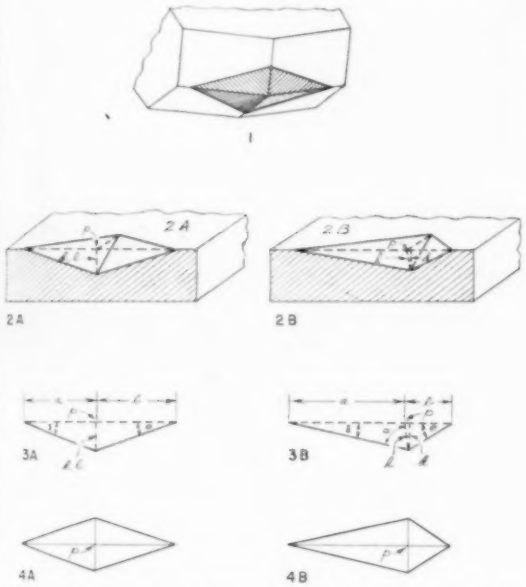

FIGURE 5. *Schematic drawing of indentation made by McKee wear gage.*

$(a+b)$ represents the length of the indentation, which is divided into the segments a and b by the transverse axis of the rhombus that is seen in the visible image of the indentation. The significant factors involved in the mathematical analysis are the relations of the depth of the indentation to the lengths of the segments a and b and to the sines and tangents of the angles θ and δ. If the indentation is symmetrical, $a=b$, and $\delta=\theta=4°$ 17′. (The angle at the apex of the indenter is by actual measurement 171° 26′.)

Therefore when the indentation is symmetrical

$$d=b \tan 4°17'$$

$$d=\frac{a+b}{2} \tan 4°17'$$

$$d=0.0749 \frac{(a+b)}{2}=0.03745(a+b).$$

The graduated scale of the microscope used in this work is divided into 100 divisions, each 0.0099 mm long. Using these values, we find that $d=0.0000146\ (a+b)$ in. if a and b are expressed in McKee gage scale divisions.

If the indentation is not symmetrical, there is a decrease in its depth due to asymmetry. This type of indentation is shown in figure 5 by drawings 2B, 3B, and 4B. The loss in depth may occasionally be as much as 5 percent, although most cases in actual practice are found to be nearly symmetrical. (In 94% of a typical group of marks, the correction for asymmetry was less than 0.5%.)

Figure 6 shows the magnitude of the correction

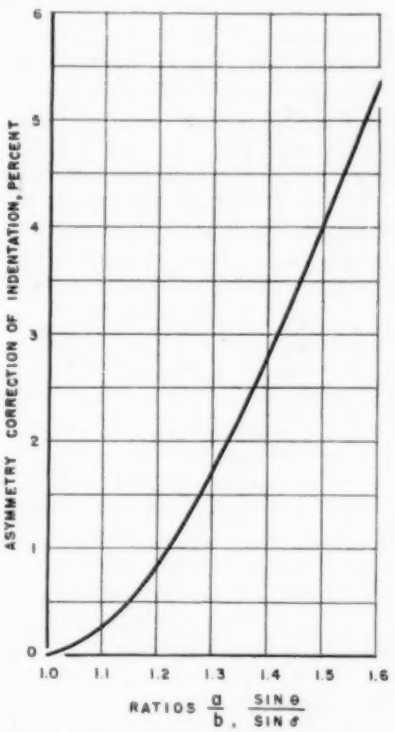

FIGURE 6. *Correction for asymmetry of the indentation.*

necessary for various amounts of asymmetry. The mathematical analysis on which this chart is based is given in the appendix.

As the indentations were made with the long axis along the curved surface of the cylinder wall, there is a correction for curvature. This varies from 2 to 8 percent, depending on the length of the indentation and the size of the cylinder. The value of the correction is closely approximated by the expression $(a+b)^2/8r$, where $(a+b)$ is the length of the mark, and r is the radius of the cylinder.

The indentation is somewhat distorted by springback of metal after the indenter is removed. Our data indicate that this springback will average about 20 percent in cast-iron cylinders. This will be discussed further below.

5. Corrections in Instrument Readings

Within certain limits, metal pushed out of position by an indenting tool will tend to return to its original position, but after the limit of elasticity is reached at least part of the deformation is permanent. The shape of the indentation will therefore not be the same as that of the indenter, because some of the metal has a tendency to spring back when the indenting tool is removed. The final impression may depend on hardness, homogeneity, and elasticity of the metal, and the rate at which the load is applied. Because of these factors, the relation between the length of the mark (indentation) and its depth varies. This relation may change as the mark wears away. It is believed that in homogeneous materials the depth of the mark cannot be more than the theoretical depth represented by the shape of the indenter before its removal.

No satisfactory method was developed to determine accurately the depth of individual marks. All corrections used in analysis of the test results were based on averages. However, the American Instrument Co. furnished a chart in which the corrections were based on the Knoop hardness of the material. In practice this chart could not be used, because the Knoop hardness could not be determined accurately in an engine cylinder.

The calibration for springback of metal in the indentation is shown on figure 7. This plot was derived as follows: Flat metal blocks bearing a considerable number of indentations made with a McKee indenter were lapped off in measured

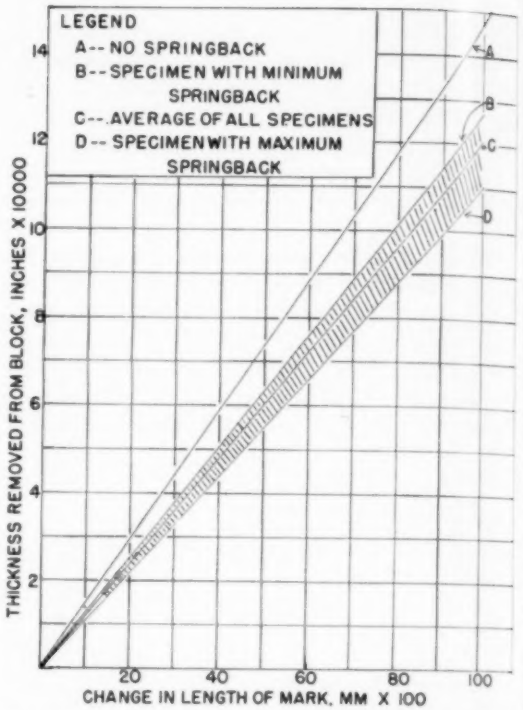

FIGURE 7. *Calibration of wear gage for cast iron and steel specimens.*

A, No springback; B, specimen with minimum springback; C, average of all specimens; D, specimen with maximum springback.

increments, the length of each mark being measured with the McKee microscope after each lapping. In this way a plot of the average loss in length of the mark against loss in thickness of the block was obtained for representative samples of cast iron of a wide range of hardness. Another similar set of measurements was made from a section of steel cylinder liner of the type used in test engine 3. The thickness of the blocks was measured with a special type of gage accurate to 0.00001 in. The blocks were lapped parallel to within about 0.00001 in. Therefore, a thickness measurement might be locally in error by 0.00002 in., although the error would normally be smaller. As this local error would be a considerable part of any measurement that would normally be made with the McKee gage, it was not known whether variations in changes of length of individual marks were due to differences in the proportion of springback or to slight local differences in the amount of metal lapped off. It was therefore

decided that the correction should be applied to a group of several indentations.

It was expected that the amount of springback would vary with the hardness of the metal. However in the work done in the investigation of cast iron specimens, no relation of springback to hardness of the metal was found. The maximum springback found was 25 percent, (fig. 7, curve *D*) the minimum 15 percent, (curve *B*) and the average 18 percent, (curve *C*). The correction found for the steel cylinder liner was 16.5 percent. The probable maximum error in the use of the average value of 18 percent would therefore be about 7 percent.

Skilled operators were able to agree on individual measurements with McKee microscope within 0.01 of the length of the scale, usually within 0.005. When the marks are considered as a group, the error of reading is not therefore believed to be large enough to be considered in relation to the correction for springback. The length of the scale represents 0.00146 in. of depth before corrections for springback are made.

The precision of the method may be illustrated by the following example. Assuming that errors of reading the instrument are nearly eliminated by use of averages, the average length of the marks on cylinder No. 2 at the start of a wear measurement is 85 scale divisions. After a period of engine operation, the average length of the same marks is 75 scale divisions. The net average change in length is 10 scale divisions. The average original depth of the marks allowing for 18 percent correction for springback is 0.00102 in. The average depth at the end of the operating period is 0.00090 in. The change in depth (wear) is 0.00012 in. The correction for springback is believed to be precise within 7 percent. The error in reading, 0.0001 in. of wear, is therefore believed to be less than 0.00001 in. when the marks are considered as a group.

6. Sensitivity of McKee Wear Gage

The McKee indenter is of greatest value in measurement of small increments of wear. The limit to which inside micrometers may be used with any degree of accuracy is probably about 0.0001 in. The accuracy of measurements made with a micrometer is affected to a considerable extent by the temperatures at which measurements are taken. The expansion of metal over a 3- to 4-in. diameter may be as much as 0.0001 in. for a temperature difference of 3 deg C. A further source of trouble when micrometers are used is distortion of the cylinder walls. With the McKee wear gage, both difficulties are very nearly eliminated. The change in depth of an indentation due to a temperature change of 3 deg C is less than one one-hundredth of 1 percent. With micrometers, errors in measurement will vary in proportion to the diameter of the cylinder. In the use of the McKee wear gage, only the amount of metal worn from the cylinder wall is measured. The change in diameter of the cylinder not being a significant factor, distortion of the cylinders may affect the wear at a given point, but the accuracy of measurements is not affected.

7. Test Equipment and Operating Conditions

Five 1942 model engines, of three different makes, were used in the tests. The engines were direct-connected to dynamometers or electric generators and were operated 24 hr a day on a common test cycle that included 20 min operating time and a 10-min shut down in each half-hour. The 20-min operating time consisted of four 5-min periods, during which the engine was operated for 3½ min under conditions equivalent to road operation at about 40 mph, then was idled for 1½ min at 500 rpm. During the shut-down period cold water was forced through the cooling systems of the engines and through special cooling coils in the oil pan, in order to have normal starting conditions at the beginning of each operating period. Throttle operations of the engines were controlled simultaneously by solenoids operated by an electric clock. Speeds and temperatures were recorded after 15 min of operation.

A recording vacuum gage was connected to the intake manifold of each engine. As the manifold pressure is a direct function of the throttle position at any given speed, an excellent record of events of operation was obtained. A typical 24-hr recording is reproduced in figure 8. Temperature and speed readings for a typical 30-min cycle are shown in figure 9.

Twelve indentations were made at each of four levels (½ in., ¾ in., 1 in., and 1¼ in. below the top of the block in each cylinder), one mark on the center line of the thrust face and the others spaced 30 degrees apart around the cylinder. The lengths of the indentations were measured with the McKee

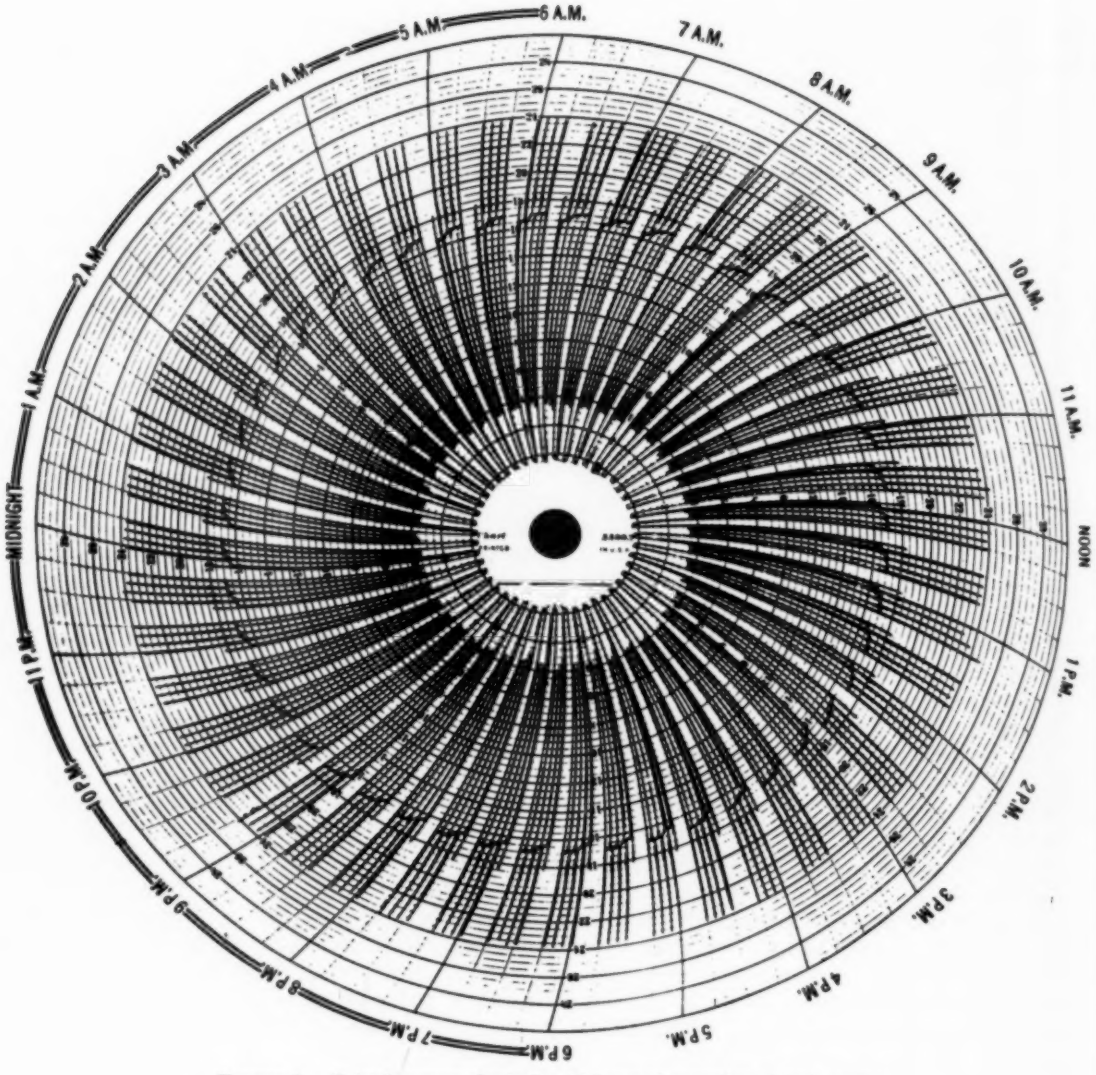

FIGURE 8. *Bristol vacuum chart after 24 hours of operation of test engine.*

gage before the start of the test and after 144 hr of operation. The indentations were made with the long axis perpendicular to the axis of the cylinder.

It was soon discovered that the temperature of the water circulated through the engine during the 10-min shut-down period had a significant effect on the cylinder wear. Thereafter the circulated cooling water was drawn from two storage tanks in which the temperature could be accurately controlled at any desired level.

8. Test Results

There was much variation in wear at the various points. Some of this may be attributed to (1) Slight local depressions and elevations of the cylinder walls, (2) changes in contour of the cylinder walls resulting from unequal torque in tightening of the cylinder head bolts, (3) location of the marks with reference to the height on the cylinder wall or to the circumference of the cylin-

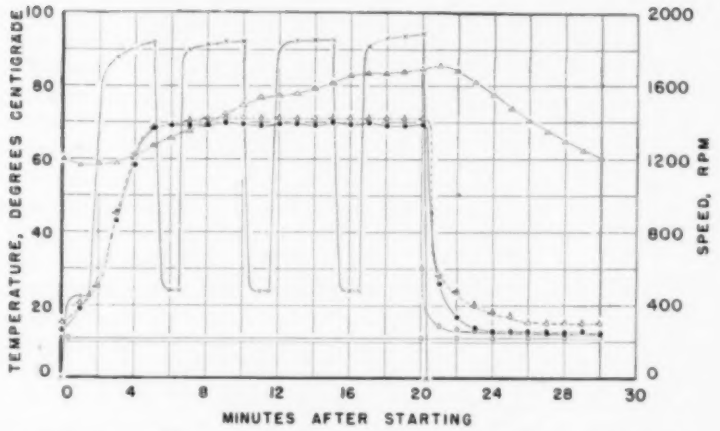

FIGURE 9. *Engine temperatures during typical wear-test operating cycle.*

○, Tapwater; ◇, outlet, oil cooler; ●, outlet, cylinder head; -◇-, jacket water; △, crankcase oil; ×, speed.

der, and (4) inhomogeneities in the composition of the metal.

The cylinder wear was somewhat greater when the engines were operated on gasoline than when some of the substitute fuels were used. There was, however, a considerable variation in the amount of wear from week to week. This variation could not always be accounted for by known factors, but was found to depend to some extent on the temperature of the cooling water, cycle of operation, and other factors. These factors will be discussed further below.

The wear around the circumference of the cylinder did not always follow a consistent pattern. The least amount of wear in nearly every case appeared on the side of the cylinder opposite the one receiving the maximum thrust of the piston. The maximum amount of wear was usually on the sides of the cylinder in line with the engine, although in a very few cases the maximum wear was on the thrust face of the cylinder. Table 2 shows the average wear of five engines with reference to the position of the marks on the circumference of the cylinder.

TABLE 2. *Wear on circumference of cylinder, average for five engines*

Position on cylinder	Engine 1, average wear	Engine 2, average wear	Engine 3, average wear	Engine 4, average wear	Engine 5, average wear
	in.	*in.*	*in.*	*in.*	*in.*
Thrust	0.000074	0.000060	0.000032	0.000050	0.000070
Front	.000098	.000066	.000048	.000067	.000097
Antithrust	.000034	.000028	.000031	.000052	.000095
Rear	.000084	.000058	.000067	.000066	.000088

An 18-percent correction was made for metal springback in the indentation, and an average correction of 5 percent was used for curvature of the cylinder wall. Most values are averages of 240 or more readings and represent at least 10 weeks of engine operation.

A definite vertical pattern of cylinder wear was found to exist with all of the engines tested. This is shown graphically in figure 10 and in table 3 below. This table is a general average of the wear by levels in the cylinder in a large number of tests made with gasoline and alcohol. Each value in the table is an average of the results of

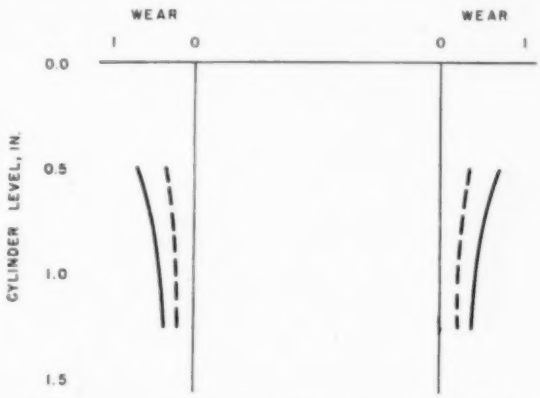

FIGURE 10. *Vertical wear pattern in engine cylinder.*

Units of wear at top of figure are ten-thousandths of an inch. Dotted lines indicate wear with alcohol, solid lines gasoline.

TABLE 3. *Wear by cylinder levels with alcohol and gasoline*

All measurements were made in the upper one-third of piston travel

Distance to top of cylinder	Average wear with gasoline [a]	Average wear with alcohol [b]	Alcohol wear, percentage of gasoline wear
in	*in*	*in*	
½	0.000078	0.000039	50
¾	.000057	.000030	53
1	.000047	.000024	51
1¼	.000041	.000024	58

[a] Average of 4,200 readings.
[b] Average of 936 readings.

tests made on all engines. The corrections for cylinder wall curvature and metal springback are the same as in table 2.

9. Factors Affecting Wear

During the course of the investigation it was observed that the amount of wear varied considerably with changes in operating conditions. As these variations did not always seem consistent, surveys of test conditions were made for a comparatively long operating period, with particular reference to operating temperatures, humidity, starting, etc. In regard to this survey, the following conditions were considered significant. (1) *At low operating temperatures, wear appeared to be greatly accelerated.* In figure 11 the wear in all tests made with five engines on gasoline is plotted against the temperature of the cooling water circulated through the engine during the 10-min. stopping period of each half-hour cycle. Although

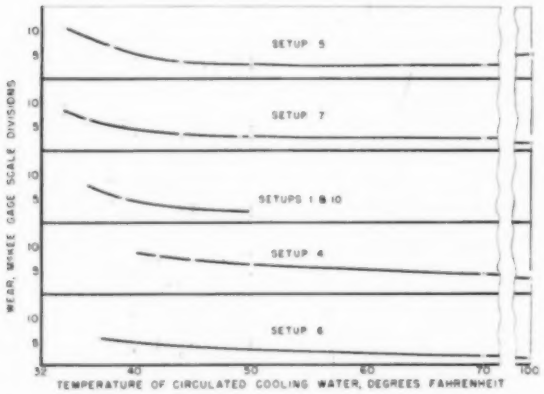

FIGURE 11. *Relation of wear to temperature of circulated cooling water.*

there is a considerable scatter of the points, it is seen that there is a definite trend toward increased wear as the temperature was decreased below about 50° F. The decrease in wear as the temperature is increased beyond this point appears to be small, but it does seem to continue up to 100° F, the highest temperature used in these tests. In two tests where the engines were operated continuously, without the usual 10-min. stop for cooling in each half-hour, the wear was found to be negligible. Presumably most of the wear in the other tests must have occurred during the engine warmup. (2) *During starts made at very low temperatures, wear was found to be greatly accelerated.* Indentations of the usual length (about 1 mm), made on the cylinder walls of an engine used only in starting tests at low temperatures, had completely disappeared after a total operating time of a little more than 200 hr. In these tests the engine was started at atmospheric temperatures ranging from +60° to −25° F and was operated until the engine temperatures had reached equilibrium. The rate of wear in this case was at least six times as great as the maximum found in the usual test cycle at 34° F or above. (3) *No definite relation of wear to atmospheric humidity could be established.* (4) *Some fuels are more corrosive to the engine than are others* (see table 3). In this connection, Williams [10] showed that wear is much accelerated by high sulfur content of the fuel.

The cause of the increase in wear at low operating temperatures is not definitely known. One theory advanced [11, 12, 13, 14] is that there is a deficiency in lubrication during starting and engine warmup. This may be due to a delay in the lubricant reaching the cylinder wall or to loss in viscosity of the lubricant through dilution. A second theory holds that the wear at low engine temperatures is due to corrosion [10, 13, 15]. Williams believed that low temperatures permitted the condensation of moisture on the cylinder walls, thus favoring the formation of corrosive acids. He pointed out that wear was greatly accelerated when the temperature of the cylinder walls was just below the dewpoint. Further support for the corrosion theory is found in the results shown in table 3. The wear with alcohol fuels was found to be about half that with gasoline in tests made under comparable conditions. It is reasonable to assume that the difference in wear may have been

due to differences in the corrosive characters of the fuels.

It is improbable that much corrosion occurs during the actual stop. Studies have shown [16] that the corrosion film formed on iron tends to protect the surface from further corrosion, unless this film is removed by mechanical means as by piston rings during operation of an engine. Further support for the theory that corrosion occurs during the warmup is found in the fact that the test engines were connected to heavy dynamometers or generators, so that when switched off they rotated a number of revolutions before stopping. In this way the cylinders were left filled with a mixture of fuel and air that was not particularly corrosive. During the warmup a considerable number of explosions occur before the temperature of the walls is raised above the condensation point. The dewpoint temperature for exhaust gas [10] is about 126° F at atmospheric pressure and about 300° F at 500 lb/in.^{2}, approximately the maximum pressure reached in an automotive engine. It is seen in figure 9 that with the circulated tap water at 52° F approximately 4 min of operation was required to raise the water jacket to 140° F, the temperature generally accepted by the automotive industry as the minimum for satisfactory operation.

Assuming that 4 min of the cycle would be required for the engine to reach the dewpoint temperature, there would be more than 2,500 explosions in each cylinder that might be followed by condensation of corrosive gases, and more than 10,000 strokes of the piston during which the piston rings would wipe oil and corroded material from the cylinder wall. In successive strokes of the piston there would be further corrosion that would in turn be wiped off so that more corrosion could take place.

It should be observed that these tests were run in a laboratory where there was comparative freedom from dust and other abrasive materials ordinarily picked up in road operation.

Sparrow and Scherger point out [11] that much wear results from faulty distribution of cooling water. This may result in condensation from too low a wall temperature or in hot spots that cause the oil to lose its viscosity. It was observed that in some of the engines tested at the National Bureau of Standards the front cylinders (nearest the water pump) always had a greater wear than any of the other cylinders.

Further discussion of the cause of wear is given by Williams, who made an extensive review of the literature [17 to 28] on the subject. In view of the above evidence, it is therefore believed that a considerable part of cylinder wear may be due to the corrosion occurring during the engine warmup when condensation on the cylinder walls is possible. The wear might be much reduced if the jacket temperatures could be kept above the dewpoint or if some method could be developed to make the cylinders, pistons, and rings completely corrosion resistant.

V. Combustion Chamber Deposits

After each 144-hr run, the deposits of carbon were carefully removed from the cylinder head, valves, and engine block. The deposits were weighed and extracted with naphtha to remove traces of oil and moisture remaining and were analyzed for iron and lead. The iron in a weighed and dried sample is first dissolved in a mixture (1:5) of nitric and sulfuric acids, then precipitated as a hydroxide, dissolved in 6 *N* hydrochloric acid and determined by titration with potassium dichromate after reduction with stannous chloride. The total amount of noncombustible ash is determined by heating a weighed sample of the engine deposits at about 1,000° C to constant weight The remainder of the sample is assumed to be carbonaceous material.

A total of 49 samples were weighed and analyzed. The samples represented 62 weeks of engine operation. The analyses are summarized in table 4.

TABLE 4. *Combustion chamber deposits*

Total operating time	Fuels	Average total deposits per week	Average oil-free deposits per week	Average iron deposits per week
Weeks		*g*	*g*	*g*
17	Gasoline	18.08	16.67	0.268
1	200-proof alcohol	3.66	3.11	.152
2	190-proof alcohol	6.15	5.09	.302
5	Fuel blend 1	11.51	9.69	.266
2	Fuel blend 2	11.04	9.01	.393
2	Fuel blend 3	10.89	8.74	.265

It is shown that the combustion chamber deposits are considerably less with 190-proof and

200-proof alcohols than with gasoline. Experimental work has indicated that most engine deposits are due to incomplete combustion of the lubricating oil [29]. It is therefore believed possible that the smaller carbon deposits occur with alcohol and its blends because of the fact that there is no dilution of the oil such as occurs with gasoline. When the lubricant is diluted with gasoline it loses much of its viscosity, so that presumably more of it can reach the cylinders, making more engine deposits possible. The differences in iron deposits may be due to metal removed from the cylinder head, etc., by the sampling tools. Consequently the amount of iron has no significance.

VI. Analysis and Consumption of Lubricating Oil

Twenty-eight samples of crankcase oils from engines operating on gasoline and alcohol were analyzed. There was no indication of dilution of the lubricant by an alcohol fuel. Gasoline shows a dilution of 2 percent by weight, estimated by ASTM method D–322–35. The ASTM method employs steam distillation and is not applicable to crankcase oils from engines operating on alcohol and other water soluble fuels.

The percentage by weight dilution of the alcohols was based on the loss by evaporation upon heating for two 1-hr periods at 105° C, and the results were compared with a sample of new oil. This method was not satisfactory for gasoline, as it involved prolonged heating with an uncertain endpoint.

Five engines were in operation over the period during which the oil consumption was taken, but due to the fact that in most of the tests the engines were operated on gasoline, some of the data on the other fuels may not be representative of average conditions. Figure 12 shows the average oil consumption of one of the engines in which a number of tests were made with each fuel. These tests gave no indication that there was any significant difference between the oil consumption in operation with gasoline or alcohol fuels.

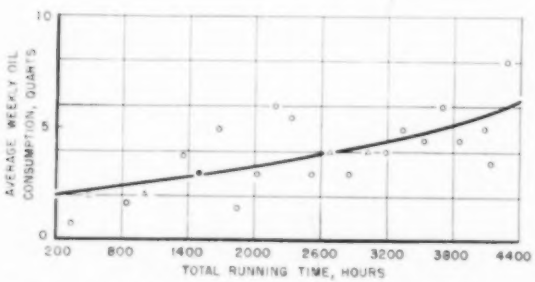

FIGURE 12. *Oil consumption of wear-test engine with various fuels.*

○, Gasoline; △, 190-proof alcohol; ●, fuel 1; □, 200-proof alcohol.

VII. Operating Temperature Limits of Blends

The starting lines shown in figure 13 were taken from data reported by R. E. Streets [6]. It is shown that starting is possible at temperatures somewhat below normal winter temperatures in this country if ether is used in the alcohol blend, but vapor lock results at fairly low temperatures. Acetone is not as good as ether in lowering the minimum starting temperature, but it is not as likely to cause vapor lock.

Vapor lock is partial or complete interruption of fuel flow due to formation of vapors in the fuel lines or carburetor. The net result of vapor lock is a considerable increase in the leanness of the mixture ratio. This is usually indicated by one or more of the following phenomena: (1) Loss of power, (2) backfiring and/or surging, (3) abnormally high engine temperatures, (4) detonation and (5) complete stoppage of the engine or failure to start. Closely related to vapor lock is another hot weather fuel trouble, carburetor percolation. This is the result of the accumulation of excessive quantities of vapor in the carburetor bowl. It usually occurs during idling or during a stop with ignition off after a hard run, and is evidenced by stalling of the engine during idling or by difficulty in starting because of an over-rich mixture.

Unblended 190-proof alcohol is not subject to vapor lock at any atmospheric temperature likely to be encountered. However, it cannot be used for starting at temperatures much below 60° F unless it is blended with a more volatile fuel. In order to determine the permissible fuel volatility for adequate starting with reasonable freedom from vapor lock, a series of tests was run with a 1942 model automobile. The test car was equipped with nickel resistance thermometers for measurement of temperatures of outside air, carburetor air, fuel in the carburetor bowl, carburetor flange, fuel in tank, water jacket, and crankcase oil. A gage was

connected to the fuel line to indicate pump discharge pressure. Fuel from the tank was sampled at intervals through a coil packed in dry ice so that no vapors would be lost in sampling. The test procedure was to (1) charge the fuel tank with alcohol to which a volatile blending agent had been added in proportions estimated to cause vapor lock; (2) drive the car at 50 mph for 1 hr, taking readings of the temperatures in the fuel system, etc., at 15-min intervals; (3) stop the car facing the wind and the engine idling; (4) read temperatures of nickel resistors 4 min after stop and turn off ignition 5 min after the stop; (5) take another set of readings 14 min after the ignition was switched off, restart the engine 1 min later; and (6) get the car into high gear as soon as possible and attempt to accelerate with wide open throttle. Cutting out of the engine due to lack of fuel was considered an indication of vapor lock. A further indication of vapor lock was a fall of the fuel-pump pressure to zero.

If the system did not vapor lock, more of the volatile blending agent was added to the fuel, the car was driven about 6 miles at 50 miles per hr, and the above procedure was repeated. Further additions of the blending agent were made until vapor lock occurred. Samples of each fuel blend with which the engine was operated were taken for laboratory study. The Reid vapor pressure was measured by ASTM method D 323–41. The refractive indices of the samples were determined so that the composition of the blends could be estimated.

Control tests were made to determine the operating characteristics of the test car using blends of gasoline and isopentane. Vapor lock occurred at an atmospheric temperature of 100° F with a blend having a Reid vapor pressure of 7.3 lb/in.^{2}. This is considered as a normal vapor-locking tendency. As the carburetor used in the tests had a mixture control, this carburetor was replaced with a standard carburetor after incipient vapor lock was obtained and the test repeated with the same result, indicating that the use of the special carburetor did not change the vapor-locking tendency of the car.

The Reid vapor pressure of the alcohol blend that gave vapor lock at 100° F is low as compared with that of gasoline being 3.5 lb/in.^{2} for the blend and 7.3 lb/in.^{2} for gasoline. Due to the fact that the Reid method is designed for a V/L ratio of 4 and the vapor handling capacity of the car is about 30, comparisons cannot be made of fuels whose V/L relations are as different as those of alcohol and gasoline. The data on the alcohol blends are therefore presented in volume percentage of the blend rather than giving the Reid vapor pressure.

The results of the tests are shown graphically in figure 13. The useful operating range of a

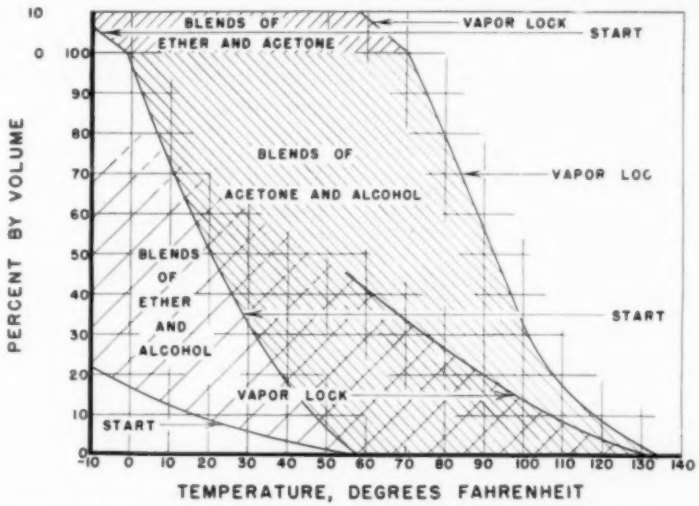

FIGURE 13. *Operating limits of alcohol blends with ether and acetone.*
The blending agent is the first of each pair. The temperatures are atmospheric temperatures.

blend containing any given percentage of a blending agent is indicated on figure 13 by the abscissae of the points at which the percentage line indicated intersects the lines for starting temperature and vapor lock. The lines for minimum starting temperature and vapor lock are the heavy lines that cross the page diagonally. For example the ordinate for 10-percent ether in alcohol crosses the lines for starting and vapor lock at points that indicate that starting is possible at 16° F, while vapor lock will occur at 107° F. It will be seen that small percentage of ether will lower the starting temperature somewhat more than the same percentage of acetone. The useful range of a blend containing 10-percent ether in alcohol is from 16° to 100° F, or 84 degrees. Sixty percent of acetone must be added to alcohol before an engine can be started at 16° F, and the blend will cause vapor lock at 88° F, a useful range of 72 degrees. Therefore, disregarding cost and availability, ether is a better blending agent for alcohol than is acetone.

VIII. Conclusions

This series of tests indicates that 190-proof alcohol blended with ether for starting at low temperatures is a satisfactory substitute for gasoline. In general, power and engine performance are comparable for the two fuels. Fuel system parts are not adversely affected by alcohol or ether.

The relative rate of evaporation, combustion chamber deposits, and crankcase oil dilution are less with alcohol than when operating on gasoline.

The disadvantages of using alcohol are that the range of atmospheric temperatures for operation is less than with gasoline, and that larger quantities of the more expensive fuel (alcohol) are required.

IX. References

[1] Donald B. Brooks, J. Research NBS **35,** 1 (1945) RP1660.

[2] Afton D. Puckett, J. Research NBS **35,** 273 (1945) RP1673.

[3] Jesse T. Duck and C. S. Bruce, J. Research NBS **35,** 439 (1945) RP1681.

[4] F. A. Middleton and C. S. Bruce, J. Research NBS **36,** 171 (1945) RP1698.

[5] Donald B. Brooks, J. Research NBS **36,** 425 (1945) RP1712.

[6] R. E. Streets, J. Research NBS **39,** 39 (1947) RP1811.

[7] George Beck, Zylinder und Kolbenring Verschleiss Deutsche Kraftfahrtforschung **29** (1939).

[8] Frederick Knoop, Chauncey G. Peters, and Walter B. Emerson, J. Research NBS **23,** 39 (1939) RP1220.

[9] S. A. McKee, J. Research NBS **39,** 155 (1947) RP1819.

[10] C. G. Williams, Collected researches on cylinder wear (British Institution of Automobile Engineers, London, 1940).

[11] S. W. Sparrow and T. A. Scherger, SAE J. **38,** 117 (1936).

[12] Frank Jardine, Automotive Ind. **51,** 242 (1924).

[13] Otto M. Bur'hardt, SAE J. **19,** 657 (1926).

[14] A. E. Becker, Automotive Ind. **64,** 401 (1931).

[15] GMC Research Staff, Automotive Ind. **50,** 956 (1924).

[16] U. R. Evans, Metallic corrosion, passivity, and protection E. Arnold, & Co., (London, 1937).

[17] C. E. Summers, SAE J. **16,** 243 (1925).

[18] Symposium, SAE Summer Meeting, June 27, 1924, SAE J. **15,** 10 (1924).

[19] A. H. Hoffman, SAE J. **25,** 625 (1929).

[20] Symposium, Baltimore SAE Section Meeting, SAE J. **27,** 518 (1930).

[21] E. J. Lowery, SAE J. **20,** 277 (1927).

[22] E. Zimmerman, Metals & Alloys **2,** 95 (1931).

[23] E. Piwowarsky, Giesserei-Ztg. **24,** 553 (1927).

[24] N. Stern, Motorwagen **29,** 479 (1926).

[25] Anonymous, Metallurgist **7,** 132 (1931).

[26] H. Bornstein, ASTM Proc. **20,** part II, 166 (1929).

[27] Gusseisen, Z. Ver. deut. Ing. (1930).

[28] Staff of the John I. Thorncraft Co., Nickel Bul. (London) 4, 295 (1931).

[29] Donald B. Brooks, SAE J. **18,** 48 (1926).

X. Appendix

1. Mathematical Relationships in the Indentation

The angle at the apex of the diamond used in the tests was 171°26′. The sum of the angles δ and θ in both triangles of figure 5 is therefore 8°34′. In 3A, $\angle\delta=\angle\theta$ and the depth of the indentation may be determined by the equation

$$\left.\begin{aligned} d_A &= a_A \tan\theta \\ a_A &= \frac{d_A}{\tan\theta} \end{aligned}\right\} \quad (1)$$

In the above equations, and those that follow, the subscript A denotes a symmetrical indentation and the subscript B denotes an asymmetrical indentation. The amount of rotation of the indenter is indicated by the angle ρ included between d and l

$$\left.\begin{aligned} \delta_B &= \theta_A - \rho \\ \theta_B &= \delta_A + \rho \end{aligned}\right\} \quad (2)$$

By the law of sines

$$\frac{a_B}{b_B} = \frac{\sin(\theta_A+\rho)}{\sin(\theta_A-\rho)} \quad (3)$$

$$a_B = b_B \frac{\sin(\theta_A+\rho)}{\sin(\theta_A-\rho)} \quad (4)$$

The sine ratio,

$$\frac{\sin\ (\theta_A+\rho)}{\sin\ (\theta_A-\rho)} \tag{5}$$

may be expressed as R, so $a_B=b_BR$.

$$a_A=b_A,\ 2b_A=b_B+b_BR=b_B(1+R) \tag{6}$$

$$l_B=a_B\frac{\sin\ (\theta_A-\rho)}{\sin\ \alpha} \tag{7}$$

$$d_B=l_B\cos\ \rho=\frac{a_B\sin\ (\theta_A-\rho)\ \cos\ \rho}{\sin\ \alpha} \tag{8}$$

$$b_A=b_B\frac{(1+R)}{2} \tag{9}$$

and

$$d_A=b_B\frac{(1+R)\ \tan\ \theta_A}{2}$$

$$\frac{d_B}{d_A}=\frac{\dfrac{a_B\sin\ (\theta_A-\rho)\ \cos\ \rho}{\sin\ \alpha}}{b_B\dfrac{(1+R)\ \tan\ \theta_A}{2}} \tag{10}$$

$$a_B=b_BR,$$

so

$$\frac{d_B}{d_A}=\frac{2R\sin\ (\theta_A-\rho)\ \cos\ \rho}{(1+R)\ \tan\ \theta_A\sin\ \alpha} \tag{11}$$

Substituting for R,

$$\frac{d_B}{d_A}=\frac{\dfrac{\sin\ (\theta_A+\rho)\ \sin\ (\theta_A-\rho)\ \cos\ \rho}{\sin\ (\theta_A-\rho)}}{\dfrac{[\sin\ (\theta_A-\rho)+\sin\ (\theta_A+\rho)]\tan\ \theta_A\sin\ \alpha}{\sin\ (\theta_A-\rho)}}$$

$$=\frac{2\sin\ (\theta_A+\rho)\ \sin\ (\theta_A-\rho)\ \cos\ \rho}{[\sin\ (\theta_A-\rho)+\sin\ (\theta_A+\rho)]\tan\ \theta_A\sin\ \alpha}. \tag{12}$$

Expanding

$$\frac{d_B}{d_A}=\frac{2(\sin\theta_A\cos\rho+\cos\theta_A\sin\rho)(\sin\theta_A\cos\rho-\cos\theta_A\sin\rho)\ \cos\rho}{(\sin\theta_A\cos\rho-\cos\theta_A\sin\rho+\sin\theta_A\cos\rho+\cos\theta_A\sin\rho)\tan\theta_A\sin\alpha}$$

Simplifying

$$\frac{d_B}{d_A}=\frac{\sin^2\theta_A\cos^2\rho-\cos^2\theta_A\sin^2\rho}{\sin\theta_A\tan\theta_A\sin\alpha}.$$

But

$$\alpha=90-\theta_A,$$

and

$$\sin\alpha=\cos\theta_A$$

$$\tan\theta_A=\frac{\sin\theta_A}{\cos\theta_A},$$

so substituting, we find that

$$\left.\begin{aligned}\frac{d_B}{d_A}&=\frac{\sin^2\theta_A\cos^2\rho-\cos^2\theta_A\sin^2\rho}{\sin^2\theta_A}\\&=\cos^2\rho-\frac{\cos^2\theta_A}{\sin^2\theta_A}\sin^2\rho=\cos^2\rho-\mathrm{ctn}^2\theta_A\sin^2\rho\\&=1-\sin^2\rho-\mathrm{ctn}^2\theta_A\sin^2\rho\\&=1-(1+\mathrm{ctn}^2\theta_A)\sin^2\rho\end{aligned}\right\} \tag{13}$$

The difference between the depths of the symmetrical and asymmetrical indentations is expressed by the equation

$$1-\frac{d_B}{d_A}=(1+\mathrm{ctn}^2\theta_A)\sin^2\rho. \tag{14}$$

If $\theta_A=4°17'$, $\mathrm{ctn}^2\theta_A=178.22$ and $1-\frac{d_B}{d_A}=179.22\sin^2\rho$. (15)

Using the equation above and the sine ratio from eq 5, a correction chart for asymmetrical indentations may be set up, as shown in table 5. As the sine ratio is the same as the ratio of the visible segments of the mark, a and b, the angle of rotation, ρ, is determined from the ratio a/b

TABLE 5. *Correction chart for asymmetrical indentations if* $\theta_A=4°17'$

The correction for asymmetry is found by comparison of columns 2 and 3

Angle of rotation of indenter	Ratio of a/b*	Correction for asymmetry
		Percent
0.0	1.000	0.0000
.1	1.048	.0546
.2	1.098	.218
.3	1.150	.490
.4	1.206	.87
.5	1.264	1.36
.6	1.325	1.96
.7	1.390	2.68
.8	1.458	3.50
.9	1.531	4.42
1.0	1.608	5.46

* Also ratio of $\sin\theta/\sin\delta$.

WASHINGTON, June 12, 1947.

794450—48——5

U. S. Department of Commerce
National Bureau of Standards

Research Paper RP1914
Volume 41, August 1948

Part of the Journal of Research of the National Bureau of Standards

Applications of Magnetochemistry to Polymers and Polymerization [1]

By Pierce W. Selwood [2]

After a brief review of fundamental definitions, experimental methods, theoretical and semiempirical results on diamagnetic substances, two topics are considered: First, studies of the diamagnetic anisotropy of crystalline and oriented materials. Using solid naphthalene as an illustration, it is shown how to obtain the principal molecular susceptibilities from the measured parameters of the single crystal and the molecular orientations in the unit cell as derived from X-ray studies. Conversely, the direction cosines for solid diphenyl are calculated from the measured macroscopic susceptibilities and the susceptibilities of the molecule. Results recently obtained on the anisotropy of cellulose, protein fibers, and stretched rubber indicate the value of such methods, particularly for oriented polymers containing aromatic groups, because of the large effects of the latter. Next, attention is devoted to the paramagnetism of oxygen and free radicals that can be utilized as a measure of the concentration of the species. Radical concentrations as low as 10^{-6} mole per liter may be estimated by means of a modification of the Gouy-balance. It has been employed in a study of the thermal polymerization of styrene at 66° C. From the changes in diamagnetism in the course of the reaction, the rate of consumption of oxygen present is determined. Assuming this to be due to combination with styrene radicals, the rate of thermal initiation is estimated to be 3.8×10^{-14} mole^{-1} liter sec^{-1}. However, in order to obtain by magnetic methods directly the free radical concentration in ordinary chain polymerization processes, the sensitivity would have to be improved by several orders of magnitude.

I. Introduction

There are two principal types of magnetic measurements from which polymer chemistry may gain information. These are (1) the study of diamagnetic anisotropy, and (2) the *in situ* study of free radicals and other paramagnetic components, such as oxygen. Neither of these methods has so far received much attention from polymer chemistry. There is reason to believe, however, that they will both make important contributions to our knowledge of polymers and polymerization in the not too distant future.

The numerical quantity with which magnetochemists are chiefly concerned is the magnetic susceptibility, χ. This quantity is defined as follows: Let H be the intensity of a magnetic field and B be the magnetic induction in any substance placed in the field. We then have $B=H+4\pi\mathfrak{d}$, where $\mathfrak{d}$ is the intensity of magnetization, and $\mathfrak{d}/H$ is the magnetic susceptibility per unit volume, K. Taking d as the density of the substance: $K/d=\chi$, which is the magnetic susceptibility per unit mass.

For nearly all organic compounds the magnetic susceptibility is negative. Such substances are said to be diamagnetic; they are repelled by a magnet. The order of magnitude of the susceptibility for organic compounds is -0.3×10^{-6} to -0.8×10^{-6}. The susceptibility of water is -0.720×10^{-6}. For diamagnetic substances the susceptibility is independent of field strength and virtually independent of temperature.

For many transition group elements and their compounds, and for organic and inorganic free radicals, the magnetic susceptibility is positive. These are said to be paramagnetic. The susceptibility of paramagnetic substances is often 10 to

[1] This paper was presented as part of the 1946-47 series of lectures on the Properties of High Polymers given at the National Bureau of Standards.
[2] Professor of chemistry, Northwestern University.

100 times as large numerically as that of diamagnetic substances. Paramagnetic substances are attracted to a magnet. Positive magnetic susceptibilities are substantially independent of field strength, but they frequently vary approximately inversely as the absolute temperature. More often, they follow the Curie-Weiss law, $\chi = C/(T+\Delta)$, where C and Δ are constants and T is the absolute temperature.

Magnetic susceptibilities are most frequently measured by the method of Gouy (fig. 1). A

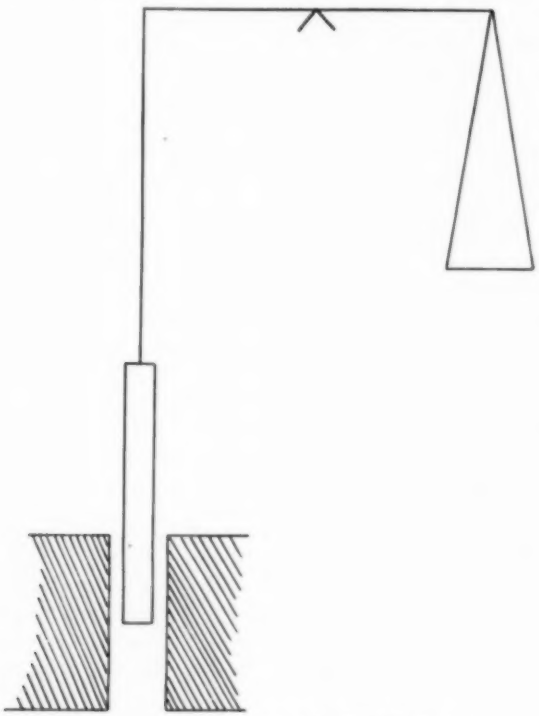

FIGURE 1. *Principle of the Gouy method.*

cylindrical sample is suspended from a balance so that one end of the sample is in a region of high magnetic field intensity, and the other end is in a field of negligible intensity. The fields commonly used are produced by large electromagnets and are of the order of 5,000 to 20,000 gauss. On application of the field the sample will, if diamagnetic, seem to lose in weight, or if paramagnetic, seem to gain in weight. The changes so observed are of the order of milligrams.

If the sample is a liquid or a powder, it may be contained in a calibrated glass tube. For most measurements on organic compounds, it is necessary to use a microbalance to gain adequate sensitivity. Temperature control is generally necessary, and for paramagnetic substances it is frequently necessary to make measurements over a wide range of temperature. With all refinements, a sensitivity of four significant figures is attained without too much difficulty.

There have been innumerable modifications of the Gouy method and many other methods operating on somewhat different principles. Thus, the sample may be suspended horizontally rather than vertically, the force may be measured by springs, or by hydrostatic pressure. In all methods related to the Gouy method the force, f, exerted on application of the field is given by

$$f = 1/2(\mathrm{K} - \mathrm{K}_0)AH^2,$$

where K is the magnetic susceptibility of the substance per unit volume, K_0 is the volume susceptibility of the atmosphere surrounding the sample, A is the cross-sectional area of the sample, and H is the field strength. The susceptibility of hydrogen as an atmosphere is generally negligible, but air is appreciably paramagnetic.

The Faraday method for measuring susceptibilities measures the force exerted on a small sample by a field having a fairly high gradient in the direction of motion of the sample. The Quincke method is often used for liquids; it measures the capillary rise, or depression, produced when a strong field is applied to the liquid [1 to 5][1].

Some 30 or 40 years ago, efforts were made to apply standard induction techniques to the measurement of magnetic susceptibilities. These methods all failed because the susceptibilities are so very small. But recently Broersma [6] has developed an induction method that is as sensitive as the best Gouy determinations. At present the method is considerably more complicated than the Gouy method, but further development may make it the method of choice for routine susceptibility measurements.

II. Atomic and Molecular Diamagnetism

The classical theory of diamagnetism shows that the susceptibility per gram atom, χ_A, is given by the expression

[1] Figures in brackets indicate the literature references at the end of this paper.

$$\chi_A = -2.832 \sum \overline{r^2} \times 10^{10},$$

where $\overline{r^2}$ is the mean square radius of the electronic orbits. The same result is obtained in the quantum-mechanical theory of magnetism, from which diamagnetic atomic susceptibilities may in theory be directly calculated [7]. For hydrogen

$$\chi_A = -2.832 \times 10^{10} \left(\frac{h^2}{4\pi^2 Ze^2 m} \right) \left[\frac{5}{2} n^4 - \frac{3}{2} n^2 l(l+1) + \frac{1}{2} n^2 \right]$$

where n and l are principal and subordinate quantum numbers, respectively, Z is the atomic number, h is Planck's constant, and m is the electron mass. Unfortunately, atomic hydrogen is not only difficult to study, but is paramagnetic. This paramagnetism is far larger than the underlying diamagnetism could possibly be. However, indirect methods for estimating the atomic diamagnetism give results in good agreement with theory. Similar calculations give fair agreement with experiment for the inert gases and for mercury vapor.

Unfortunately, theoretical calculations of susceptibility for polyatomic molecules are in a rudimentary state. For the calculation of molecular susceptibilities our only recourse, at present, is the use of empirical constants derived from the consideration of experimentally found susceptibilities for a large number of organic compounds. These constants, known as Pascal's constants, may be used in much the same way that molecular refractivities are used in calculating molar refraction. The molar susceptibility is in general given by

$$\chi_M = \sum n_A \chi_A + \lambda$$

where n_A is the number of atoms of susceptibility, χ_A is the molecule, and λ is a constitutive correction depending on the nature of the bonds between the atoms. Tables of Pascal's constants and constitutive corrections are available in works on magnetochemistry [2]. With their aid some surprisingly accurate estimations of susceptibilities have been made.

These considerations suggest that the process of polymerization should bring about a change of magnetic susceptibility. Farquharson [8] has examined the polymerization of 2,3-dimethylbutadiene. Consider a dimerization $2\ B \rightarrow B_2$. The molar susceptibility of the dimer must be $\chi_M = 2\chi_B + \lambda$, where λ is the constitutive correction for formation of the new bond. If n molecules of B polymerize to form B_n, then $\chi_M = n\chi_B + (n-1)\lambda$, and the relationship between molar suceptibility and n will be a straight line. The susceptibility of the polymer per unit mass will be

$$\chi = \frac{n\chi_B + (n-1)\lambda}{nM_B},$$

where M_B is the molecular weight of the monomer. The change of χ with n will then be represented by a hyperbola. Farquharson has found that such is the case for 2,3-dimethylbutadiene, and for certain other polymerizations. Whether the susceptibility increases or decreases during polymerization depends on the nature of the bonds broken and formed. Both cases are known.

From the above it would appear that measurement of magnetic susceptibility may afford a measure of the extent of polymerization and also an estimate of the molecular weight. Applications of the latter have been made by Farquharson [9] to the polyoxymethylenes. So far, however, there is no evidence to show that the magnetic method can compete in these respects with any of the standard procedures in polymer chemistry. It might possibly be adapted to certain *in situ* types of studies where other methods are awkward. But the small differences of susceptibilities encountered and the effect of isomerism, hydrogen bonding, and impurities, is such as to discourage further attempts along this line.

III. Diamagnetic Anisotropy

We turn now to a much more promising application of magnetism to high polymers, namely, the diamagnetic anisotropy.

A substance, such as a gas, in which the molecules are all arranged at random, is truly isotropic. Effective isotropy may be shown by a solid, the microcrystals of which have completely random orientation. In crystals of low symmetry there are three mutually perpendicular directions known as the axes of principal magnetism. Along these axes the direction of magnetism corresponds with the direction of the applied field. The magnetic susceptibilities along these axes are called principal susceptibilities. Their values are often

unequal. If such an anisotropic substance is powdered, the average susceptibility of the powder is the mean of the three principal susceptibilities,

$$\bar{\chi}=1/3(\chi_1+\chi_2+\chi_3).$$

Cubic crystalline matter is isotropic, but if a piece of noncubic matter is supended in a magnetic field it will tend to orient itself so that the axis of maximum (algebraic) susceptibility in the plane of rotation lies along the lines of force. In orthogonal crystals the axes of principal susceptibility coincide with the crystal axes. In the monoclinic system one principal magnetic axis coincides with the symmetry axis of the crystals. Many organic compounds crystallize in the monoclinic system.

The additivity of average suceptibilities of organic compounds shows that even in the solid state the mutual influence of neighboring molecules on the magnetic susceptibility must be neglibible. (This is not true for paramagnetic compounds.) It follows that the anisotropy of a single crystal must be due to the anisotropy of the unit cell, and that this, in turn, depends only on the resultant anisotropy of the individual molecules in the cell. If the molecule is essentially magnetically isotropic, then the crystal will show little or no anisotropy. But if the molecule is anisotropic then the resultant anisotropy of the crystal depends only on the relative orientation of the molecules. If the molecules are arranged in layers, then the resultant crystal anisotropy will be large, but if the molecules are arranged haphazardly, or so that their anisotropies cancel each other, then the crystal will be isotropic.

An obvious way to measure magnetic anisotropy is to orient a single crystal so that one axis lies in the field gradient in one of the conventional methods for measuring susceptibilities. But Krishnan [10] has developed a far more elegant method. Krishnan's method gives the difference between any two principal susceptibilities.

If an isotropic sample is cut to spherical shape it will suffer no orientation in a nonuniform field. Alternatively, an isotropic sample of any shape will suffer no orientation in a uniform field. This is the basis of the Krishnan method.

The sample is suspended by a fine torsion fiber in a homogeneous field (fig. 2). A field of sufficient homogeneity may be found in a small region

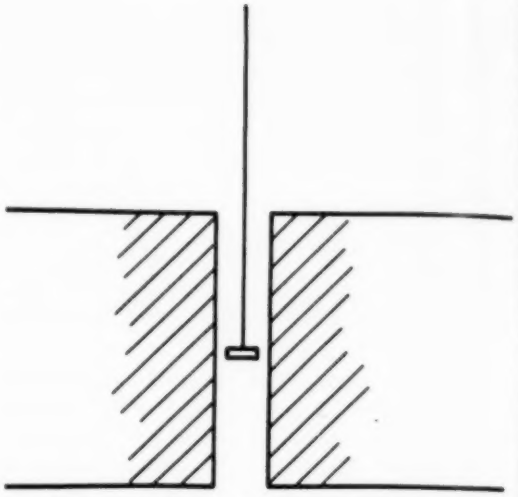

FIGURE 2. *Principle of the Krishnan anisotropy balance.*

between relatively large plane pole pieces. The field may be 5,000 to 10,000 gauss. For reasons of economy a permanent magnet, mounted on a sliding table, has some advantages for these measurements. In general one magnetic axis of the sample is in the axis of the torsion fiber. If the crystal is isotropic it will suffer no orientation on application of the field, but if it is anisotropic it will turn until the algebraically largest susceptibility approaches the direction of the lines of force. The torsion head may now be turned until the crystal suffers no orientation on application of the field. The largest algebraic susceptibility is now parallel to the field.

If the crystal is made to oscillate, the period of oscillation is related to the molar magnetic anisotropy as follows:

$$\Delta\chi=\frac{C}{H^2}\frac{M}{m}\frac{t_0^2-t^2}{t^2},$$

where t_0 and t are oscillation periods with the field off and on, respectively, C is the torsional constant of the fiber, m is the mass of the crystal, M is the molecular (or formula) weight, H is the field, and $\Delta\chi$ is the difference between the two principal susceptibilities in the plane of rotation.

The anisotropy so obtained is that which exists in the plane of oscillation. The third principal susceptibility may be investigated by reorienting the crystal. Absolute principal susceptibilities may be obtained by measuring one susceptibility

by a direct method; or by using the average (powder) susceptibility.

Krishnan [11] has also developed a modification of the above method. This second procedure has some practical advantages over the first, especially for very small crystals. The crystal orientation in the field is adjusted as before so that the largest algebraic susceptibility in the plane of rotation lies in the direction of the field. Now if the torsion head is turned through an angle α, the crystal will turn through a smaller angle ϕ. The relation between α and ϕ is such that

$$c(\alpha-\phi)=\frac{1}{2}\frac{m}{M}H^2\Delta\chi 2\phi,$$

where the terms have the same significance as before. If the torsion head rotation is continued until $\phi=\pi/4$ the crystal will suddenly flip around to a new equilibrium position. For this to occur the torsion head must be turned through an angle α_c, and we have:

$$c(\alpha_c-\pi/4)=\frac{1}{2}\frac{m}{M}H^2\Delta\chi,$$

or

$$\Delta\chi=\frac{c}{H^2}\frac{M}{m}(2\alpha_c-\pi/2).$$

The largest diamagnetic anisotropies are shown by graphite, and by aromatic compounds, the molecules of which contain benzene, cyanuric, or phthalocyanic rings. Carbon in the cubic (diamond) form is isotropic with a molar susceptibility of -6×10^{-6}. But the principal molar susceptibility of graphite parallel to the hexagon axis is -264×10^{-6}, which is over forty times numerically as great as the susceptibility normal to the hexagonal axis. For naphthalene and anthracene the principal susceptibilities are given below [12]:

Principal susceptibilities for single crystal $\times 10^6$

	$-\chi_1$	$-\chi_2$	$-\chi_3$
Naphthalene	56.0	146.4	76.6
Anthracene	75.5	211.8	102.9

For many organic compounds the complete structure has been determined by X-ray diffraction studies, and the orientations of the molecules in the unit cell are known. It is possible to deduce the principal susceptibilities of the individual molecules from the principal susceptibilities of the crystal and the molecular directional cosines. Principal molar susceptibilities for individual molecules of two compounds are shown below.

Principal susceptibilities for individual molecules $\times 10^6$

Compound	$-K_1$	$-K_2$	$-K_3$
Naphthalene	56.1	53.9	169.0
Anthracene	75.8	62.6	251.8

Conversely, if the principal susceptibilities of the individual molecules are known or can be estimated, and if the anisotropy of the crystal is measured, it is then possible in favorable cases to find the arrangement of molecules in the unit cell. In other words, the magnetic anisotropy may be used for a complete structure determination. More frequently, the anisotropy is of use in simplifying structural determinations by X-rays. Examples of these calculations will be given below.

Various suggestions have been made to explain the abnormal diamagnetism shown along one axis by aromatic compounds. The most popular explanation is that the aromatic, or resonance, electrons occupy orbits of molecular instead of atomic size. A satisfactory general theory of anomalous diamagnetic anisotropy in aromatic compounds has been developed by London [13]. London's theory corresponds to the method of molecular orbitals in the theory of chemical binding.

We shall now show how the observed principal susceptibilities in the crystal may be used to find the principal susceptibilities for the individual molecule. Naphthalene is chosen as the example.

Naphthalene belongs to the monoclinic class. The crystalline and magnetic axes of a monoclinic crystal are shown in figure 3, and figure 4 shows the relation of a naphthalene molecule to these axes. Two of the principal magnetic axes lie in the (010) or *ac* plane; the magnetic susceptibilities along these axes are χ_1 and χ_2. The angle ψ, which the χ_1 axis makes with the *c* axis of the crystal, taken as positive toward the obtuse angle β between the *c* and *a* axes, determines the positions of the two magnetic axes. The angle θ is connected

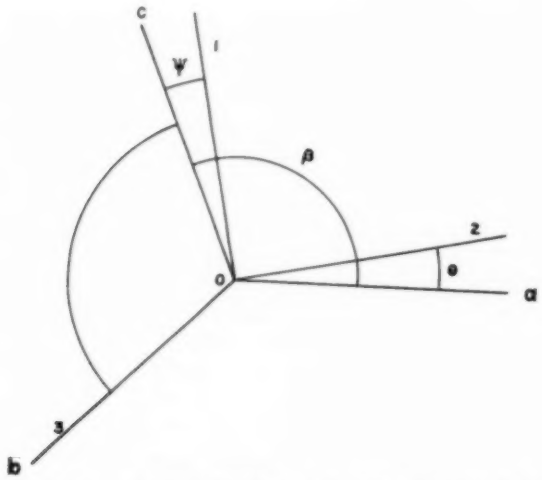

FIGURE 3. *Principal crystal (a, b, c) and magnetic (1, 2, 3) axes in a monoclinic crystal.*

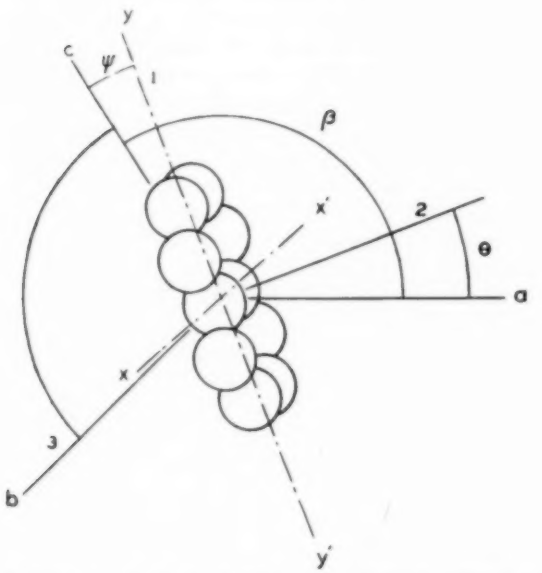

FIGURE 4. *Position of naphthalene molecule relative to crystal and magnetic axes.*

with ψ by the relation $90°+\theta+\psi=$obtuse β. The third magnetic axis is along the b axis, and the susceptibility along it is χ_3.

X-ray studies show that the unit cell of naphthalene contains two molecules, for each of which the structure is plane. Both molecules have their lengths, the lines that join centers of constituent rings, almost in the (010) plane, making an angle of 12° with the c axis. Considerations of symmetry show that the long axis of the naphthalene molecule must be one of its magnetic axis. We should, therefore, expect the above direction in the crystal to be one of the magnetic axes of the crystal. Direct observation of the magnetic axes confirms this view, and the angle ψ is actually found to be 12°. The other two magnetic axes are along the breadth of the molecule in the plane of the rings, and along the normal to the plane of the rings, respectively.

X-ray studies show that the planes of the molecules are inclined at +65° and −65°, respectively, to the (010) plane. We have, therefore, all the information necessary to find the magnetic susceptibilities of the individual molecule

$$\chi_1=K_1,$$
$$\chi_2=K_2\cos^2 65°+K_3\sin^2 65°,$$
$$\chi_3=K_2\sin^2 65°+K_3\cos^2 65°,$$

where χ and K are principal molar susceptibilities of crystal and of molecule, respectively. Substituting the experimentally determined values for χ_1, χ_2, χ_3, we obtain the numerical values for K_1, K_2, K_3 given above.

Biphenyl will be chosen as an example to illustrate the type of calculation in which the anisotropy is used to find the orientation of molecules in the unit cell. We shall assume that the rings in biphenyl have the same structure as in benzene and that the molecule is planar.

The average (powder) molar susceptibility of biphenyl is -102.9×10^{-6}, which is numerically less than twice that of benzene by 7.7×10^{-6}. This difference is obviously the contribution of the two hydrogen atoms that have been dropped. As a first approximation, we assume that this diminution is the same along the three principal axes of the molecule. The principal susceptibilities for the benzene molecule are $K_1=-37.3$, $K_2=-37.3$ $K_3=-91.2(\times10^{-6})$. We then obtain for the principal molar susceptibilities of the biphenyl molecule, all $\times10^{-6}$,

$$K_1=K_2=-(2\times37.3)-7.7=-66.9$$
$$K_3=-(2\times91.2)-7.7=-174.7.$$

The principal molar susceptibilities for the biphenyl crystal are

$$\chi_1=-63.4\times10^{-6}$$

$$\chi_2 = -146.5$$

$$\chi_3 = -98.9,$$

and the angle ψ is 20.1°.

There are two molecules in the unit cell. Place both molecules with their planes parallel to (100) and their lengths along the c axis. To bring the molecules to their actual orientations, they are given the following rotations (fig. 5):

First, a rotation about the c axis of one of the molecules through an angle λ, and of the other through an angle $-\lambda$.

Second, a rotation of both molecules about the b axis through an angle δ, the positive direction of the rotation being defined as from the c axis to the a axis, through the obtuse angle β.

Third, a rotation of the molecules through $+\nu$ and $-\nu$, respectively, about the normal to the plane that contains the b axis and the direction of lengths of the molecules after the second rotation has been performed.

It is clear that $\delta = \psi = +20.1°$, and λ and ν can be obtained from the following relationships:

$$\chi_1 = K_1 \cos^2 \nu + (K_2 \cos^2 \lambda + K_3 \sin^2 \lambda) \sin^2 \nu$$

$$\chi_2 = K_2 \sin^2 \lambda + K_3 \cos^2 \lambda$$

$$\chi_3 = K_1 \sin^2 \nu + (K_2 \cos^2 \lambda + K_3 \sin^2 \lambda) \cos^2 \nu.$$

It has already been assumed that $\chi_1 + \chi_2 + \chi_3 = K_1 + K_2 + K_3$; therefore, only two of the above relationships are independent.

Solving, we get

$$\lambda = 31°, \qquad \nu = 0°.$$

The lengths of the molecules lie in the (010) plane in the obtuse angle β at 20.1° to the c axis, and the planes of the molecules are inclined at plus and minus 31°, respectively, to the b axis. This structure determination is confirmed by X-ray analysis. ($\psi = 20°$, $\lambda = 32°$, $\nu = 0°$).

In the above analysis we have evaluated the principal susceptibilities of the molecule from structure considerations that may not be applicable for molecules more complicated than biphenyl. In such cases it is possible to obtain the molecular susceptibilities from measurements of magneto-optical rotation, according to methods described by Raman and Krishnan [14].

The structure determination given for biphenyl

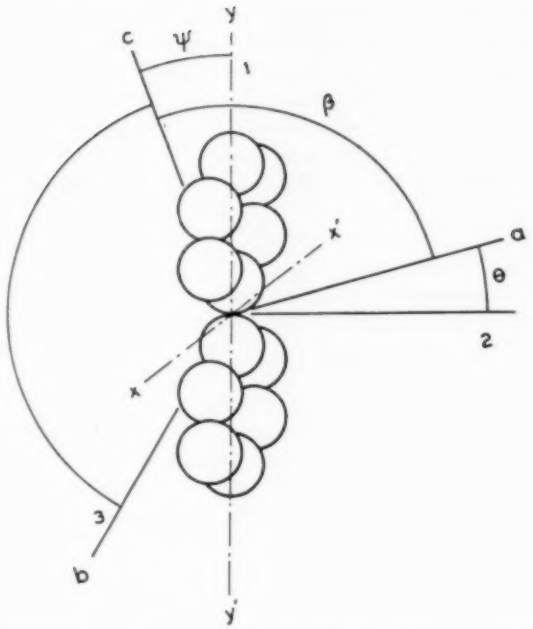

FIGURE 5. *Position of biphenyl molecule relative to crystal and magnetic axes.*

is unfortunately not generally applicable to organic solids. The simplicity of the derivation comes from the special case of $\mu \approx \upsilon$. For other classes of substances the information obtainable from magnetic anisotropy is often less, but any aid from such a source is welcome if it lessens the labor of complete structure determinations from X-ray data. The applicability of the magnetic method is described by Lonsdale and Krishnan [12]. It may be summarized as follows:

In the triclinic system, magnetic anisotropy measurements give directly the molecular orientations.

In the monoclinic and orthorhombic systems the magnetic method is of aid in structure determinations and is very valuable in a few special cases.

In crystals of high symmetry the magnetic measurements are of little or no use [15].

The literature does not reveal many studies on the magnetic anisotropy of polymeric material. A few studies have been made that show the existence of the property in high polymers. But the obvious applicability of the method in the study of polymers containing aromatic groups seems to have escaped attention.

Mme. Cotton-Feytis [16, 17] has recently dem-

onstrated the anisotropy of several natural types of fibers and of crude rubber. These substances can, to a first approximation, be considered as uniaxial crystals. The largest numerical susceptibility is sometimes longitudinal, sometimes perpendicular to the long axis. Various types of cellulose (cotton, sisal, etc.), silk fiber, keratin, and collagen all show varying degrees of anisotropy. The magnitude of the anisotropy roughly parallels the degree of molecular orientation as revealed by X-ray studies. For example, a normal sample of collagen showing a high degree of molecular orientation has an anisotropy ten times as large as the same sample shrunk and rendered amorphous by treatment with formaldehyde.

Nilakantan has investigated the anisotropy of wood and cellulose. Wood is anisotropic, apparently because of a molecular anisotropy in the cellulose molecule and the more or less regular orientation of these molecules along the fiber axis. Lignin and the hemicelluloses are amorphous.

The greatest diamagnetism of cellulose is along the fiber axis, which is presumably along the length of the molecule. This anisotropy in α-cellulose derived from teakwood is about $\chi_{\parallel}-\chi_{\perp}=-0.1\times 10^{-6}$. The average susceptibility of α-cellulose in powder form is -0.508×10^{-6}. The method appears to have some utility in confirming the molecular orientations of cellulose shown by X-ray studies.

Crude rubber normally has a certain degree of anisotropy, and this is altered by hot and cold working, and by compression and tension. Plexiglass is said by Cotton-Feytis to yield somewhat similar results, but no details are given.

When crude rubber is stretched, the anisotropy increases but seems to tend toward a limit. This parallels the effects observed with X-ray methods and suggests more or less complete molecular orientation in one direction at high elongations. The anisotropy observed in stretched rubber is, incidentally, quite large. The figures reported by Cotton-Feytis for oscillation periods with the magnetic field off and on, respectively, are 85 seconds and about 5 seconds. There is no doubt that the method is a sensitive one for detecting molecular orientation in such systems.

The effects observed will doubtless be much more valuable in the study of high polymers containing aromatic groups. It seems probable that degrees of molecular orientation quite beyond detection by other methods will be readily estimated by the anisotropy measurements. There are obvious applications of such studies to changes occurring under compression, tension, extrusion, and hot and cold working. The establishment of relationships between anisotropy and physical properties such as hardness, tensile strength, optical properties, and second-order transitions, is also a possibility.

IV. Atomic and Molecular Paramagnetism

We turn now to applications in which the paramagnetism of certain molecules or groups may be used for the elucidation of certain problems in polymerization. First, however, we shall present some general information on atomic and molecular paramagnetism.

The classical theory of Langevin develops an expression for paramagnetic susceptibility on the assumption that each atom is a small permanent magnet. These atomic magnets tend to aline themselves with an applied field, but the alinement is resisted by thermal agitation. In modern terminology we identify the atomic magnets with the magnetic moments produced by orbital and spin movements of the electrons.

Langevin's expression for the molar paramagnetism is

$$X_M=\frac{N\mu^2}{3kT},$$

where N is Avogadro's number, μ is the permanent magnetic moment, k the Boltzmann constant, and T the absolute temperature. The corresponding quantum mechanical expression derived by Van Vleck [7] is

$$X_M=\frac{N\overline{\overline{\mu}}^2}{3kT}+N\overline{\alpha},$$

where $\overline{\overline{\mu}}^2$ is the square of the low frequency part of the magnetic moment vector, averaged over time, and this average being itself average over the various normal states appropriately weighted according to the Boltzmann factor. The quantity $\overline{\alpha}$ is a combination of high frequency elements of the magnetic moment, and of the diamagnetic part of the susceptibility.

In general, the paramagnetic moment consists of a part derived from an orbital contribution and a part derived from a spin contribution. The only major cases in which the orbital contribution

is important is for isolated paramagnetic atoms and for rare earth ions. For those substances in which only the spin contribution is important the paramagnetism is approximately represented by

$$X_M = \frac{N\beta^2}{3kT}[4S(S+1)],$$

where S is the resultant spin moment, and β is the Bohr magneton, which is given by

$$\beta = \frac{eh}{4mc} = 0.917 \times 10^{-20} \text{ erg gauss}^{-1},$$

where e is the electronic charge, h is Planck's constant, m is the mass of the electron, and c is the velocity of light.

The effective magnetic moment in such cases is given by

$$\mu_{eff} = 2\sqrt{S(S+1)},$$

where S may be found from the spectral multiplicity, or, if the number, n, of unpaired electrons is known,

$$\mu_{eff} = \sqrt{n(n+2)}.$$

Finally, the magnetic moment may be found experimentally from

$$\mu_{eff} = 2.84\sqrt{\chi_M T},$$

or more accurately from

$$\mu = 2.84\sqrt{\chi_M(T+\Delta)}.$$

These expressions are of great value in connection with studies of transition group ions, such as Fe^{+3}, Cr^{+3}, Ni^{+2}, and their respective complexes. However, for all but a very few cases of paramagnetism in molecules there is only one unpaired electron, and the "spin only" formula applies. Furthermore, in almost all such cases the quantity Δ is not far from zero. Hence, for paramagnetic molecules such as triphenylmethyl, we find that the molar paramagnetic susceptibility at 20° C is about $1{,}270 \times 10^{-6}$, and that this varies inversely as the absolute temperature.

Among paramagnetic molecules of interest we may mention NO, NO_2, ClO_3, the triarylmethyls, semiquinones, and metal ketyls. All these substances are characterized by having an odd number of electrons. The existence of an unpaired electron is essential for paramagnetism. Molecular oxygen is paramagnetic, although it contains an even number of electrons. The paramagnetism in this case results from the peculiar electronic state in which two electrons remain unpaired. A similar situation exists in a few complex organic compounds related to the Chichibabin hydrocarbons. Such substances are called biradicals.

It will be clear from the above that a major application of magnetochemistry is in the detection and estimation of molecules containing an unpaired electron spin, that is to say, of free radicals.

V. Free Radicals

There have been many magnetochemical studies of free radicals reported in the past 10 years, during which this has become the leading physical method in free-radical chemistry. The general nature of the results obtainable will be surveyed briefly [2, 19].

Inasmuch as the most characteristic property of a free radical is its unpaired electron, the magnetic susceptibility is a most direct measure of free radical existence. Whereas molecular weights, colors, and chemical reactivity may depend upon secondary factors, it is difficult to see how a molecule that does not contain a transition group element can be paramagnetic unless it is a free radical. We choose to define a free radical as a chemical entity, neutral or ionic, which contains one or more unpaired electrons, transition elements being, of course, excluded.

In this way the free radical nature has been established for such substances as diaryl nitric oxide, Fremy's salt, a great variety of hexaarylethanes, the hydrazyls, semiquincnes, Wurster's salts, the metal ketyls, certain diaryl peroxides, diaryl disulfides, and of certain materials in the phosphorescent state. On the other hand, certain organometallic compounds of which hexaphenyldilead is an example, have been shown to be diamagnetic, although molecular weight determinations seem to indicate dissociation to the free radical form.

The magnetic method has a further advantage in its flexibility. Measurements may conveniently be made on free radicals in solution at various temperatures and concentrations, and in various solvents. The importance of this type of measurement lies in the possibility of obtaining equilibrium constants at several temperatures, and thus

opening the way for calculations of heats of dissociation, free energies, and entropies. A considerable number of hexaarylethanes have been studied in this way with a view to finding the effect of different substituents on the heats of dissociation. Such data are of interest in connection with the resonance theory of free radical stability.

Other information obtainable from magnetic measurements on hexaarylethanes includes the rate and activation energy of the disproportionation reaction undergone by some free radicals, the relationships between color and free radical concentration, and rate studies on certain photochemical reactions shown by these substances. One of the most valuable features of the magnetic method is the possibility of studying, *in situ*, reactions as they take place, provided the concentration of a paramagnetic component changes with time, as is the case with free radical reactions [21, 22].

It should be mentioned that the magnetic method is not infallible. Short-lived radicals cannot be studied with the magnet unless the steady state concentration is sufficiently high. With the most refined apparatus a free radical concentration of 10^{-6} mole per liter might be just detectable. Furthermore, there is one case reported in the literature in which the substance appears to be a biradical but is diamagnetic. This is the simple Chichibabin hydrocarbon, to derivatives of which reference was made above. The simple hydrocarbon appears to catalyze the *ortho-para* hydrogen conversion, which is evidence of a paramagnetic component, but the compound shows no trace of paramagnetism as measured in the usual way [23].

VI. Magnetic Measurements on Reacting Systems

As applied to reacting systems, magnetic susceptibilities have been used as described above to study the rate of disproportionation of hexaarylethanes [24]. The transitory existence of semiquinone free radicals has been demonstrated magnetically by Michaelis [25], who studied the concentration of these substances as a function of time, and in some cases by a process that might be called "magnetic titration," that is, the change of susceptibility during the quantitative addition of an oxidizing or reducing agent. A typical example of a reaction that may be studied *in situ* magnetically is the slow reduction of dichromate with glucose in dilute solution. This reaction produces a large calculable change of susceptibility owing to the change from the practically nonmagnetic dichromate ion to the strongly paramagnetic chromic ion. No change of phase complicates this reaction, which has been used to calibrate the very sensitive magnetic balance described below.

The possibility of studying reacting systems *in situ* has suggested the use of magnetic measurements in polymerization reactions. The information obtainable in this way would appear to be of two kinds. First, it would certainly be possible to detect very small concentrations of molecular oxygen and to estimate their changes with time. And second, the free radical theory of polymerization suggests the attractive possibility of obtaining quantitative information on free radical concentration during polymerization.

The magnetic study of reactions such as these requires a degree of sensitivity far beyond that normally obtainable with the classical Gouy balance. An apparatus using the Gouy principle, but with several refinements leading to greatly increased sensitivity, will be described (fig. 6). This

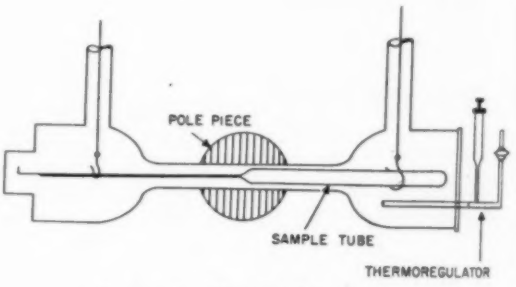

FIGURE 6. *Horizontal Gouy balance.*

uses a horizontal, rather than a vertical, mounting of the sample tube. The horizontal mounting has actually been used for many years, and has recently been adopted by Theorell and by Calvin for high sensitivity measurements.

The sample tube is suspended horizontally from long delicate fibers. One end of the tube is between the poles of a magnet. A permanent magnet has a great advantage in that the field is quite steady over long periods of time. This is a condition very difficult to attain with an electromagnet. The substance under investigation is

placed in the sample tube, which then moves horizontally as the susceptibility increases or decreases with time as the reaction proceeds. The whole apparatus is, of course, mounted so as to reduce the effects of vibration and of drafts to a minimum.

Displacements of the sample tube are observed for approximate readings with the aid of a micrometer microscope focussed on a fiduciary point. Refined measurements are made with a Fabry and Perot type of interferometer, one plate of which is mounted on the end of the sample tube. With this apparatus the sensitivity is such that 10^{-6} mole of free radicals may just be detected [26].

Some of the results obtained with this apparatus are shown in figure 7. These results are for the thermal polymerization of styrene. It will be noted that the magnetic susceptibility suffers relatively large changes during the first few hours of reaction. Under the experimental conditions this corresponds to a few percent of polymerization. The changes in susceptibility generally take the form of a large increase in diamagnetism followed by a much slower increase. The changes are markedly influenced by the purity of the styrene and the method of handling the monomer prior to its introduction into the apparatus.

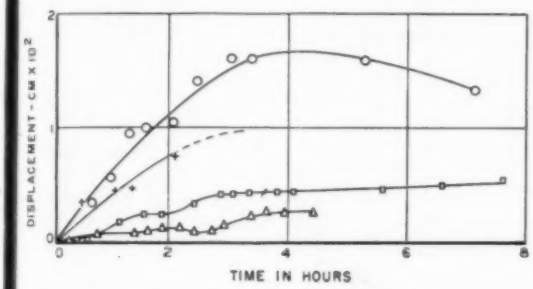

FIGURE 7. *Changes of diamagnetic susceptibility during polymerization of styrene.*

Thermal polymerization of styrene. ○, stock room styrene, vacuum distilled (+ degassed); □, styrene prepared from cinnamic acid, and △, degassed.

The initial increase of diamagnetism is often much greater than would be found for complete polymerization. This "anomalous" diamagnetic increase is believed to be due to the consumption of dissolved molecular oxygen. The inhibiting action of oxygen on vinyl polymerization is well known. Assuming that no normal polymerization takes place during the induction period (a small amount of polymerization would have a negligible effect on the susceptibility), then the displacement of the sample tube from zero time to the time at which the curve levels out, approximately represents the initial concentration of oxygen present. For curve 1, figure 7, the initial concentration of oxygen thus found is 2.9×10^{-4} mole per liter, and this concentration steadily falls. At 2 hours the concentration is 0.99×10^{-4} mole per liter.

The rate of oxygen consumption is shown by these results to be zero order. Reasonably concordant results are obtained on different samples of styrene, although the initial oxygen concentration may be quite different.

These results may be used to calculate the rate constant for initiation. If the initiation process is represented as forming a biradical, oxygen reacts with these free radicals very rapidly.

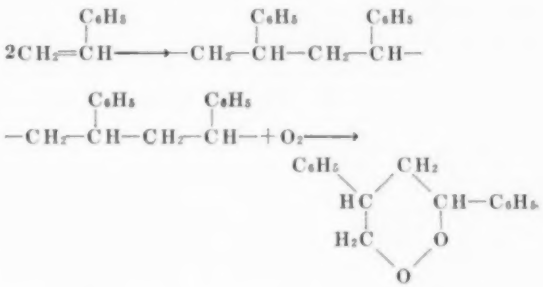

Such a process is represented by the equations

$$2M \xrightarrow{k_1} R$$

$$R + O_2 \xrightarrow{k_2} RO_2,$$

where R is a free radical and represents the concentration of free radicals in the kinetic equations and M is the monomer and its concentration.

$$\frac{dR}{dt} = K_1M^2 - k_2[O_2]R \qquad (1)$$

$$-\frac{d[O_2]}{dt} = k_2[O_2]R. \qquad (2)$$

Since the rate of consumption of oxygen is experimentally zero order, it follows that eq 1 is the rate-determining step. That is, the free radicals are consumed as rapidly as they are formed owing to the rapid action of the oxygen. A steady state is therefore reached, free radicals being used up

at the same rate at which they are formed and $dR/dt=0$, therefore

$$k_1M^2=K_2[O_2]=-\frac{d[O_2]}{dt}$$

and

$$k_1=-\frac{d[O_2]}{dt}\frac{1}{M^2}.$$

$-d[O_2]/dt$ may be found from the rate of oxygen loss, and is equal in one of the runs to 2.8×10^{-8} mole per liter per second, and M (for pure styrene monomer) is 8.56 moles per liter.

Hence

$$k_1=2.8\times10^{-8}\times1/(8.56)^2$$

$$=3.8\times10^{-14}\text{ mole per liter per sec.}$$

This figure is not unreasonable. Bartlett [27] gives a rate constant for initiation in the photopolymerization of vinyl acetate (which should be much higher than for thermal polymerization at 66° C) as $\sim3\times10^{-8}$.

The above results are preliminary and are given to indicate the probable direction of magnetochemical research on polymerization rather than with the idea of presenting a completed program.

If vinyl polymerization actually goes through a free radical mechanism there is presented the attractive possibility of determining the free radical concentration by magnetic measurements on reacting systems. There have been some reports in which this possibility is claimed to have been realized [28]. However, the best estimates of free radical concentrations give values of the order of 10^{-9} moles per liter. These estimates are made indirectly and are possibly subject to fairly large error. Nevertheless, opinion at the present time is that the sensitivity of the best magnetic balances is still several orders from the detection of free radicals in this way. It may be that an appropriate choice of reacting system would yield free radical concentration much higher than that normally believed to be present. But it must be admitted that such a possibility seems to be somewhat remote.

VII. References

[1] E. C. Stoner, Magnetism and matter (Methuen and Co., Ltd., London, 1934).
[2] P. W. Selwood, Magnetochemistry (Interscience Publishers, Inc., New York, N. Y., 1943).
[3] W. Klemm, Magnetochemie (Akademische Verlagsgesellchaft, Leipzig, 1936).
[4] S. S. Bhatnagar and R. N. Mathur, Physical principles and applications of magnetochemistry (Macmillan and Co., Ltd., London, 1935).
[5] R. W. Asmussen, Magnetokemiske Undersøgelser over Uorganiske Kompleksforbindelser (Jul. Gjellurups Forlag, Copenhagen, 1944).
[6] S. Broersma, Magnetic measurements on organic compounds (Martinus Nijhoff, The Hague, 1947).
[7] J. H. Van Vleck, The theory of electric and magnetic susceptibilities (Oxford University Press, Oxford, 1932).
[8] J. Farquharson, Trans. Faraday Soc. **32,** 219 (1936).
[9] J. Farquharson, Trans. Faraday Soc. **33,** 824 (1937).
[10] K. S. Krishnan, B. C. Guha, and S. Banerjee, Phil. Trans. Roy. Soc. (London) [A] 231, 235 (1933).
[11] K. S. Krishnan and S. Banerjee, Phil. Trans. Roy. Soc. (London) [A]234, 265 (1935).
[12] K. Lonsdale and K. S. Krishnan, Proc. Roy. Soc. (London) [A]156, 597 (1936). This paper corrects certain erroneous data given in one of Krishnan's earlier papers. The incorrect data were unfortunately repeated in a review article by P. W. Selwood and J. Parodi, J. Chem. Education **23,** 574 (1946).
[13] F. W. London, J. phys. radium **8,** 397 (1937).
[14] C. V. Raman and K. S. Krishnan, Proc. Roy. Soc. [A]113, 511 (1927).
[15] W. A. Wooster, Physics of crystals (Cambridge University Press, Cambridge, Eng.).
[16] E. Cotton-Feytis, Compt. rend. **214,** 485, 996 (1942); **215,** 299 (1942).
[17] E. Cotton-Feytis, Rev. gen. Caoutchouc **21,** 26 (1944).
[18] P. Nilakantan, Proc. Indian Acad. Sci. 7A, 38 (1938).
[19] W. A. Waters, The chemistry of free radicals (Oxford University Press, Oxford, 1946).
[20] R. F. Preckel and P. W. Selwood, J. Am. Chem. Soc. **63,** 3,397 (1941).
[21] M. F. Roy and C. S. Marvel, J. Am. Chem. Soc. **59,** 2,622 (1937).
[22] H. G. Müller, Z. Elektrochem. **45,** 593 (1939).
[23] G. M. Schwab and N. Agliardi, Ber. 73B, 95 (1940).
[24] P. W. Selwood and R. F. Preckel, J. Am. Chem. Soc. **65,** 895 (1943).
[25] L. Michaelis, G. F. Boeker, and R. K. Reber, J. Am. Chem. Soc. **60,** 202 (1938).
[26] H. Boardman and P. W. Selwood, not yet published.
[27] P. O. Bartlett, J. Am. Chem. Soc. **68,** 2,381 (1946).
[28] J. Farquharson and P. Ady, Nature **143,** 1,067 (1939).